HELSINKI UNIVERSITY OF TECHNOLOGY
Faculty of Chemistry and Materials Sciences

Annukka Santasalo

Electrocatalysis of organic molecules on platinum catalyst surfaces: from the fundamentals to the polymer electrolyte fuel cell applications

Thesis for the degree of Licentiate of Science in Technology submitted for inspection, Espoo, 9 October, 2009.

Supervisor Professor Kyösti Kontturi

Instructor Docent Tanja Kallio

HELSINKI UNIVERSITY OF TECHNOLOGY
Faculty of Chemistry and materials Sciences

ABSTRACT OF LICENTIATE THESIS

Author

Annukka Santasalo

Title of Thesis

Electrocatalysis of organic molecules on platinum catalysts surfaces: from the fundamentals to the polymer electrolyte fuel cell applications

Abstract

Polymer electrolyte fuel cells (PEFC) fuelled with organic compounds can be used as energy sources in small, portable applications due to their high power density. Organic fuels such as low molecular mass alcohols have been studied for these applications due to their uncomplicated and relative safety when compared to gaseous fuels. However, although studied already for decades, the adsorption and oxidation mechanisms are still not well understood which is vital for the development of fuel cell applications. In the literature part electrocatalaysis of organic molecules is discussed: the electrode material, ions and molecules in the liquid phase and the electrode potential applied have highest influence on the adsorption and oxidation of these molecules. The probability of a metal to be a suitable catalyst for a certain organic molecule can be estimated by using the molecular orbital theory of both phases.

The experimental part includes two published articles and auxiliary experiments with stepped single crystal electrodes. In the first publication, crossover through the Nafion® 115 membrane as a function of time and performance in a PEFC for several organic molecules is studied. Methanol as the smallest uncharged molecules has the highest crossover rate through the studied membrane, however, also it produces superior performance in a platinum ruthenium catalysed PEFC. Even if other molecules do not reach the current densities produced with methanol, the open circuit potential obtained with isopropanol is dramatically higher compared to methanol.

Consequently, in the second publication the oxidation of methanol, isopropanol and their mixtures has been studied on platinum single crystal electrodes. On Pt(111) the alcohol mixture produces higher current densities than pure alcohol solutions in acidic electrolytes ($HClO_4$ and H_2SO_4). As a result stepped single crystals with Pt(111) terraces and steps of Pt(100) or Pt(110) configuration have also been studied. The only stepped surface which produced higher current densities has wide Pt(111) terraces and Pt(100) steps. In addition, the oxidation of 2-propanol and alcohol mixture is studied with IR spectroscopy and the results indicated that both isopropanol and methanol co-adsorbed on the Pt(111) surface, however, the explanation for the higher activity of an alcohol mixture compared to the isopropanol oxidation is still under investigation..

Supervisor Professor Kyösti Kontturi	Instructor Docent Tanja Kallio
Chair Physical Chemistry	Chair code Kem-31
Pages 56	Language English
Keywords Polymer electrolyte fuel cell, electrocatalysis, oxidation of alcohols	Date 9th October 2009

TEKNILLINEN KORKEAKOULU
Kemian ja materiaalitieteiden tiedekunta

LISENSIAATINTUTKIMUKSEN TIIVISTELMÄ

Tekijä

Annukka Santasalo

Lisensiaatintutkimuksen nimi

Orgaanisten molekyylien elektrokatalyysi platinapohjaisten katalyyttien pinnalla: perusteista polymeerieletrolyyttipolttokennoihin

Tiivistelmä

Orgaanisia polttoaineita käyttäviä polymeerielektrolyyttipolttokennoja (PEPK) voidaan käyttää energianlähteinä pienissä, kannettavissa sovellutuksissa korkeiden tehotiheyksiensä vuoksi. Nestemäiset polttoaineet kuten alkoholit ovat kiinnostavia polttoaineita kuluttajasovellutuksiin, koska ne ovat turvallisempia ja helpompia käyttää kuin kaasumaiset polttoaineet. Vaikka orgaanisia polttoainevaihtoehtoja on tutkittu jo vuosikymmeniä, niiden adsorptiota ja hapettumista platinakatalyyttien pinnalla ei vielä tunneta kunnolla, mikä on edellytyksenä käytännön sovellusten suunnittelussa. Työn kirjallisessa osassa käsitellään orgaanisten molekyylien elektrokatalyysiä eli niiden adsorboitumista sekä hapettumista erilaisille platinakatalyyttipinnoille. Näihin ilmiöihin vaikuttavat erityisesti valittu elektrodimateriaali, liuoksissa olevat ionit ja molekyylit sekä elektrodin potentiaali, joiden matemaattisia tarkasteluja voidaan käyttää hyväksi arvioitaessa elektrodimateriaalin soveltuvuutta tietyn orgaanisen aineen elektrokatalyysiin.

Kokeellinen osa koostuu kahdesta julkaistusta artikkelista sekä lisämittauksista yksikide-elektrodeilla. Ensimmäisessä artikkelissa on tutkittu erilaisten orgaanisten, pienimolekyylimassaisten komponenttien kulkeutumista paljon käytetyn Nafion® 115 membraanin läpi ajan funktiona sekä näiden polttoaineiden suorituskykyä PEPK:ssa. Metanoli pienikokoisimpana, varautumattomana molekyylinä kulkeutui nopeitten tutkitun membraanin läpi, mutta sillä saatiin korkeimmat virrantiheydet platina-ruteniumkatalysoidussa polttokennossa. Vaikka muut molekyylit eivät saavuttaneet metanolin kaltaisia virrantiheyksiä, isopropanolilla saavutettiin metanolia huomattavasti korkeampi avoimen virtapiirin jännite.

Toisessa julkaisussa on näiden tulosten pohjalta tutkittu metanolin, isopropanolin sekä niiden muodostaman seoksen hapettumista elektrodeilla, joiden pinta-atomit ovat järjestäytyneet yhden kiderakenteen mukaisesti. Korkeimmat virrantiheydet alkoholiseokselle kummassakin happamassa elektrolyytissä saatiin Pt(111) kidepinnalla, joten lisämittauksia suoritettiin elektrodeilla, joilla oli Pt(111) suuntautuneet terassit sekä Pt(100) tai Pt(110) suuntautuneet askelmat. Tämän lisäksi 2-propanolin sekä alkoholiseoksen hapettumistuotteita tutkittiin infrapunaspektroskopialla, jolla havaittiin että molemmat puhtaat alkoholit alkoholiseoksesta sekä adsorboituvat että hapettuvat Pt(111) pinnalla. Valitettavasti selvyyttä siihen miten alkoholiseos edesauttaa isopropanolin hapettumista, ei näillä mittausmenetelmillä saatu.

Työn valvoja Professori Kyösti Kontturi	Työn ohjaaja Dosentti Tanja Kallio
Professuuri Fysikaalinen kemia	Koodi Kem-31
Sivumäärä 56	Kieli Englanti
Avainsanat Polymeerielektrolyyttipolttokenno, elektrokatalyysi, alkoholien hapettuminen	Päiväys 9.10.2009

Preface

The experiments for the publications have been performed at the Research Group of Physical Chemistry and Electrochemistry, Helsinki University of Technology between July 2006 and December 2007 and at Universidad de Alicante, Spain at time period January – June 2008. The writing process for the publications and this thesis has been carried out from since at Finland. The financial possibility to travel and work in Spain has been provided by Finnish cultural foundation and Helsinki University of Technology and is gratefully acknowledged.

First I would like to address my gratitude for Prof. Kyösti Kontturi for providing me an opportunity to start my PhD studies with fuel cell topic and for all help he has given me at the founding process for my exchange period in Spain. My supervisor Dr. Tanja Kallio I would like to give my sincere gratitude for filling me up with ideas and offering her guidance also from a distance. I would like to thank all other staff members of the laboratory especially other PhD students for filling up the coffee room and being there for me when the help was urgently needed.

Secondly I would like to thank Prof. Juan Feliu for the opportunity to work for half a year in Spain and my supervisors Dr. Fran Vidal-Iglesias and Dr. Jose Solla-Gullón for introducing me into the world of electrocatalysis and single crystal electrodes; slowly but firmly in Spanish with a lot of patience. I would also like to address my special thanks for my lunch group for providing me company at the long hours of Spanish *almuerzo* and *comida*.

This work could not have been performed without a strong support of my family and friends in all my choices. Finally, I would like thank my wonderful fiancé Matti for inventing the interesting idea of working abroad and travelling between France and Spain.

Otaniemi 9th October 2009

Annukka Santasalo

List of Symbols

c	concentration	mol
e	charge of a proton	0.16027×10^{-18} C
E	electrode potential	V
E_{OCP}	open circuit potential	V
E_{PCZ}	electrode potential at the potential of zero charge	V
F	Faraday's constant	96485 C mol^{-1}
n	number of the electrons	
z	charge number	
θ	surface coverage	
μ	chemical potential	J/mol
Φ	work function	eV
ϕ	inner potential (Galvani potential)	V
χ	surface potential	V
ψ	outer potential	V

List of Abbreviations

2-PrOH	Isopropanol
CB	Conduction Band
DEMS	Differential Electrochemical Mass Spectroscopy
DMFC	Direct Methanol Fuel Cell
fcc	Face centred cubic
hkl	Miller indices
HOMO	Highest Occupied Molecular Orbital
IR	Infrared
LUMO	Lowest Unoccupied Molecular Orbital
MEA	Membrane Electrode Assembly
MeOH	Methanol
OCP	Open Circuit Potential
OLEMS	On-Line Electrochemical Mass Spectroscopy
Pt[n(111) x (100)]	Platinum stepped single crystal electrodes with Pt(111) terraces and Pt(100) steps.
Pt[n(111) x (110)]	Platinum stepped single crystal electrodes with Pt(111) terraces and Pt(110) steps.
PEFC	Polymer Electrolyte Fuel Cell
PZC	Potential of Zero Charge
RHE	Reversible Hydrogen Electrode
SCE	Single Crystal Electrode
SSCE	Stepped Single Crystal Electrode
VB	Valence Band

Index

1 Introduction

Polymer electrolyte fuel cells using liquid fuels are promising electrochemical power generators, especially for portable applications, due to their capability to maintain high power densities for a long time period. To become user friendly, the temperature of the fuel cell must remain near room temperature, the weight of the cell must decrease and the refuelling interval should be extended. However, the main obstacle for fuel cell commercialisation is the high cost of the cell components. Firstly, the commercial membrane used as an electrolyte is very expensive due to its complicated fabrication process. Secondly, in order to oxidise organic fuels at low temperatures precious noble metal catalysts such as platinum or platinum-ruthenium alloys are needed.

These components cannot be replaced with cheaper ones because the basic mechanisms behind the oxidation reactions of different fuels on these catalyst materials are not clearly understood. In particular, the oxidation of liquid fuels in the fuel cells proceeds on a three phase boundary which is very complex to model. To simplify the systems, well-defined single crystal surfaces can be used in aqueous media to expand the knowledge of the adsorption and oxidation processes occurring on catalyst surfaces.

The aim of this thesis is to obtain better understanding of the electrooxidation process of organic fuels on platinum based material surfaces. This thesis includes two published papers and additional specific measurements related to the second paper. The first publication outlines how the different organic fuels perform in a PtRu catalyst fuel cell using a Nafion® 115 membrane as an electrolyte. The objective of the second publication is to deepen understanding of the electrooxidation of two alcohols and their mixture that have been shown to perform well in the fuel cell tests of the first publication.

The scientific papers included are:

Appendix I

A. Santasalo, T. Kallio and K. Kontturi, Performance of Liquid Fuels in a Platinum-Ruthenium-Catalysed Polymer Electrolyte Fuel Cell, *Platinum Metals Rev.*, **53** (2) (2009) 58.

Appendix II

A. Santasalo, F. J. Vidal-Iglesias, J. Solla-Gullón, A. Berná, T. Kallio and J. M. Feliu, Electrooxidation of Methanol and 2-propanol Mixtures at Platinum Single Crystal Electrodes, *Electrochim. Acta*, **54** (2009) 6576.

2 Literature

2.1 Polymer Electrolyte Fuel Cell (PEFC)

Different fuel cell types are classified by the electrolyte material used to separate the anode and cathode from each other and one of these types is the polymer electrolyte fuel cell (PEFC) which possesses a proton conductive membrane as an electrolyte. This membrane requires water to be functional and consequently, the use of these types of fuel cells is limited to a temperature range where water is in liquid phase. Thanks to high energy densities, PEFCs fuelled with liquid organic fuels are normally used as power sources for small portable devices such as cell phones or laptops where near room temperature conditions are required.

2.1.1 Principle of the liquid fuelled PEFC

A membrane electrode assembly (MEA) of the PEFC is made by adding at both sides of the proton conductive membrane electrolyte electrodes, which are mixtures of supported catalyst nanoparticles and conductive polymer ionomer (Figure 1). At both ends of the sandwich complex there are two composite material endplates working as electron conductors. Liquid fuel is fed to the anode compartment and oxidised further while protons and electrons are produced. Protons are transported though the membrane to the cathode side and to maintain electrical neutrality, the electrons circulate from the anode endplate to cathode through an external load and this movement of electrons can be utilised as electric power. At the cathode protons and electrons come together in an oxygen rich atmosphere and the oxygen is reduced to water.

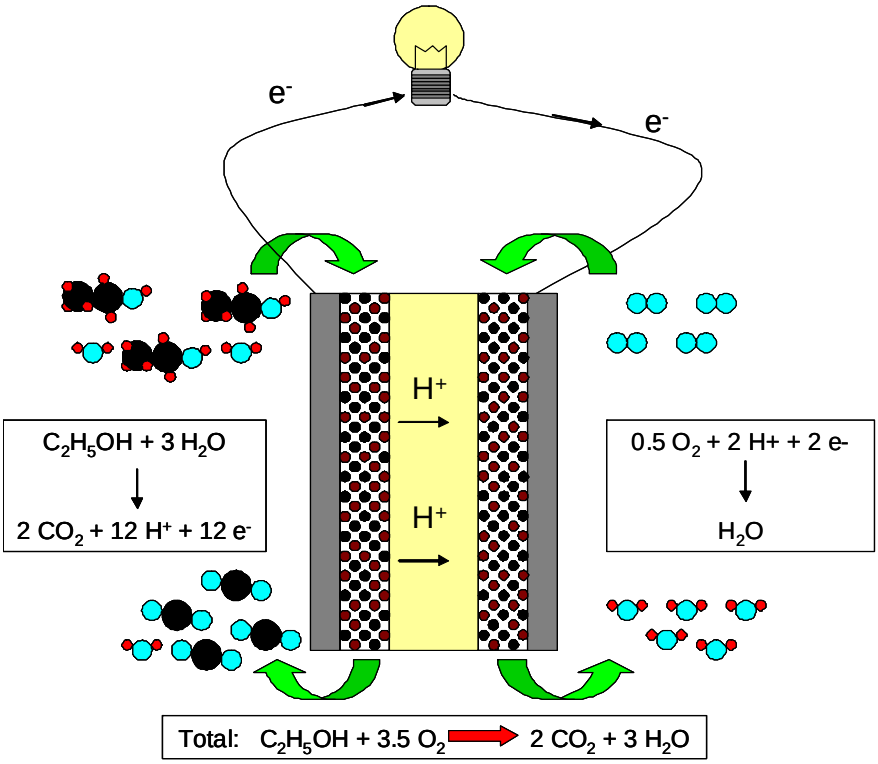

Figure 1. Working principle of the direct ethanol fuel cell.

In principle, liquid fuelled fuel cells can use whatever liquid fuel as long as it can be oxidised at the anode and thus, produce protons and electrons. Liquid organic fuels have been the focus of interest due to their high energy density and more facile storage compared to standard gaseous hydrogen [1 - 7]. However, the electrochemical reactions with organic fuels are more complex: the overall reactions for complete methanol oxidation in the PEFC are:

Anode: $CH_3OH + H_2O \rightarrow CO_2 + 6H^+ + 6e^-$ (i)

Cathode: $\frac{1}{2}O_2 + 2H^+ + 2e^- \rightarrow H_2O$ (ii)

Total: $CH_3OH + \frac{3}{2}O_2 \rightarrow CO_2 + 2H_2O$ (iii)

The corresponding reactions for ethanol oxidation are presented in Figure 1. However, for none of the organic molecules are the electrochemical reactions as simple as outlined in i-iii. On the contrary, several side reactions occur on highly

active catalyst materials such as platinum. These side reactions for a wide range of small organic molecules on bulk platinum electrode have been presented in previous work [8]. In addition, in section 2.3.5 the structural sensitivity of methanol electrooxidation is discussed in details.

Another important phenomenon that needs to be taken into account when studying liquid fuels in the PEFC is a crossover of small, uncharged molecules from the anode to cathode through the water channels of the polymer electrolyte membrane. At the cathode side crossover of the alcohols enables direct reactions between the alcohol and oxygen resulting in power loss within the cell. Moreover, due to the fact that pure platinum is often used as a catalyst material on the cathode, the formation of CO blocks the catalytic surface and reduces the performance of the cathode catalyst. This phenomenon has been widely studied for methanol [9- 12] but less so for other organic fuels such as formic acid [13- 15], ethanol [16-17] and isopropanol [18].

2.2 Single Crystal Electrodes (SCE)

In order to understand electrocatalysis of the fuel cell catalyst materials, detailed information about the surface structure of the catalyzing metal surface and its effect on adsorption and oxidation of the reactant molecules is needed. However, electrocatalysis in the PEFC takes place on bulk polycrystalline surfaces, which are complicated and difficult to model. Taken into account that adsorption and oxidation is happening on three phace boundary that includes the liquid organic fuel, solid metal particles and gaseous product the complexity increases notably. As a result, single crystal electrodes (SCE) having known surface structure are used to reduce the amount of variables. Moreover, even though the SCEs cannot be used in real application they provide crucial information about the surface structure sensitivity of the electrooxidation mechanisms that can be utilised when new applications are designed.

The surface of a SCE is made atomically flat by laser beam and all the atoms on the surface possess only one crystal orientation. For many noble metal catalysts the crystal lattice is face centred cubic (fcc) indicating that the atoms are at the centre of the lateral surfaces and at the corners of the unit cell (Figure 2). The surfaces of the SCE are characterised by Miller indices (hkl) that represent the reciprocal of the intercepts of the plane defined by the x-, y- and z-axes.

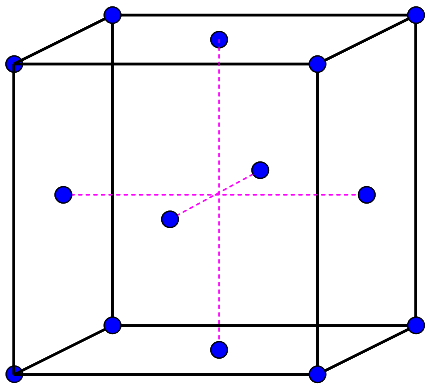

Figure 2. Face centred cubic crystal lattice.

For fcc systems, there are three ways to arrange the surface atoms. These surfaces are called low-index planes and in the case of fcc lattice they are represented by Miller indices as (111), (110) and (100) representing atomically flat surfaces with square, hexagonal and rectangular arrangement of the surface atoms, respectively (Figure 3).For fcc systems monoatomic stepped surfaces can be defined as a combination of these three basal planes.

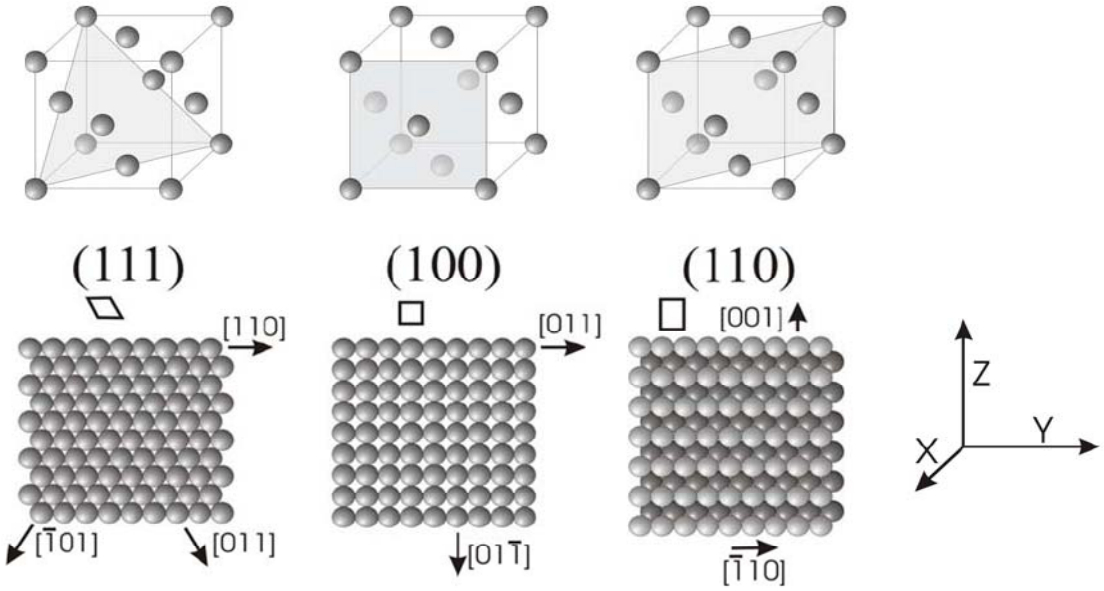

Figure 3. Low-index planes (111), (100) and (110) of fcc systems [19]. (Reprinted by the permission of the author.)

The preparation and cleaning of the single crystal surfaces is crucial to obtain perfectly oriented surfaces, otherwise, the advantage of having a known surface structure is lost. The most common surface defects are adatoms, islands, vacancies, holes and monoatomically high steps (Figure 4). For each different surface configuration there is a different probability for organic molecules to adsorb, thus, making several competing adsorption processes possible and hence, changing the whole behaviour of the catalyst material. For this reason important adsorption and oxidation mechanisms are often the first studied on low-index SCE to obtain more information of the basic electrooxidation processes before defects are added.

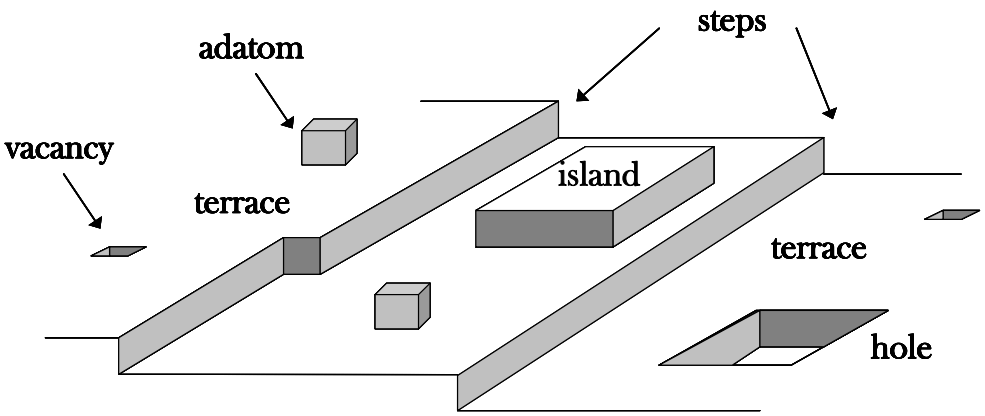

Figure 4. Different surface defects that can be found from a regular electrode surface.

Surfaces containing controlled surface defects are called stepped single crystal surfaces (SSCE) and they are a combination of terraces with the geometry of one basal plane and steps of another. From an applied point of view these crystal surfaces are closer to real bulk catalyst surfaces, but still the surface structure can be carefully controlled. The side of the stereographic triangle (Figure 5) represent the order of different step surfaces for fcc metals and the Miller indices of these surfaces can be determined with the formulas presented in the Table 1; the upper formula gives the Miller index and the lower one tells how the length of the terraces and the steps determines the n.

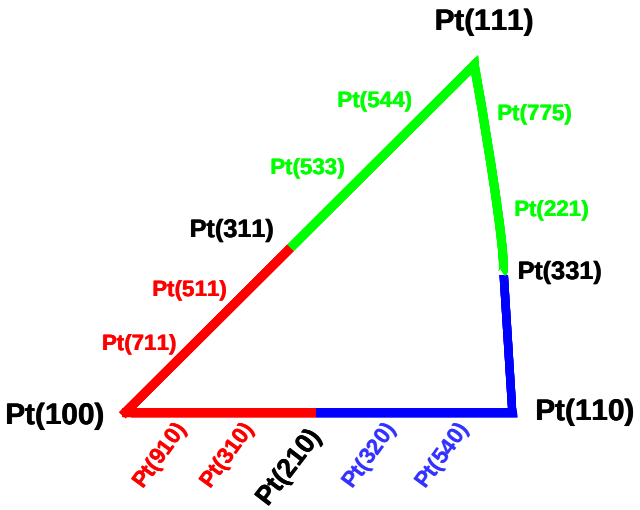

Figure 5. Stereographic triangle.

Table 1. The Miller indices for stepped single crystal surfaces.

	Terraces (100)	Terraces (110)	Terraces (111)
Steps (100)	-	**(2n 2n-2 0)** [n(110)x(100)]	**(n-1 n-1 n+1)** [n(111)x(100)]
Steps (110)	**(n 1 0)** [n(100)x(110)]	-	**(n n n-2)** [(n-1)(111)x(110)]
Steps (111)	**(2n-1 1 1)** [n(100)x(111)]	**(2n-1 2n-1 1)** [n(110)x(111)]	**(n n n-2)** [n(111)x(111)]

In Figure 6 there is an example of how SSCE are formed and named for fcc metals. Pt(511) single crystal surface has 3-atom length (100) terraces (square shaped in Figure 6) and one atom high (111) steps (triangle shaped in Figure 6). From the Table 1, for Pt(511) the formula for the n is

n = number of atoms in the terrace with (100) orientation

From the formulas in Table 1, Pt(511) can only be represented using the (2n-1, 1,1) nomenclature. So, 2n-1=5. Therefore, the width of the terrace with (100) orientation is 3 atoms.

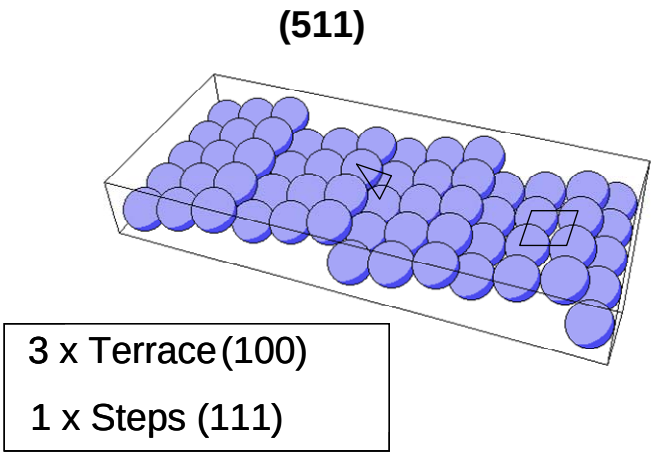

Figure 6. Platinum stepped single crystal surface with (511) orientation.

2.2.1 Preparation of well-ordered SCE surfaces

To be able to study electrooxidation on single crystal electrodes, they must be first carefully prepared. Well-ordered low-index surface must be atomically flat; have only large terraces and should possess as little surface defects as possible. First of all, a small spherical single crystal is prepared by melting a high purity metal wire of the studied metal to form a metal bead [20] this is followed by careful cutting and polishing with a laser beam.

After polishing, the surface is still contaminated by the polishing products and the resin used to fix the electrode during the polishing process. In addition, the spontaneous thermal movement of the surface atoms disorder the surface structure over time and the properties of the SCE are lost. In order to burn away all impurities [21] as well as reorder the surface atoms, the SCE is flame annealed with a Bunsen burner prior to every experiment. At the high temperature, the thermal movement of the metal atoms will progressively order the disordered parts of the surface. Moreover, with high temperature both oxidation and thermodesorption of different impurities occurs resulting in a clean electrode surface.

However, the cleaning process can experience problems when cooling the electrode down especially around 100 ºC, as the ambient impurities of air commence to oxidise on the surface due to the high catalytical activity of clean platinum surface. This can be avoided by cooling the crystal in reducing atmosphere such as in hydrogen stream. After this cooling process, the electrode is dipped into a bubbler with ultrapure water in equilibrium with H_2/Ar flow and so that the surface becomes protected by a water droplet [22].

2.2.2 Electrochemical characterization of SCE surfaces

Due to the fact that annealed single crystal surfaces have to be used in experiments right after the cleaning process, it is not possible to use spectroscopic methods every time to ensure that the annealing has succeeded. Therefore, an electrochemical cyclic voltammetry method can be used to confirm that the reorganisation of the surface has been successful. After annealing, cooling and protecting with a water droplet into the SCE electrode is transferred an electrochemical cell containing an acidic or alkaline electrolyte. Moreover, the potential of the electrode surface must be controlled all the time the electrode is in the electrolyte to avoid unwanted processes such as the electrode oxidation resulting in the loss of the surface orientation.

Cyclic voltammetry profiles of different platinum low-index planes with perchloric and sulphuric acid media are presented in Figure 7. These voltammograms are in accordance with data previously published by other groups; samples cooled down in air and studied in several media [23] and for samples cooled down in H_2 atmosphere and tested in acid [24] or alkaline [25-27] media. However, comparison of the experiments should be done with the same single crystal electrodes because all of them are individually made and have small differences, like variations in peak intensity for instance. Therefore, when using the same electrode, not only the peak positions need to remain the same but also the peak intensity must remain the same as in the previous experiments if a successful annealing process has been performed.

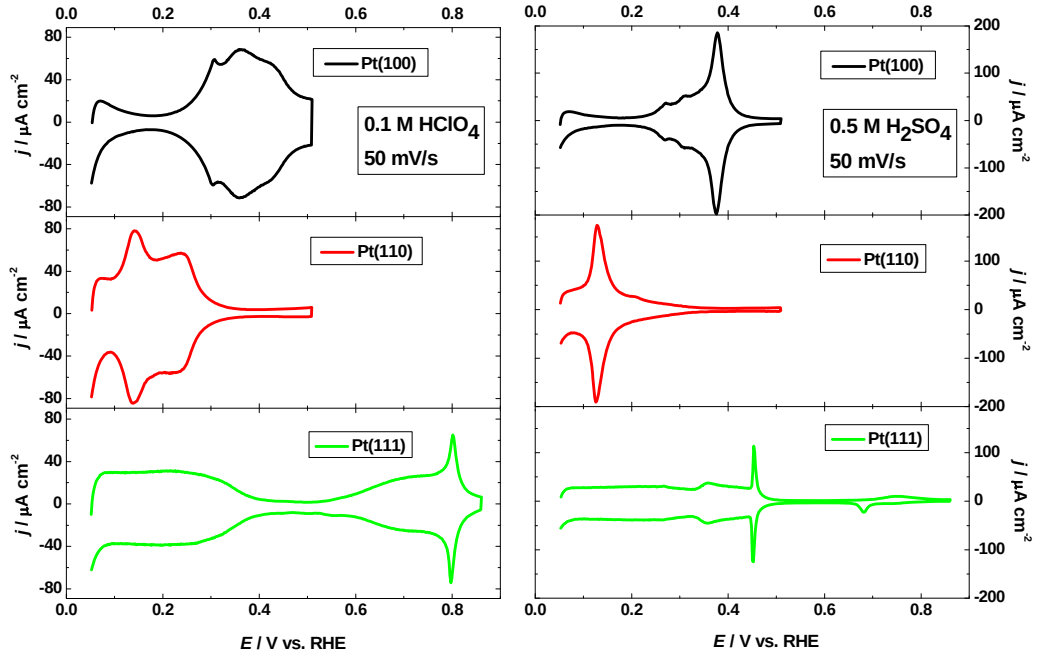

Figure 7. Cyclic voltammetry profiles for platinum low-index planes in 0.1 M $HClO_4$ (left) and 0.5 H_2SO_4 (right), 50 mV s^{-1}, third scans are shown.

As it can be seen from Figure 7, the cyclic voltammograms of Pt(100) and Pt(110) have only been cycled to 0.5 V vs. RHE because the crystal structure will rearrange if higher potentials is applied [28]. Every single crystal surface has its own fingerprint cyclic voltammetry profile that depends on the potential at which the protons and anions of the solutions are adsorbed and desorbed on/from the surface (Figure 7). For Pt(110) proton adsorption starts at very low potentials and in perchloric acid there are two main peaks (0.14 V and 0.25 V vs. RHE) corresponding the Pt(110) terraces and Pt(110) steps. When interpreting the voltammograms it has to be taken into account that no anion adsorption/desorption takes place in $HClO_4$. In the case of H_2SO_4 all the protons/anions in the electrolyte will adsorb/desorb a potential of 0.14 V.

In the case of Pt(100) in H_2SO_4 the main peak related to the presence of Pt(100) terraces is seen around 0.37 V. In $HClO_4$ the main peak is observed at 0.35 V and there is also a small shoulder at 0.30 V. With all the surfaces the peaks appearing in the voltammograms of $HClO_4$ are wider and the intensity is lower than in H_2SO_4.

This confirms that different adsorption mechanisms occur depending on the electrolyte. Finally, for Pt(111) the main adsorption potentials are 0.8 V and 0.45 V for $HClO_4$ and H_2SO_4, respectively.

If any other peaks appear in the voltammogram it is normally due to unsuccessful annealing and cooling process of the SCE or impurities in the electrolyte (contamination). Examples of surface defects formed without flame treatment are outlined by Clavilier [29]. For the H_2SO_4 electrolyte it is known that also the sulphate ion adsorbs on the electrode surface resulting in competitive adsorption [30], which is the main reason for the differences in the cyclic voltammograms presented in Figure 7.

In the case of stepped surfaces, narrowing the terrace width decreases the peaks related to the low-index plane present at the terraces and the contributions due to the step geometry will increase. Therefore, a SSCE with wide terraces will have a cyclic voltammetry profile resembling closely the basal plane of the terrace with only small features of the basal plane of the steps. This can be also noted in Figure 8 where cyclic voltammetry of different SSCEs with Pt(111) terraces and Pt(100) steps are presented.

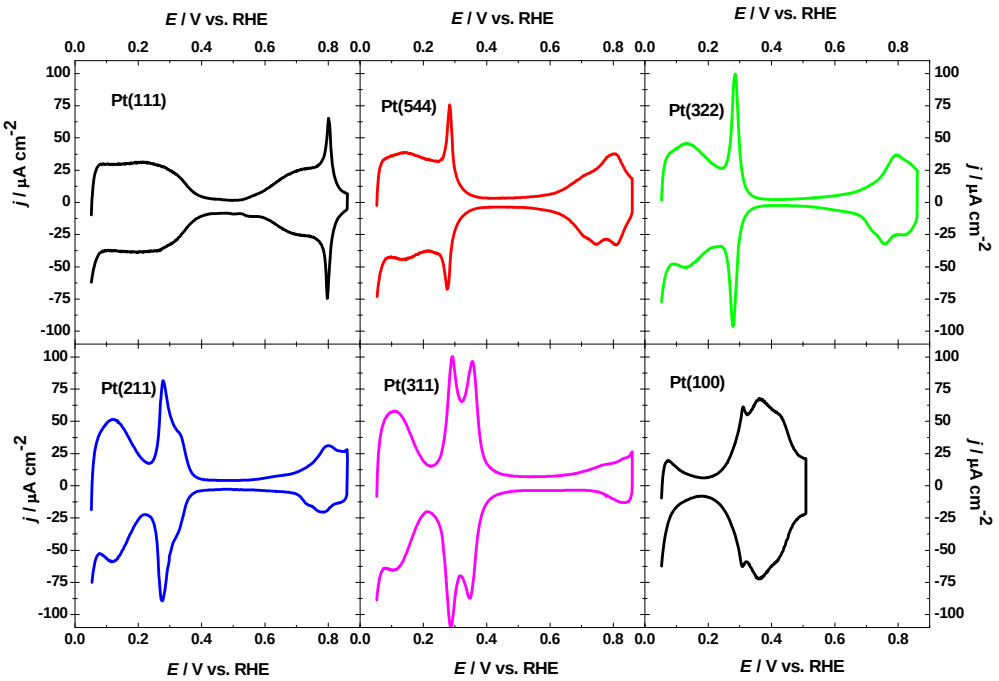

Figure 8. Cyclic voltammetry profiles for Pt(111), Pt(100) and platinum stepped surface with (111) terraces and (100) steps in 0.1 M $HClO_4$. Scan rate 50 mV s^{-1}, third scans are shown.

The (100) step density decreases in the order Pt(311) > Pt(211) > Pt(322) > Pt(544) (Figure 8). Pt(311) is a SSCE having Pt(100) terraces and Pt(111) steps that are both only one atom long (Table 1). Accordingly, there are two main adsorption peaks. At the low potential there is a contribution related to the presence of (100) sites and at higher potentials there is a very low peak indicating small influence of Pt(111) step (Figure 8). For instance, Pt(211) has short Pt(111) terraces which are three atoms wide implying that this (111) contribution must be more noticeable, than in the case of Pt(311). This can be clearly seen from the voltammogram; there is only one main adsorption peak and a little shoulder for the Pt(100) sites, in addition, there is a peak at 0.8 V indicating the stronger influence of Pt(111) terraces. On the voltammogram of Pt(322) the shoulder has vanished and the Pt(100) peak is very sharp. Also the peak at higher potentials continues increasing towards (544) but does not reach the (111) sharpness even with wide terraces.

2.3 Electrocatalysis

Electrocatalysis is officially defined as effect of the electrode materials on the electrode reaction rate meaning that the electrode materials influence on the adsorption and oxidation rate of an organic molecule used as a fuel in a fuel cell. Even if there already exists working consumer fuel cell applications, there still remains a lack of understanding as to the basic reaction of organic molecules on metal surfaces that are currently used as fuel cell catalyst materials.

Electrocatalysis happens in two distinct parts: first, a molecule must be able to adsorb on the surface and form a bond with the electrode (chemical adsorption). Secondly, the molecule must exchange a charge with the metal surface by changing its chemical structure (electrochemical reaction that in the case of oxidable species is called electrooxidation). However, catalyst sites of a metal surface are never free of adsorbed species in an electrolyte solution. For instance when a metal electrode surface is introduced into a water solution the water molecules will instantly cover the surface sites of the electrode (Scheme 1A). If no potential is applied to the electrode, the surface will stay covered by water molecules and the adsorption of other molecules is inhibited.

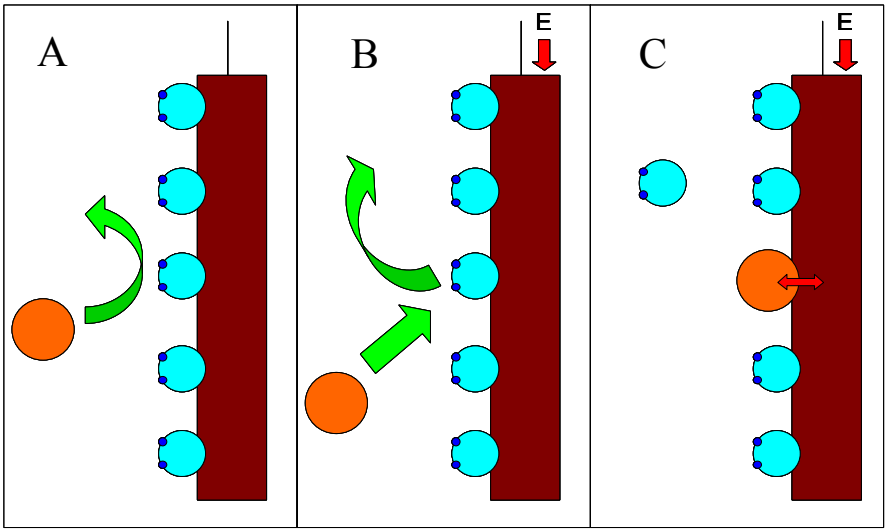

Scheme 1. The adsorption and electrooxidation of an organic molecule on a metal surface with controlled potential.

When more positive potential is applied to the electrode adsorption of the water molecules becomes less favoured and they will diffuse away from the electrode (Scheme 1B). At these free catalyst sites other molecules, e.g. organic compounds, can adsorb, however, the electrochemical reaction cannot occur until the electrochemical potentials of the electrons in both phases are equal. Therefore, even if the potential of the electrode is positive enough to allow the adsorption to occur, it is necessarily proper for the electrochemical reaction. When more positive potentials are applied, the Fermi level shifts to lower energies enabling the movement of the electrons from the highest occupied molecular orbital (HOMO) of the organic molecule to the electrode (Scheme 1C).

2.3.1 Properties of the metal electrode surfaces

To understand the mechanisms occurring on an electrode surface it is first crucial to consider the situation excluding the influence of a liquid electrolyte and concentrate on the electron movement in the solid metal phase. When two metal atoms form a bond two kinds of orbitals are generated: a bonding orbitals and antibonding orbitals. In case more electrons are located on the bonding orbital, the bond is stable.

A metal electrode structure comprises of numerous metal atoms and therefore various bonding and antibonding orbitals are incorporated into continuous energy bands. The band with highest energy is completely occupied by electrons at T = 0 K and is called the valence band (VB) (Figure 9). An electron band with higher energy is called conduction band (CB) and is totally unoccupied at temperature of absolute zero. Metal electrodes are conductors because the valence band and the conduction band are overlapping and electrons can move from one energy level to another by their thermal movement.

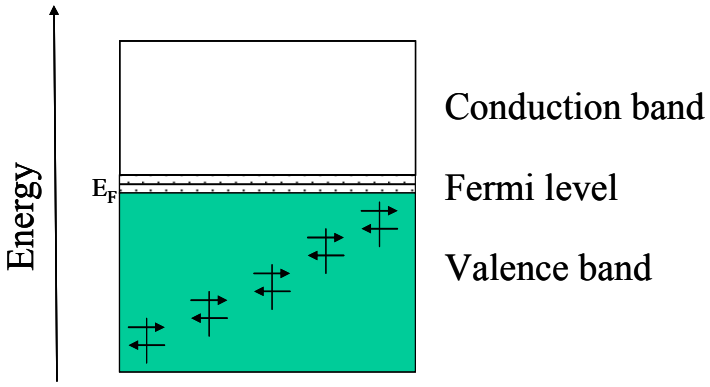

Figure 9. The energy levels of the metal electrode.

At the temperatures of absolute zero the highest energy of the occupied valence band is called Fermi energy and defines the interface between the valence band and the conduction band (Figure 9). Accordingly, the probability to find an electron below the Fermi level is 1 for all energies lower than the Fermi level and similarly zero for the energies higher than the Fermi level. The thermal movement of the electrons

ensures that when temperature is increased they move from the VB to the CB indicating that all cases where the temperature is higher than 0 K the conduction band is never totally unoccupied, moreover, the Fermi-Dirac distribution is not anymore a unit function but instead the Fermi level is defined as the energy level where the probability to find an electron is 0.5.

The Fermi level is used as an energy concept because it can be connected to a reference value providing information about the metal electrode. The uncharged metal electrodes can be classified by their work function Φ which is defined as the electrical work needed to remove an electron from the Fermi level of the metal to a vacuum. For known surface structured single crystal surfaces, the work function can be measured with an accuracy of ± 0.01 eV. The closer the atoms are packed the larger the work function of the metal is; in other words work function will decrease in order (111) > (100) > (110) for single crystal planar planes (Table 2). Because exact values of metal work function can be used in calculations, single crystal electrodes are an important tool for studying electrocatalysis on different metals. However, even if it is difficult to accurately determine work functions for the bulk polycrystalline surfaces, a rough estimation can be obtained if the surface coverage of each crystal surface is known:

$$\Phi_{poly} = \sum_i \Phi_i \theta_i \qquad (1)$$

Table 2. Work function values, in E_h (1 E_h = 27.2114 eV), for low-index platinum single crystal electrodes.

SCE	Experiment	Theory
Pt(100)	0.214 [31]	0.240 [32]
Pt(110)	0.215 [33]	0.227 [32]
Pt(111)	0.223 [31]	0.240 [32]

In addition, the Fermi level of the metal phase can be also defined as the chemical potential of the electrons in the metal phase because by the definition the chemical potential is the same as the work function but has the opposite sign:

$$E_F^M = -\Phi^M = \tilde{\mu}_e^M = \mu_e^M - e\phi^M \tag{2}$$

where μ_e^M is the chemical potential of electron in metal phase and ϕ^M the Galvani potential (inner potential) of the metal electrode which can be defined as the work when a charged particle is brought from the vacuum to the inner part of the metal phase (Figure 10).

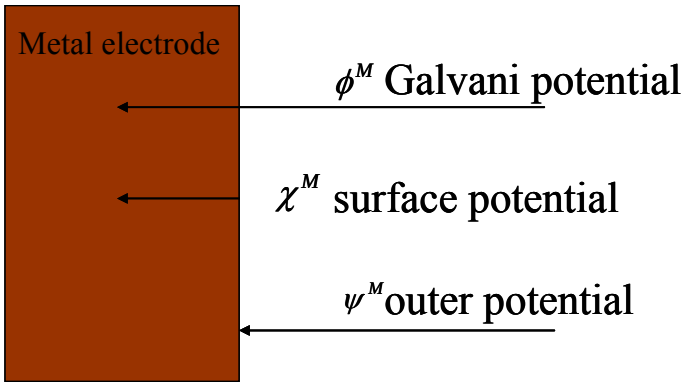

Figure 10. Definitions of Galvani potential, surface potential and outer potential.

For every charged phase, the inner part of the phase is always neutral and the charge is accumulated to the surface of the phase. The Galvani potential can be divided to two different potentials: firstly, the work that is needed to bring the charged electron from the surface of the metal to the neutral inner part of the metal phase is called the surface potential χ^M and even though this potential cannot be measured, the concept is very important when studying surface phenomena such as adsorption or electrooxidation. Secondly, the work that is required to bring the electron from a vacuum to the surface of the metal phase is defined as the outer potential ψ^M and it is a measurable variable. The difference between the outer potentials of the metal

electrodes is called the Volta potential. The Galvani potential can be written with the concepts of the outer potential and the surface potential:

$$\phi^M = \chi^M + \psi^M \tag{3}$$

when the Galvani potential is replaced by the concepts of surface potential and outer potential, the equation (2) becomes:

$$\tilde{\mu}_e^M = \mu_e^M - e\chi^M - e\psi^M \tag{4}$$

For the case of uncharged metal phase the outer potential of the metal is zero and the equation (4) can be defined as:

$$\tilde{\mu}_e^M = \mu_e^M - F\chi^M \tag{5}$$

As already discussed above, the chemical potential of the electron in the metal phase is equal to the work function of the metal but with a reversed sign. When combining equations (2) and (5), the work function of the metal can be written into this new from:

$$\Phi^M = F\chi^M - \mu_e^M \tag{6}$$

This formula shows that the work function of the metal influences the surface potential of the electrode thus affecting surface attractiveness for adsorption of molecules. Therefore, metals with suitable work functions are good catalyst materials for organic molecules.

2.3.2 Properties of the interface between metal and electrolyte

To a fuller understand of electrocatalysis the interaction between the solid electrode surface and liquid electrolyte must also be taken into account. When a metal electrode is introduced into an electrolyte solution, the chemical potentials of the electrons in these two phases are not equal, however, until an exchange of electrons between the phases can occur there has to be equilibrium between the phases and this can be expressed as equal electrochemical potentials of the electrons at both phases:

$$\tilde{\mu}_e^M = \tilde{\mu}_e^L \tag{7}$$

where the superscript letters are M and L indicating metal and liquid phase, respectively. When the chemical potentials in both phases are written as in equation (2) the equation (7) is modified to:

$$\mu_e^M - F\phi^M = \mu_e^L - F\phi^L \tag{8}$$

by rearranging this formula, the interfacial potential difference between the phases can be obtained:

$$\phi^M - \phi^L = \frac{\mu_e^M - \mu_e^L}{F} \tag{9}$$

The electrode potential [34] can be expressed as:

$$E^M = (\phi^M - \phi^L) - \frac{\mu_e^M}{F} + const \tag{11}$$

where the constant term depends on the nature of the reference electrode and is not investigated in this work.

When the system is studied at the microscopic scale, the interfacial potential difference $\phi^M - \phi^L$ describes the electric work generated by the electron crossing the electrode-electrolyte interface and therefore, depends on three different parts [35]:

i) the surface potential of the metal χ^M which is modified by the effect of the solvent ($\sigma\chi^M$).

ii) the potential drop across any preferentially oriented layer of solvent molecules being in contact with the metal ($g = \chi^L + \sigma\chi^L$) where χ^L is the surface potential of the solvent and $\sigma\chi^L$ the same potential taking also into account the effect of the metal.

iii) the potential drop caused by the free charges (σ) moving in the opposite direction than the electrons crossing the interface.

In the particular case of the potential of zero charge (PZC) there is no electron movement across the interface resulting in negligible movement of free charges and therefore excluding iii). Electrode potential in the case of the potential of zero charge can be written as:

$$E^M_{PZC} = (\chi^M + \sigma\chi^M + \sigma\chi^L + \chi^L) - \frac{\mu^M_e}{F} + const \tag{12}$$

The work function of the metal has already been determined earlier (6) and therefore equation can be simplified to:

$$E^M_{PZC} = \frac{\Phi^M}{F} + \Delta\chi + const \tag{13}$$

where $\Delta\chi = \sigma\chi^M + \sigma\chi^L + \chi^L$ is called as the interfacial term and represents the modification occurring on the surface of two phases in contact. Though, the important part of the equation (13) is that the potential of zero charge depends directly on the work function of the metallic electrode. For different electrolytes,

potentials of zero charges can be defined and for aqueous solutions these values for most commonly used fuel cell catalyst metals are presented in the Table 3.

Table 3. Potential of zero charge as V vs. RHE in aqueous solution for most commonly used bulk fuel cell catalyst [35,36*].

Pt	Ru	Sn	Ni	Ag	Au
0.18	-0.25*	-0.39	-0.33	-0.70	0.20

For the sake of simplicity, the potential of zero charge is one of the main reasons why metals behave so differently as catalyst materials. Accordingly, PZC has become an important tool for understanding the electrocatalytical behaviour of organic molecules on metal catalyst materials.

2.3.3 Adsorption

Before the adsorption of organic molecules can be discussed, the adsorption of the solvent molecules is considered as a function of potential. When an uncharged electrode is introduced into as electrolyte solution, the solvent molecules will instantly adsorb onto the surface sites (Scheme 1A). The potential needed to weaken the bond between the catalyst surface and the water molecules is individual for each metal and is related to the potential of the zero charge that has been outlined in the previous section.

In the case of water molecules on platinum surfaces, the water molecules can adsorb onto the metal surface with two different configurations: positively or negatively charged atom towards the metal surface (Figure 11). The direction of the adsorbed water molecules on the metal surface depends on the potential of the electrode. If the potential is more negative than the PZC of the metal, the water molecules will adsorb with the positive atom (hydrogen) towards the metal surface and when the potential reaches the PZC the molecule will turn to another configuration as presented in Figure 11 [37].

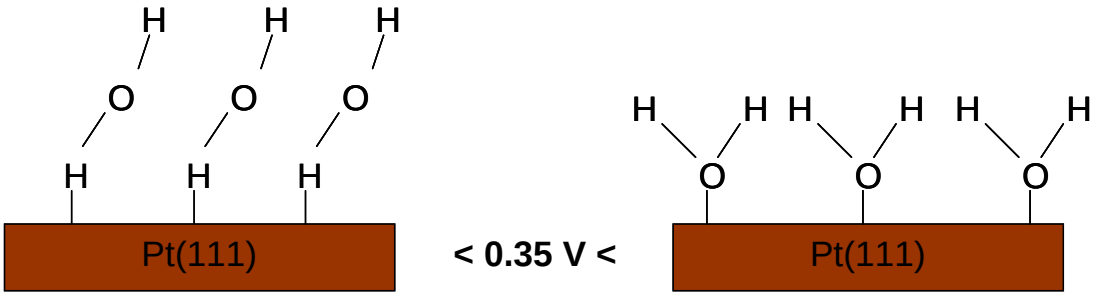

Figure 11. The orientation of the water molecule on the Pt(111) surface depends on the potential of the electrode. The PZC of Pt(111) is 0.35 V [37].

Unfortunately, the phenomenon is more complex because water does not only form one adsorbed monolayer on the metal catalyst surface but an ice-like net structure instead as presented in Figure 12. The first layer of the water molecules are adsorbed onto the metal surface with weak chemical bonds simultaneously influencing the

metal surface by lowering the work function of the metal electrode. Furthermore, the water molecules - due to their strong dipole moment - form hydrogen bonds with the other water molecules and arrange into a more complicated net structure starting from the adsorbed layer and continuing to the direction of the bulk solution.

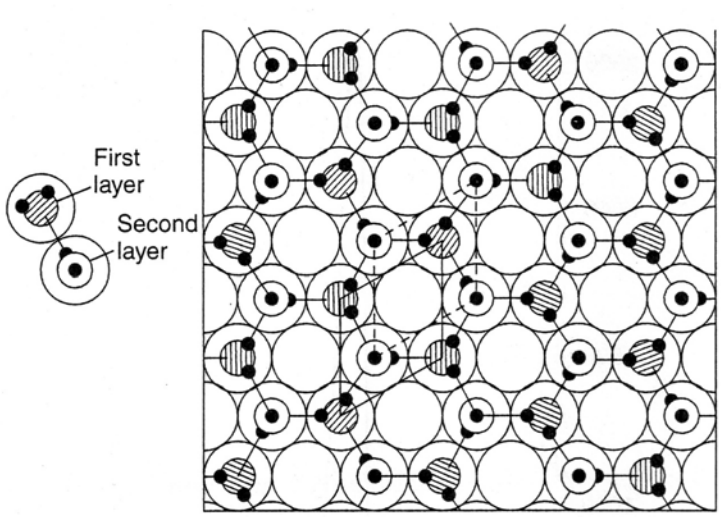

Figure 12. The structure of the water molecule net on the metal surface. Molecules in the first layer are shown with a darker colour and the molecules that are not directly on the surface but have a hydrogen bonds with the adsorbed molecules, with a lighter colour [38]. (Reproduced with permission from Elsevier)

As mentioned earlier, the applied electrode potential has a strong influence on the adsorption phenomena and it also influences the net structure of the solvent or water molecules. The effect of potential on water molecule adsorption on Au(111) surface is presented in details at Figure 13.

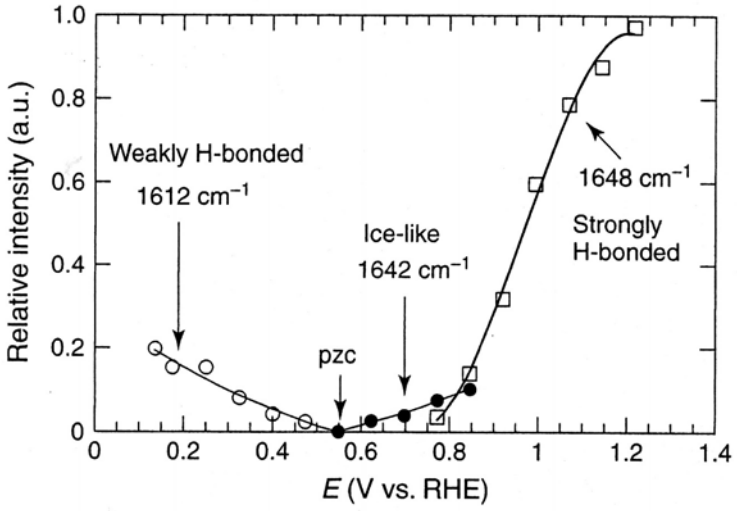

Figure 13. The plot of the integrated intensities of adsorbed water molecules bending infrared modes as a function of potential on Au(111) surface [39].(Reproduced with permission from American Chemical Society)

PZC of the Au(111) surface is around 0.55 V and at more negative potentials, water molecules are adsorbed with positive hydrogen atoms towards the metal. Moreover, at these potentials formation of hydrogen bonds with other water molecules is weak and no real net structure is formed. When the PZC is reached the water molecules rotate the oxygen atom towards the metal surface and start to form ice-like net structures away from the metal surface. Finally, when the potential is increased more the loose bonds between the water molecules begin to form stronger hydrogen bonds in the vicinity of the surface hindering diffusion from the bulk.

2.3.3.1 Factors influencing adsorption

In the case of more complex adsorbates than water molecules, additional factors need to be taken into account when the phenomenon is studied. One factor already outlined previously is the applied potential of the electrode; in particular, different potentials affect the strength of the molecule adsorption on the surface.

Secondly, the metal catalyst surface also influences the adsorption. The structure of the metal's electron shell contributes to the metal work function and the potential of the zero charge, making every metal an unique catalyst material. This can be seen in Figure 14 where cyclic voltammograms of two different bulk electrodes in the same acid electrolyte are presented. Moreover, proton adsorption occurs at different potentials for different metals as shown by two oxidation peaks on platinum and only one on palladium. Each metal surface has its own electrochemical finger print which is often used in electrochemistry to identify catalyst materials.

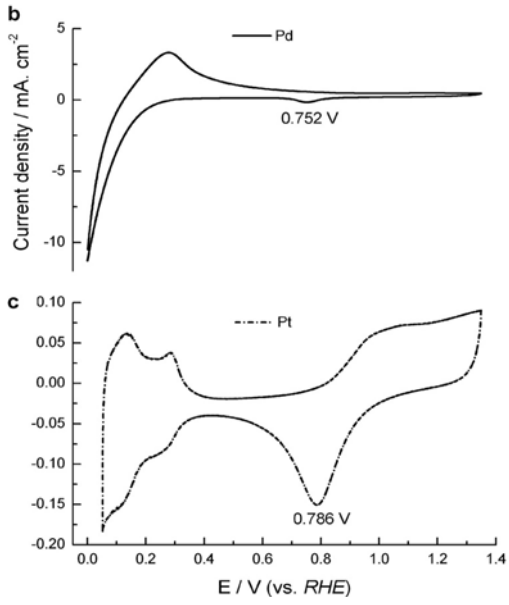

Figure 14. Cyclic voltammetry of polycrystalline palladium (b) and platinum (c) electrodes in 0.1 mol dm^{-3} H_2SO_4 deaerated with N_2, scan rate 20 mV s^{-1} [40]. (Reproduced with permission from Elsevier)

The third factor affecting the adsorption is obviously properties of the adsorbed molecule itself. By adsorbing on the surfaces this component influences on the PZC of the metal further enhancing the adsorption conditions. In addition, the probability for adsorption depends on the shape and the charge of the adsorbate. Figure 15 presents cyclic voltammograms of the same polycrystalline platinum surface in two different solvents H_2SO_4 and $HClO_4$.

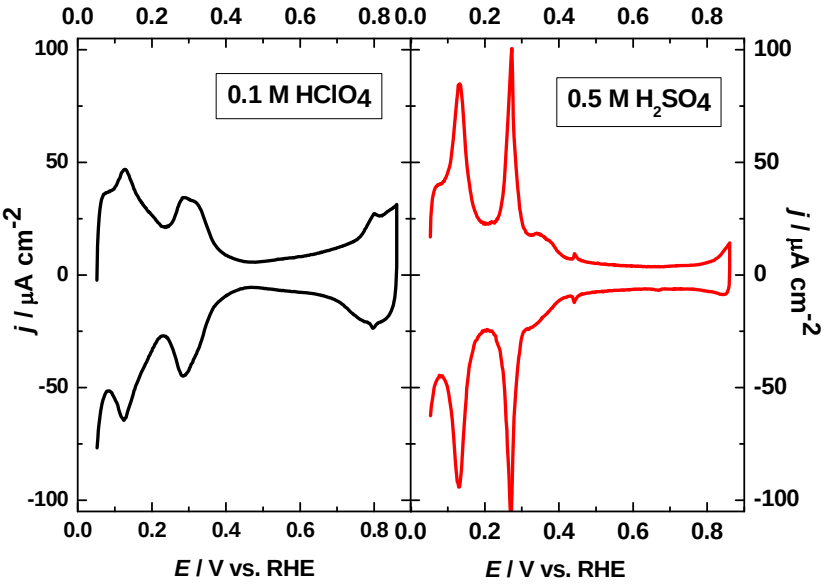

Figure 15. Cyclic voltammetries of 0.1 M $HClO_4$ and 0.5 M H_2SO_4 on polycrystalline platinum surface.

For both electrolytes there are three clearly defined adsorption peaks at 0.14 V, 0.30 V and 0.8 V vs. RHE indicating proton adsorption to Pt(110), Pt(100) and Pt(111) facets, respectively. These same peaks are the ones indicating adsorption on the single crystal terraces presented in Figure 7, however, the intensity and sharpness of these peaks and shoulders depends strongly on the electrolyte.

2.3.3.2 Adsorption of organic molecules

Most organic compounds are hydrophobic and when used as diluted aqueous solutions the organic molecules tend to escape from the bulk solution and move preferentially towards the metal electrode resulting in a different adsorption mechanism than for hydrophilic molecules. This could lead to a conclusion that the adsorption of organic molecules would be facile; however, it is on the contrary. These molecules are normally very large compared to the ions of the electrolyte and especially alcohol molecules are polar having an oxygen atom often found at one end of the molecule. Therefore, the adsorption of such a large polar molecule is only possible when the surface is approached at the right angle.

The adsorption of the organic components on the metal surfaces occurs only with a substitution reaction with some other adsorbate such as a water molecule on the surface

$$R_{sol} + nH_2O_{ad} \leftrightarrow R_{ad} + nH_2O \qquad \text{(iv)}$$

As has been seen in the previous section, the adsorbate which the organic molecule is substituting for can be a water molecule, a proton from the acid media or a hydroxyl ion in the case of alkaline media. As it has been shown in Scheme 1 this substitution reaction is not possible until a certain potential is applied and the water molecules have higher probability to diffuse away from the surface.

The adsorption of the organic molecules depend also on the concentration, implying that the more concentrated the alcohol solution the easier the adsorption. This phenomenon for several metals has been presented already in 1965 by Bockris *et al.* [41] and these plots of surface coverage versus potential are called bell shaped figures, named after the shapes of the curves (Figure 16). From this figure the potential of zero charge is also easily observed because it is the potential where the maximum surface coverage is obtained independent of the solution concentration.

Moreover, this confirms the importance of the electrode potential for the adsorption. Neutral molecules such as many organic ones are very eager to adsorb near the PZC because at this potential overcharge of the metal is at lowest and the organisation of the water molecule net is less thick making it easier for organic molecules to migrate near the electrode surface.

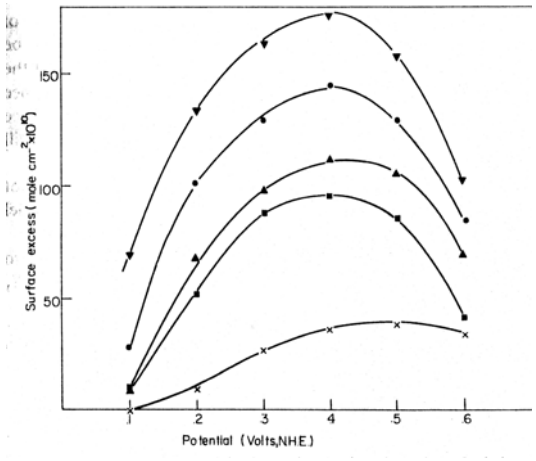

Figure 16. Coverage potential relationship in the adsorption of ethylene on polycrystalline platinum electrode in 0.5 mol dm^{-3} H_2SO_4 with different concentrations: (▼) 17 µmol dm^{-3}, (●) 9.1 µmol dm^{-3}, (▲) 4.6 µmol dm^{-3}, (■) 4.0 µmol dm^{-3}, (x) 2.1 µmol dm^{-3} [41]. (Reproduced with permission from American Chemical Society)

In particular, when other species are present in the solution, the adsorption of organic molecules is always a competitive situation where the charge, size and polarity of the molecule determine which rival is adsorbed although; the approaching angle is also vital.

Harting *et al.* [42] have been studying the probabilities for methanol molecule adsorption on the Pt(111) catalyst surface in gas and water phases with classical molecular dynamic simulations. They have reached conclusion that in aqueous solution the probability for the rupture of O-H bond is very low, denoting that the adsorption energy would be endothermic and need energy from external source (Figure 17 a). Therefore, it is more likely that the methanol molecule will adsorb to the surface forming a chemical bond between aa carbon atom and the surface (Figure 17 c). However, a methanol molecule can adsorb also with the oxygen atom towards

the surface in the case that another water molecules is adsorbed at vicinity of the oxygen atom (Figure 17 b). Hence, the adsorption of the methanol molecule by O-H bond rupture increases if the adsorption of water molecules on catalyst surface is feasible which is the case if a platinum ruthenium alloy is used as catalyst material instead of pure platinum.

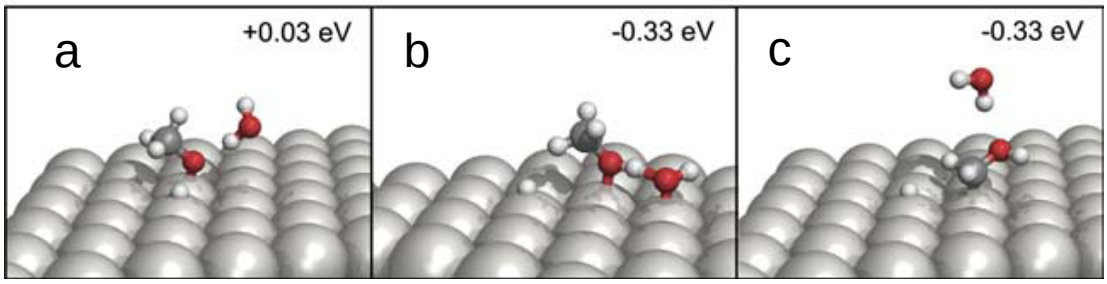

Figure 17. Minimum energy structures of methanol molecule on Pt(111) electrode in aqueous solution with the energy needed for rupture of the bonds [42]. (Reproduced with permission from Elsevier)

From these kinds of simulations we can learn how the molecule will be orientated onto the catalyst material and which would be the most facile reaction path for totally oxidised final product. However, these experiments are made for a catalyst surface without potential control, which plays an important role in the adsorption process and therefore cannot be excluded from the models.

2.3.4 Electrooxidation

As has been seen in Scheme 1C an electrochemical reaction cannot occur until the energy levels of different phases overlap enabling transfer of electrons. Changing the potential of the electrode signify that all energy levels including Fermi level of the electrode are shifted. An organic molecule has energy levels defined by the molecular orbital theory and the first transferable electron is in the HOMO (Figure 18). First the Fermi level of the electrode is at higher energy than the HOMO of the organic molecule and therefore, no electron transfer can occur (Figure 18A).

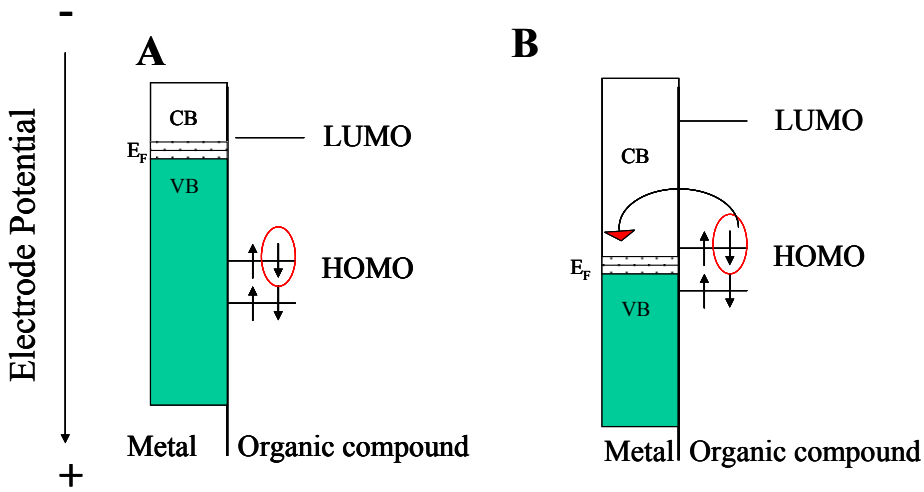

Figure 18. Electrode- organic molecule orbital structure (A) Low potential of the electrode, (B) when the potential is moved to more positive values all the energy levels of the electrode are shifted towards lower energies.

When the electrode potential is moved to more positive values, the Fermi level of the electrode is shifted to lower energy and overlaps with the HOMO of the organic molecules indicating that an electron can be transferred to the metal phase (Figure 18B). Similarly, at the cathode of the fuel cell, the oxygen molecule is reduced meaning that an electron from the valence band of the electrode is moved to the lowest unoccupied molecular orbital (LUMO) of the oxygen molecule.

2.3.5 Electrocatalysis of methanol

To better understand the adsorption and oxidation of organic molecules methanol oxidation is considered in more detail because it is the most studied organic compound in the PEFC. In Scheme 2 electrooxidation of methanol as a function of potential on a bulk platinum electrode sulphuric acid media is presented. Similar potential dependant adsorption and oxidation mechanism occurs with all other organic compounds.

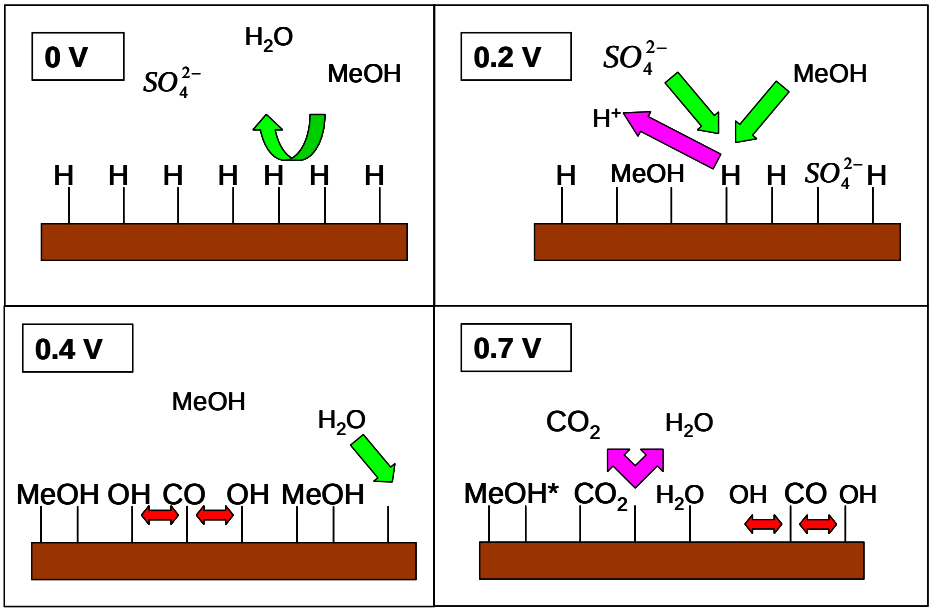

Scheme 2. The potential dependency of methanol adsorption and oxidation on bulk platinum catalyst surface. All potentials are referred to RHE.

When the potential of the platinum electrode is 0 V vs. RHE the surface is covered with protons from the acidic electrolyte inhibiting adsorption of methanol molecules or other ions such as (bi)sulphate (Scheme 2).

The potential of zero charge for a bulk platinum electrode is 0.18 V vs. RHE (Table 3) and, therefore, when a potential of around 0.2 V vs. RHE is applied the adsorption of protons on the surface weaken and other components can substitute them from the

surface sites. In a sulphuric acid solution there will not be only the methanol molecules but also the (bi)sulphate ions that have a tendency to adsorb on platinum surface [30] and, therefore, competition for the active catalyst sites is formed. The surface coverage of sulphate ions depends on the concentration of sulphuric acid, for instance at concentrations of 0.5 mol dm^{-3} every fifth active surface site is blocked by a sulphate ion [43].

Overall, it is well known that when using perchloric acid as an electrolyte instead of sulphuric acid the current density of methanol oxidation is clearly higher due to the lower adsorption strength of the perchlorate ion [44]. This is a very important to keep in mind when studying fuel cell reactions because in spite of the common believe the use of solid Nafion® type of electrolyte membranes including sulphuric acid groups does not signify that the sulphate ions would be present in the liquid phase. Therefore, a clearer image of alcohol oxidation is obtained if the electrochemical reactions are studied at the liquid phase without rival ion adsorption. Nevertheless, PZC is the first potential where methanol adsorption on platinum surface can begin, but no oxidation at this potential for either of the electrolytes is observed (Figure 19).

On platinum surfaces linearly bonded CO has been found already at a potential of 0.35 V vs. RHE implying that dehydrogenation of methanol can proceed already at these potentials [45-47]. However, oxidation to CO_2 has not been detected until the dissociation of water on catalyst surface can occur. On a pure platinum electrode the rupture of water molecule onto electrode surface cannot happen until 0.4 V - 0.45 V vs. RHE [37,48]. In order to decrease the potential where dissociation of a water molecule is possible metal alloys, particularly platinum ruthenium, are used as electrocatalyst materials for alcohol oxidation.

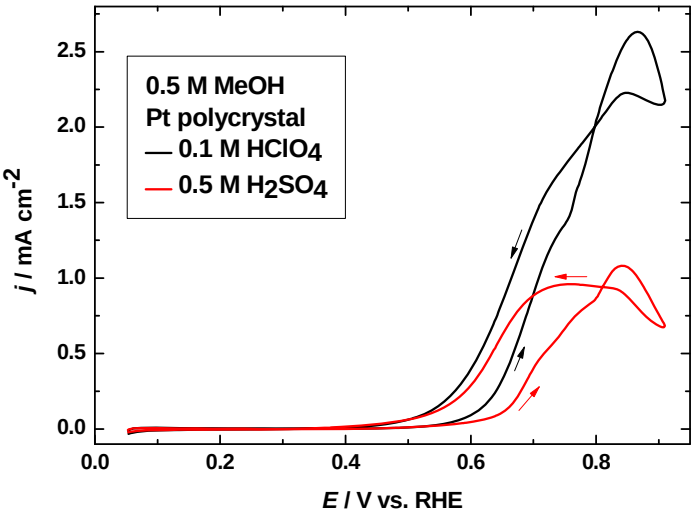

Figure 19. Methanol oxidation on a polycrystalline platinum electrode in two acidic electrolytes. Scan rate 20 mV s^{-1}, third scans shown, the arrows indicate the direction of the anodic and cathodic sweep.

Adsorbed methanol does not reach a high oxidation reaction rate until the electrode potential is increased up to 0.7 V vs. RHE (Scheme 2). At this potential the oxidation of methanol advances and the dissociation of water molecules is continuous. One CO molecule needs two adsorbed OH^- molecules to from one CO_2 and one water molecule. The CO_{ads} forms islands and the adsorbed OH^- are formed around these island formations, therefore, the adsorbates most be mobile and diffuse on the electrode surface until the reaction between these compounds is possible. If the mobility is inhibited CO_{ads} will operate as surface poison until it is further oxidised [49].

Even if the oxidation path of methanol at different potentials is very well known, the exact intermediates of methanol oxidation have been a mystery for decades. However, with new techniques of infrared spectroscopy (IR-spectroscopy) and electrochemical mass spectroscopy such as DEMS (differential electrochemical mass spectroscopy) and OLEMS (on-line electrochemical mass spectroscopy) it is possible to research the adsorbed intermediates on metal surfaces *in situ* as a function of potential. Unfortunately, only intermediates having vibration parallel with the surface

are IR active for IR spectroscopy or volatile products for DEMS and OLEMS can be detected. This is why all the reaction intermediates cannot be totally confirmed, however, an overall mechanism for methanol oxidation can be drawn.

In Scheme 3 the two different paths for electrooxidation of methanol on platinum electrode with all possible intermediates are presented**.** The reaction path through the adsorbed intermediate of CO is called the indirect path (following reactions 1-7) and similarly the path through other soluble intermediates is called the direct reaction path (reactions 8-15). These two reaction path mechanisms for methanol on pure platinum surface have been studied widely [44,50- 53] and recently the mechanism for methanol oxidation has become clear, however, in the case of higher molecular mass organic compounds the complete reaction paths still remain unsolved.

In the indirect mechanism path (Scheme 3, reaction 1-7) a methanol molecule adsorbs on the platinum surface by C-H bond cleavage and forms an adsorbed hydroxymethyl intermediate CH_2OH_{ads}. The dehydrogenation of this molecule starts from the carbon atom and the last proton disengages from the oxygen atom, resulting as adsorbed CO_{ads} intermediate [54- 59]. The oxidation from the first intermediate to CO_{ads} is energetically favoured but a problem is faced with the adsorbed CO that cannot be oxidised further until there is a suitable oxygen donor close to the molecule at 0.55 V vs. RHE potential (Scheme 2). CO is problematic as an intermediate because it is strongly adsorbed to the platinum surface and cannot be removed by any other means than oxidation and therefore becomes a surface poison blocking the surface sites at low potentials.

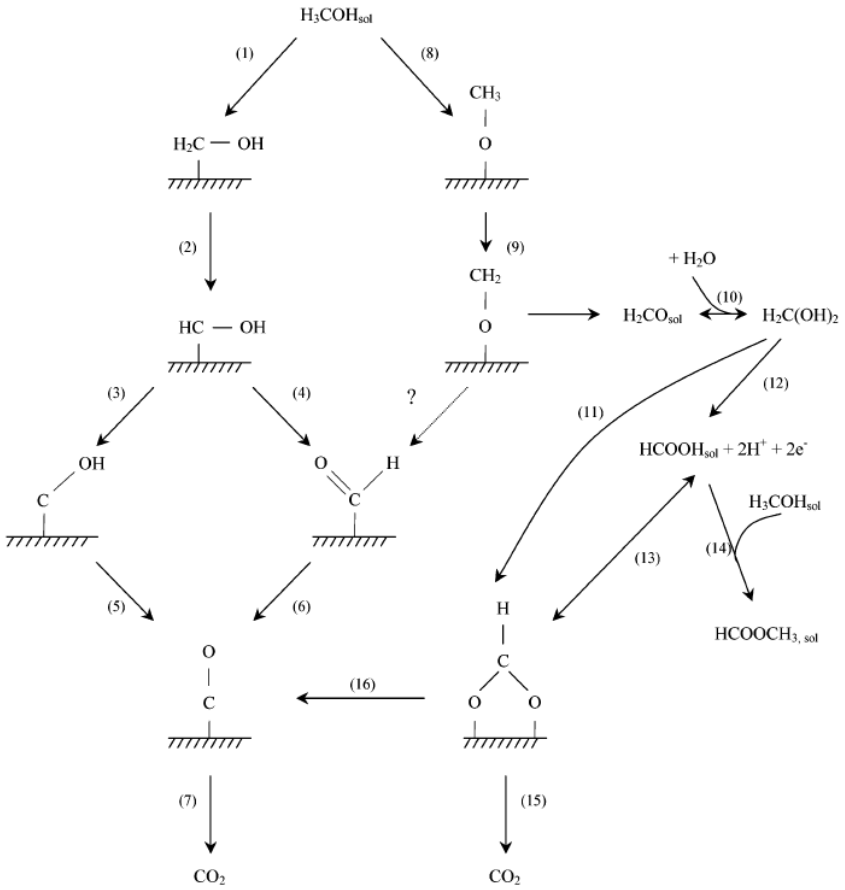

Scheme 3. Methanol oxidation on platinum surfaces with all possible intermediates and products [44]. (Reproduced with permission from American Chemical Society)

In the case of the direct mechanism path (Scheme 3, reaction 8-15) a methanol molecule adsorbs on the surface forming an adsorbed methoxy intermediate CH_3O_{ads} by O-H scission. The oxidation proceeds with one dehydrogenation step form the carbon atom resulting in soluble formaldehyde on the surface. It still remains unclear if this molecule can be further dehydrogenated on the surface or not, however, formaldehyde is a soluble product and if it is disengage from the surface it will be rapidly hydrated to methylene glycol (reaction 10) [60,61].

Finally, an adsorbed IR active formate intermediate has been detected as an oxidation product of methanol, formaldehyde and formic acid [51,62]. This intermediate can then oxidise to CO or CO_2 (reactions 15 and 16, respectively) explaining why CO_{ads} has also been found from the surfaces that favour the direct oxidation path. From this path also methylformate $HCOOCH_{3,sol}$ has been found. This molecule is formed

when formic acid intermediate reacts with methanol molecule in the solution (reaction 14). This molecule is also volatile and has a higher mass to charge ration (m/z = 60) than any other compound from the methanol oxidation intermediates and therefore, it can be used as an indicator molecule of this direct path for DEMS and OLEMS experiments.

These different paths presented in Scheme 3 have been shown to be surface structure sensitive. Already, Cao *et al*. [50] have noticed that at the potential range of 0.2 V – 0.5 V vs. RHE the Pt(111) and Pt(110) planes have a tendency to adsorb a methanol molecule on the surface as a methoxy favouring the scission of the O-H bond. In contrast, Pt(100) favours the indirect path where a carbon atom is forming the bond with the surface.

In the case of sulphuric acid electrolyte, Batista *et al.* [63,64] demonstrated that the (bi)sulphate ion can block the ensemble sites of hydromethoxyl and in this way prevent the methanol adsorption on the platinum surface. However, this ion cannot block those catalyst sites where methanol can absorb through oxygen molecule enabling the selective adsorption. This type of molecules could also be used as blocking agent to prevent unwanted adsorption paths including CO_{ads} as an intermediate; unfortunately, this surface poison is formed as well in the direct path.

Not only other co-adsorbed ions but also the surface defects influence on how the methanol molecule is adsorbed on the surface. With stepped single crystal surfaces several groups have found that even though Pt(110) terraces favour the methanol oxidation as methoxy molecule, the Pt(110) steps would prefer the hydromethoxyl adsorption via the carbon molecule [44,50]. In addition, Pt(111) steps and terraces favour the scission of C-H bond in perchloric acid electrolyte but in sulphuric acid electrolyte both prefer the direct path of the methanol oxidation. Only for Pt(100) both terraces and steps favour adsorption via oxygen molecule in both electrolytes.

3 Experimental

In the experimental part, firstly, two published papers have been reviewed and secondly, experiments for the same mixtures as used in the publication II has been studied further with stepped single crystal electrodes. The results of these further experiments have been enlightening, but have not brought enough new information on the mixture studied and therefore they have been excluded from the publication II. However, they do provide detailed information about the behaviour of the system from a practical point of view and are therefore included into this thesis.

3.1 Summary of publication I

For decades not only methanol but also several other organic molecules have been studied as fuels for polymer electrolyte fuel cell applications [65 -73]. However, in these studies only one or two of the new fuel candidates have been compared and often only with methanol performance in the same cell. A vast problem with fuel cell research is that no standardised experimental conditions are agreed and therefore straight comparison of work from different groups is difficult. The object of this publication has been to test a large amount of different light molecular weight organic molecules and their suitability for PEFC fuels in the same cell with equal conditions.

Hence, different types of organic fuels have been selected with carbon chain lengths C_1-C_3. The interest has been specially addressed to different kinds of compounds having one or more OH-groups located at different carbon atoms. The other group of interest has been organic acids but unfortunately acetic acid performed so poorly in fuel cell tests that the results have not been included in the publication. In addition, the performance of formaldehyde has also been studied to obtain a better understanding of methanol oxidation in the fuel cell. The object has been to explore if there would be a larger organic molecule that could perform in a PEFC as well as

methanol whilst having lower crossover rate through the Nafion® 115 membrane due to the larger size of the molecule.

Prior to the fuel cell experiments, the crossover of the organic components through the Nafion® 115 membrane has been determined. As has been expected already before the experiments, the crossover of methanol has been more rapid when compared to all the other molecules studied. Most of the other molecules are larger making the diffusion through a net structured membrane slower. However, the crossover of formaldehyde and formic acid has also been clearly lower. This can be explained by the charged nature of both molecules in water solution.

Nevertheless, when performances of different fuels have been studied in the PEFC with PtRu as an anode catalyst no other studied component have obtained higher performance than methanol. However, it is well known that PtRu does not catalyse C-C bond rupture at room temperature and therefore the molecules with several carbon atoms could not been oxidised to CO_2 but instead only to some intermediates. Moreover, even if no other single carbon component have performed better than methanol, formaldehyde has produced almost as high current densities as methanol even with fewer protons in a molecule, which can be explained with lower crossover rate of this compound.

Another molecule that has performed in a significantly different way from expected has been isopropanol. Even though the current density obtained has been not as high as with methanol the open circuit potential (OCP) of the cell has been more than 200 mV higher enabling the use of a wider potential range. Moreover, 2-propanol oxidation has been occurring at two different stages on the PtRu catalyst material, unfortunately, these reactions could not been identified with the fuel cell experiments. From an application point of view it would be ideal to combine the high OCP of isopropanol and the good performance of methanol.

3.2 Summary of publication II

As discovered in publication I both methanol and isopropanol have shown interesting behaviour in the PEFC and therefore, a mixture of these two compounds has been studied more closely with poly- and single crystal electrodes. In Figure 20 activity of these individual alcohols and their mixture in two different acidic electrolytes ($HClO_4$ and H_2SO_4) on platinum basal plane single crystal electrodes is presented. It can be seen from Figure 20 that in both media only on Pt(111) the oxidation of the mixture produces higher current density than neither of the individual fuels implying that the surface sites of Pt(111) some way promoted the specific adsorption of at least one component resulting in higher performance.

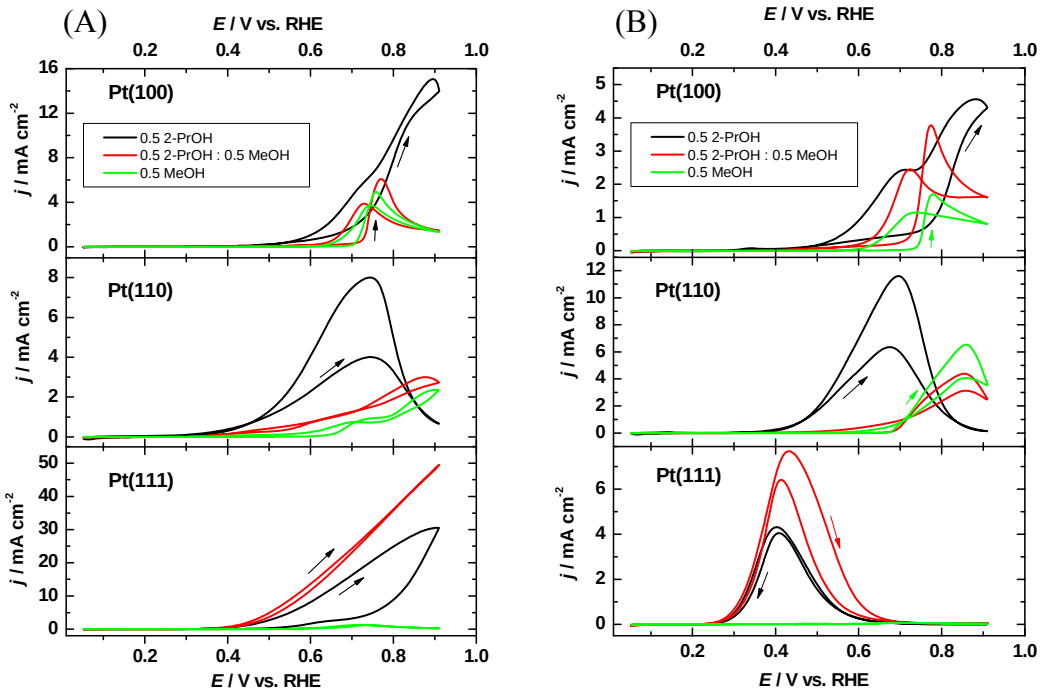

Figure 20. Electrooxidation of 2-propanol, a mixture of methanol and 2-propanol and methanol on planar plane single crystal electrodes in 0.1 mol dm^{-3} $HClO_4$ (A) and 0.5 mol dm^{-3} H_2SO_4 (B). Scan rate 20 mV s^{-1}, third scans are presented.

Due to the shape of the voltammograms (Figure 20) it has been clear that the alcohol mainly oxidised on the Pt(111) electrode is 2-propanol, therefore, the role of the methanol in the mixture has been studied by having the same amount of 2-propanol

and varying the methanol concentration systematically. The highest current density on the cyclic voltammograms has been obtained with a mixture including lowest possible amount of methanol (0.5 mol dm^{-3} 2-propanol and 0.1 mol dm^{-3} methanol). This has been explained with co-adsorption of the alcohol molecules on the Pt(111) surface and the higher the concentration of methanol the lower amount of free catalyst sites remain for 2-propanol oxidation. Therefore, when the current density has been produced mainly by oxidation of 2-propanol the highest value has been obtained with the lowest methanol concentration.

However, in the case of chronoamperometric experiments, the results obtained have been totally contradictory; the highest current density at 0.5 V vs. RHE and after 600 s. has been obtained with the mixture of 0.5 mol dm^{-3} 2-propanol and 1 mol dm^{-3} methanol. This indicates that the oxidation of 2-propanol rapidly leads to the formation of a surface intermediate blocking the catalyst sites and therefore, reducing the current density obtained dramatically. However, addition of methanol to the solution prevents the formation of this particular intermediate without obstructing the whole reaction. The more methanol is introduced into the mixture the less platinum catalyst sites have been blocked by 2-propanol oxidation intermediates.

To obtain information on the blocking intermediate of 2-propanol oxidation, IR spectroscopy has been performed. Unfortunately, no sign of intermediates of 2-propanol oxidation other than soluble acetone has been detected in the case of both 2-propanol and the alcohol mixture. However, in the IR spectra of the alcohol mixture also linear and bridge bonded CO has been detected on the surface implying that also methanol adsorbs and oxidises on Pt(111) and this co-adsorption of both methanol and 2-propanol is changing the path of isopropanol oxidation resulting as intermediates with a lower poisoning effect. Nevertheless, these experiments prove that co-adsorption of alcohols occurs and they can affect positively on the oxidation process of at least one of the components. In the case of practical applications this sort of fuel mixtures would be easily and cheaply available and if they could reduce the catalyst amount needed for specific oxidation they would address a new way for reducing the cost of a fuel cell membrane electrode assembly (MEA).

3.3 Electrooxidation of methanol, 2-propanol and their mixture on platinum stepped single crystal electrodes

Perfectly oriented single crystal electrodes provide interesting information on the adsorption and oxidation processes taking place on the electrode surfaces. However, the study on these specific electrodes is not necessarily related with bulk catalyst materials used in real applications. From a practical point of view stepped single crystal surfaces might enlighten the phenomenon also in the presence of surface defects. Therefore, in addition to the experiments made in the publication II with methanol, 2-propanol and their mixture on the low index SCEs, a study on stepped single crystal electrodes is also presented.

The low-index single crystal electrodes Pt(111), Pt(100) and Pt(110) used in this study have been the same used in the publication II, moreover, the SSCEs are prepared with the same method as the electrodes mentioned in that publication. As shown in Figure 20 Pt(111) showed the most promising results for the alcohol mixture oxidation and, therefore, a set of stepped single crystals have been selected so that the terraces of the surface have always been Pt(111) and the steps of Pt(100) or Pt(110) orientation. The selected electrodes with Pt(100) steps have decreasing step density Pt(544) < Pt(322) < Pt(211) < Pt(311). For the sake of comparison the SSCE having Pt(110) orientation but the same step densities: Pt(554) < Pt(332) < Pt(221) < Pt(331). All the experimental methods are already described in publication II.

Even though methanol oxidation on platinum has been a widely studied topic, a systematic study of single crystal electrodes with different step densities has not been done. In other publications, only a few single crystal surfaces are compared with low-index crystals. The aim of this study is to offer a comparison of alcohol oxidation on the SSCEs with vicinal planes of different length.

3.3.1 Surfaces of Pt[n(111) x (100)]

According to Figure 20 and recent studies of other groups, methanol oxidation is most active on the Pt(110) surface in a H_2SO_4 electrolyte [24,74] and on Pt(100) on $HClO_4$ [44,75]. To exclude the anion adsorption phenomena discussed in the theory part $HClO_4$ has been chosen as the electrolyte. It has been concluded from the publication II that 2-propanol has been the alcohol mainly oxidised in the mixture on Pt(111) surface. Also from previous studies it is known that methanol has a tendency to adsorb on the step sites instead of terrace sites [74]. Therefore a question remained if the oxidation of the alcohol mixture could be further improved at electrodes with Pt(111) terrace sites and different step densities with (100) and (110) geometry. The oxidation of both individual alcohols and their mixture is presented in Figure 21.

From Figure 21A it can be seen that methanol oxidation is more active on the Pt(100) surface than on Pt(111). When monoatomic steps are introduced onto the electrode surface the highest current density is obtained with the electrode having the highest step density Pt(311) in accordance with the results obtained by Tripkovic *et al.* [76]. When decreasing the step density the total current densities decrease, however, as pointed out by Tripkovic who showed that the onset potential of the oxidation shifts to lower potentials indicating higher catalytical activity. As mentioned earlier both Pt(111) terraces and steps favour the scission of C-H bond in perchloric acid electrolyte leading rapidly to formation of CO_{ads}. However, methanol adsorption on Pt(100) surface normally happens though O-H scission and therefore, forming mainly other soluble intermediates [44]. When surface sites of both basal planes are present on the surface the mechanism of methanol oxidation clearly changes, interestingly, obtaining the advantages of both basal planes; high current densities of the Pt(110) plane and low onset potential of Pt(111) plane.

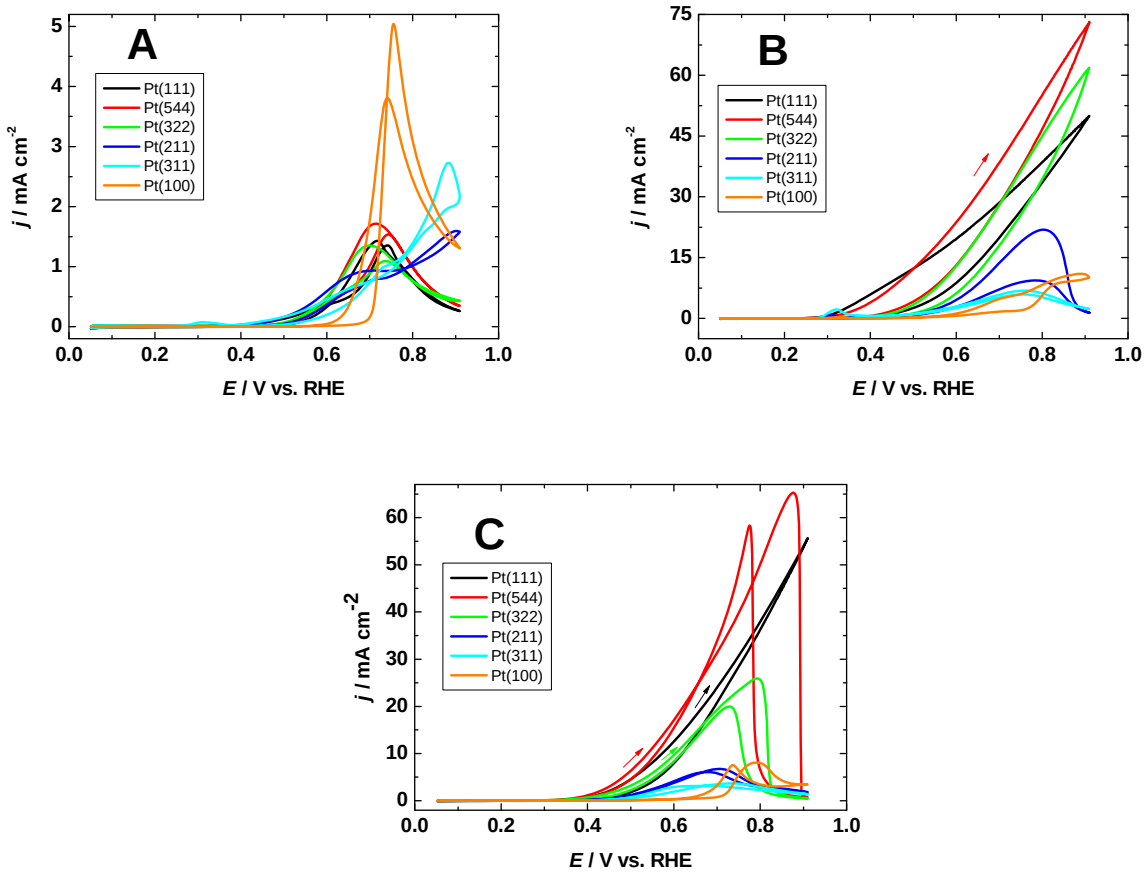

Figure 21. Oxidation of 0.5 mol dm^{-3} methanol (A), 0.5 mol dm^{-3} 2-propanol (B) and their mixture (0.5 mol dm^{-3} 2-propanol and 0.1 mol dm^{-3} methanol) (C) on Pt(111), Pt(100) and on different SSCE planes with Pt(111) terraces and Pt(100) steps. The first scan in 0.1 M $HClO_4$, 20 mV/s.

As mentioned in publication II the Pt(111) surface is blocked rapidly by intermediates of the 2-propanol oxidation even though this is also the most active surface site for the oxidation (Figure 20). Therefore, when Pt(100) steps are introduced to Pt(111) terraces the activity of 2-propanol oxidation is increased and higher current densities are obtained with high step density SSCE than with pure Pt(111) electrode (Figure 21B). This finding is in contrast with the results from Sun *et al.* [77] indicating that the activity of 2-propanol oxidation decreases in order Pt(100) > Pt(610) > Pt(211) > Pt(111) > Pt(110) at the potential region of 0.2 V – 0.8 V vs. RHE. However, the cooling of these crystals has been made in an oxidative atmosphere and the electrolyte used has been H_2SO_4. For 2-propanol oxidation in H_2SO_4 Pt(110) has been shown to be the most active surface (Figure 20) and it is

known that the reduction of the heated electrodes in air instead of hydrogen atmosphere has a crucial effect on the surface organisation of the Pt(110) surface and for this reason it is not possible to compare these results with each other.

The oxidation of the most active alcohol mixture (0.5 mol dm^{-3} 2-propanol and 0.1 mol dm^{-3} methanol) observed in publication II, shows similar voltammograms to 0.5 mol dm^{-3} 2-propanol (Figure 21C). The activity of oxidation increases with the step density, however, in contrast to the results obtained with 2-propanol on Pt(544) not only does the current density increases compared to the Pt(111) but also the onset potential is shifted to clearly more negative potentials. Furthermore, as it can be seen in Figure 21C the shape of the voltammogram of Pt(544) is different from the shape of the Pt(111) diagram indicating that a different oxidation process takes place. Voltammogram of Pt(544) is closer to all other step surfaces and Pt(100) surface implying that the oxidation reaction occurring on Pt(544) would be similar to one with Pt(100) surface, however, substantially more active.

To study closer the shapes of the voltammograms, the oxidation of all these components on individual SSCE is presented in Figure 22 and the corresponding chronoamperometric experiments are presented in Figure 23. It can be clearly seen from the former figure that the oxidation of mixture on Pt(100) occurs with the same mechanism as methanol oxidation indicating that on Pt(100) methanol is the component mainly oxidised. Nevertheless, when the step density is increased the shape of the oxidation curve starts to resemble the shape of the 2-propanol curve, however, the current density and the onset potential are superior compared to 2-propanol.

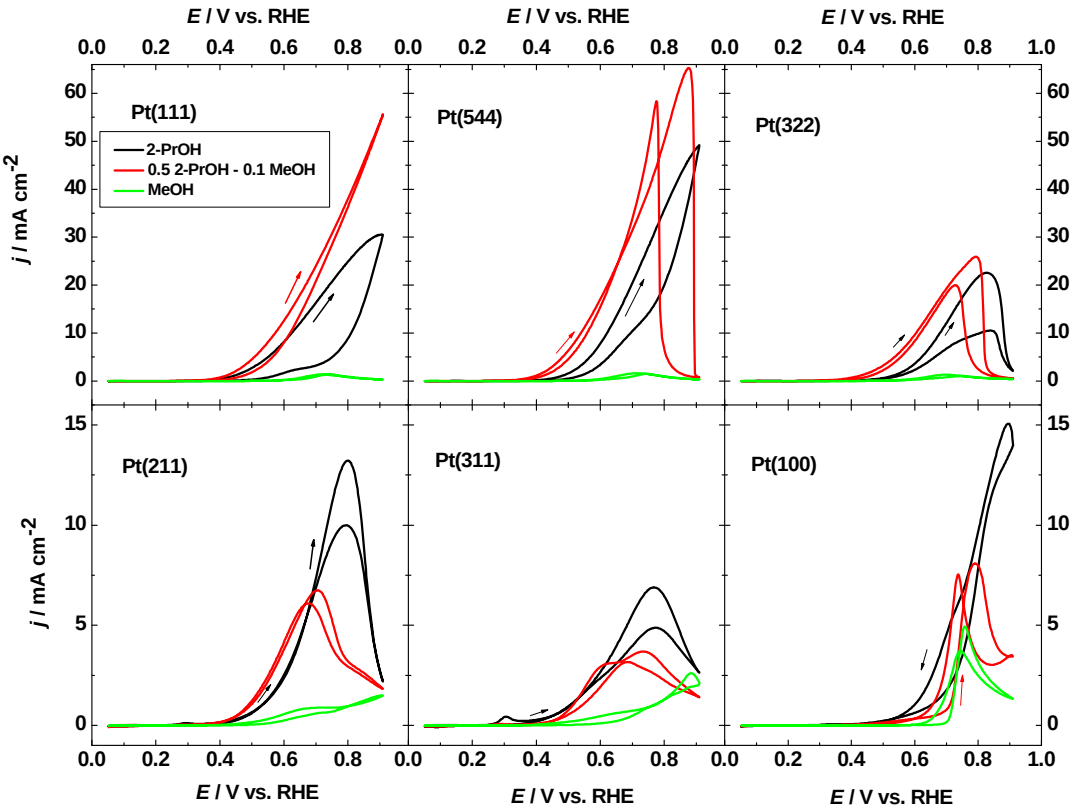

Figure 22. Difference of the oxidation of methanol, 2-propanol and their mixture (0.5 mol / dm^{-3} 2-propanol and 0.1 mol / dm^{-3} methanol) on Pt(111), Pt(100) and on different SSCEs in 0.1 M $HClO_4$, 20 mV/s, third scans are shown.

Moreover, as it can be clearly seen form Figure 23 the current density after 600 s for the pure 2-propanol solution is only slightly increased in the presence of surface defects. In contrast, for the alcohol mixture oxidation the effect of surface defects is enormous and even five times higher current densities after 600 s are obtained with Pt(544) compared to Pt(111). This indicates that the surface poisoning by a specific 2-propanol oxidation intermediate is strongly impeded in the presence of methanol within the solution and (100) steps. However, the oxidation is shifted to some other reaction route producing also high current densities.

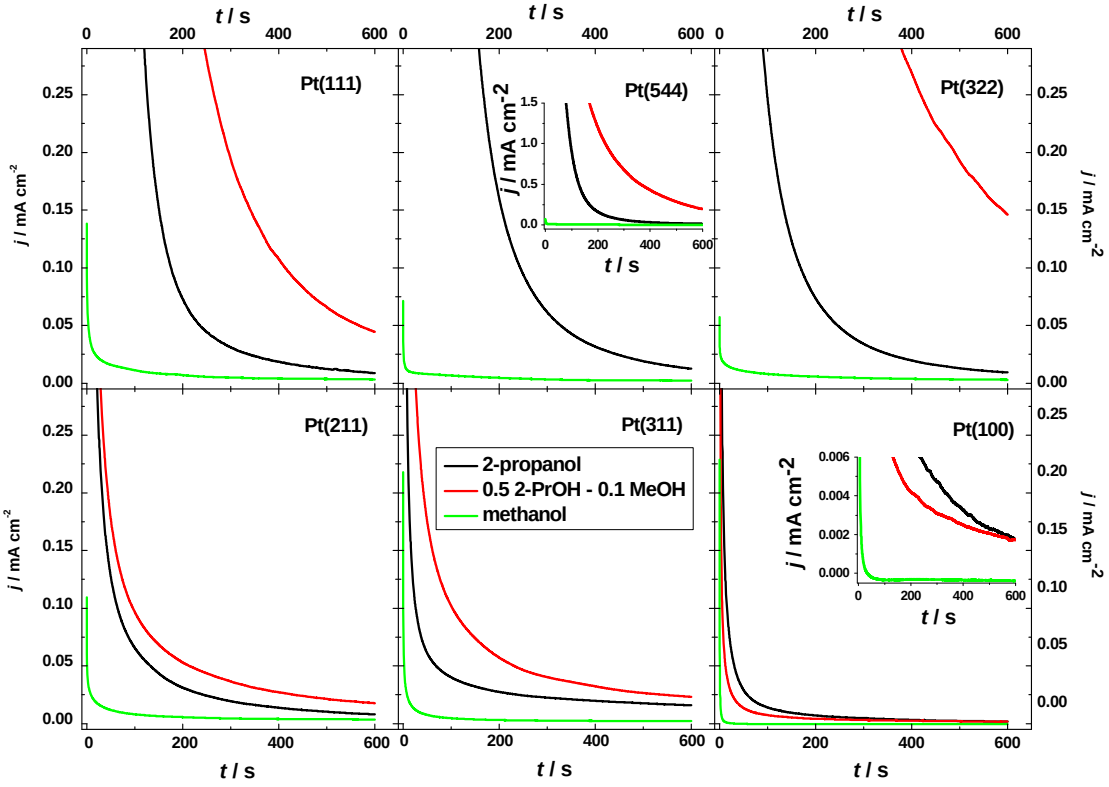

Figure 23. Chronoamperometric results for methanol, 2-propanol and their mixture (0.5 mol / dm^{-3} 2-propanol and 0.1 mol / dm^{-3} methanol) on Pt(111), Pt(100) and on different SSCEs in 0.1 M $HClO_4$, E = 0.5 V vs. RHE, 20 mV/s.

Therefore, not only the presence of methanol in the solution but also the Pt(100) steps are having strong influence on 2-propanol adsorption on Pt(544) surface. As discussed in the theoretical part, the adsorption of organic molecules is very structure sensitive and there is always a competitive situation in the presence of several components. Both factors clearly point to the selective adsorption of 2-propanol. For further research it would be interesting to discover the mechanism of this co-adsorption; however, other types of methods than electrochemical are needed to confirm these results.

3.3.2 Surfaces of Pt[n(111) x (110)]

In the case of pure methanol oxidation the Pt(110) surfaces have shown higher catalytical activity than Pt(100) in both acid electrolytes (Figure 20), therefore, similar experiments for SSCE with Pt(111) terraces and Pt(110) steps have been performed for alcohol mixture oxidation to observe if the presence of these Pt(110) surface sites would increase the activity of methanol oxidation in the alcohol mixture (Figure 24).

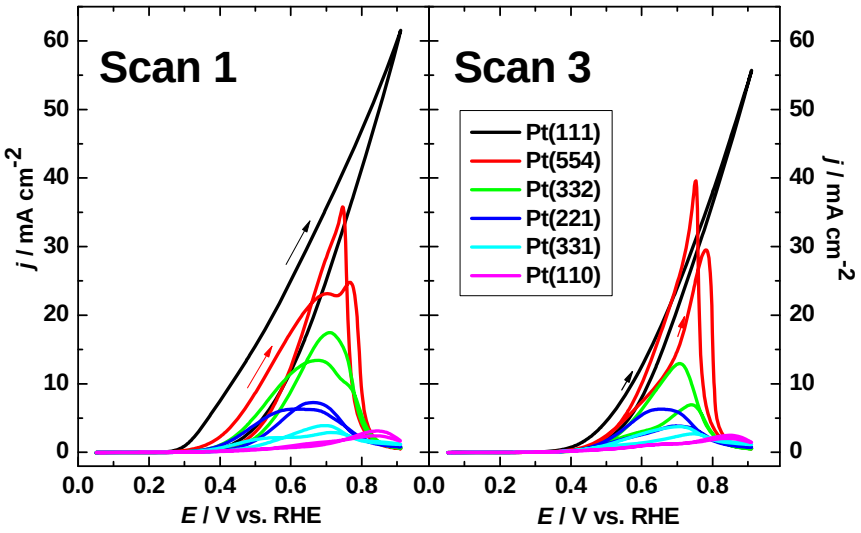

Figure 24. Oxidation of alcohol mixture of 0.5 mol / dm^{-3} 2-propanol and 0.1 mol / dm^{-3} methanol on different SSCE planes with Pt(111) terraces and Pt(110) steps. The first and third scan in 0.1 M $HClO_4$, 20 mV/s.

Housmans *et al.* [74] have studied methanol oxidation with wide terrace of Pt[n(111) x (110)] electrodes in a H_2SO_4 electrolyte and reported that the methanol oxidation increased while the step density is decreased. This is also the case with the alcohol mixture in $HClO_4$ (Figure 24); the wider the terraces became the higher current densities have been obtained, which is probably due to the facile adsorption of organic molecules on the step surfaces. However, no higher current densities nor lower onset potential of alcohol mixture oxidation is observed with the step surfaces compared to the Pt(111) surface indicating that even introducing Pt(110) step sites

for facile methanol oxidation, no improvement is obtained. This confirms that 2-propanol remains the main oxidative component and oxidation of this molecule is far more active on Pt(111) surface.

In $HClO_4$ media fast inactivation of the methanol oxidation for only three cycles has been observed on the Pt(110) electrodes in both H_2SO_4 and $HClO_4$ electrolytes. Therefore, the first and the third scans of the alcohol mixture oxidation are presented in Figure 24 confirming that also with steps surfaces the activation loss occurs rapidly. The onset potential of the oxidation at the first scan on Pt(111) is 0.30 V vs. RHE where already at third scan oxidation does not start until the potential of 0.40 V is reached. Similar results are obtained with the SSCE electrodes indicating that even the presence of step surfaces does not inhibit the surface inactivation.

Nevertheless, the co-adsorption of different organic molecules on stepped single crystal electrodes have shown very interesting results which cannot be explained by parallel oxidation of individual fuels. Use of SSCE has provided vital information about the reactions dependency on surface structure and clarified that the surface defects play an important role in the adsorption and oxidation processes of the alcohols. In future, more exact spectroscopic experiment must be executed to determine the differences in the mechanism when several rival molecules are present in the solution.

4 Conclusions and future plans

In this thesis, the electrocatalysis of small organic components have been discussed in the theory part and investigated at fuel cell and on single crystal electrodes in the experimental part. When planning a catalyst, not only the metal electrode and the organic compound but also other ions and molecules in the liquid phase and the potential applied have an influence on the electrocatalysis of organic molecules on platinum electrodes. With these theories electrocatalytical suitability of an electrode-molecule pair can also be found with theoretical calculations.

In publication I it has been found that methanol of all small organic molecules studies produces highest current densities in a PtRu catalysed anode, however, isopropanol showed higher open circuit potentials than methanol. Nevertheless, when 2-propanol oxidation has been studied on platinum electrodes in an electrochemical cell (publication II), no sign of higher activity has been noticed. From these results it can be concluded that the electrooxidation of 2-propanol is only enhanced on PtRu catalyst. For future work it is needed to study if the oxidation is more active on pure ruthenium catalyst or is the presence of platinum also needed in the alloy. Furthermore, the oxidation products on PtRu might differ from the ones on pure platinum and would be an interesting set of spectroscopic experiments.

In publication II the electrooxidation of alcohol mixtures and pure alcohols (methanol and isopropanol) have been studied on single crystal electrodes. Even though the current densities obtained with the alcohol mixtures did not perform significantly better than the pure alcohols, the interesting result has been that co-adsorption of both individual alcohols of the mixture occurs and not only 2-propanol but also methanol is oxidised according to the IR-experiments. Addition of methanol into 2-propanol solution seems to change the adsorption and oxidation route of isopropanol and leads to different reaction intermediates, unfortunately, these intermediates could not be detected with IR-spectroscopy.

5 References

1. S. K. Kamarudin, F. Achmad and W. R. W Daud, *Int. J. Hydrogen Energy*, **34** (2009) 6902.

2. A. Manthiram, *AMMTIAC Quarterly,* **4** (2009) 69.

3. N. S. Marinkovic, M. B. Vukmirovic and R. R. Adzic, *Modern Asp. Electrochem.*, **42** (2008) 1.

4. B. Viswanathan, *Catal. Today,* **141** (2009) 52.

5. E. Antolini, *J. Power Source,* **170** (2007) 1.

6. F. Vigier, S. Rousseau, C. Coutanceau, J-M. Leger and C. Lamy, *Top. Catal.,* **40** (2006) 111.

7. U. B. Demirci, *J. Power Sources,* **169** (2007) 239.

8. A. Santasalo, *"Use of liquid fuels in a polymer electrolyte fuel cell"*, Master's Thesis, Helsinki University of Technology, Department of Chemical Technology, Espoo 2007, 91 p.

9. V.S. Silva, A. Mendes, L. M. Madeira and S. P. Nunes, *J. Membr. Sci.*, **276** (2006) 126.

10. E. H. Jung, U. H. Jung, T.H Yang, D. H. Peak, D. H. Jung and S.H. Kim, *Int. J. Hydrogen Energy*, **32** (2007) 903.

11. A. A. Kulikovsky, *Advances in Fuel Cells,* **1** (2007) 337.

12. F. Liu, G. Lu and C-Y. Wang, *J. Electrochem. Soc.,* **153** (2006) A543.

13. K-J. Jeong, C. M. Miesse, J-H. Choi, J. Lee, J. Han, S. P. Yoon, S. W. Nam, T-H. Lim and T. G. Lee, *J. Power Sources,* **168** (2007) 119.

14. W. Wang, J-M. Hu, and I-M. Hsing, *J. Electroanal. Chem.,* **562** (2004) 73.

15. Y-W. Rhee, S. Y. Ha and R. I. Masel, *J. Power Sources*, **117** (2003) 35.

16. J. Ling and O. Savadogo, *Proceedings – Electrochem. Soc.* **11** (2006) 320.

17. S. Song and P. Tsiakaras, *Appl. Catal. B: Environmental,* **63** (2006) 187.

18. N. Kariya, A. Fukuokaa and M. Ichikawa, *Phys. Chem. Chem. Phys.*, **8** (2006) 1724.

19. A. López Cudero, *Estudio de la electrooxidación de CO en electrodos de Pt (poly) y Pt (hkl): El origen del pre-pico*, Universidad Autonoma de Madrid, Departamento de Química Física Aplicada, Madrid 2005, 177 p.

20. J. Clavilier, D. Armand, SG Sun and M. Petit, *J. Electroanal. Chem.,* **205** (1986) 276.

21. J. Clavilier, K. El Achi, M Petit, A. Rodes and MA Zamakhchari, *J. Electroanal Chem.,* **295** (1990) 333.

22. A. Rodes, M. A. Zamakhchari, K. El Achi and J. Clavilier, *J. Electroanal. Chem.* **305** (1991) 115.

23. M.-C. Morin, C. Lamy, J.-L. Vasquez, A. Aldaz and J.-M. Léger, *J. Electroanal. Chem.,* **283** (1990) 287.

24. E. Herrero, K. Franaszczuk and A. Wieckowski, *J. Phys. Chem.,* **98** (1994) 5074.

25. A. V. Tripkovic, K. Dj. Popovic, J.D. Momcilovic and D. M. Drazic, *J. Electroanal. Chem.* **448** (1998) 173.

26. A. V. Tripkovic, K. D. Popovic, J. D. Momcilovic and D. M. Drazic, *Electrochim. Acta*, **44** (1998) 1135.

27. A. V. Tripkovic, K. Dj. Popovic, J. D. Momcilovic and D. M. Drazic, *J. Electroanal. Chem.,* **418** (1996) 9.

28. R. Gómez and J. Clavilier, *J. Electroanal. Chem.,* **254** (1993) 189.

29. J. Clavilier, "*Flame-Annealing and Cleaning Technique",* Interfacial Electrochemistry, A. Wieckowski (Ed.), Marcel Dekker, New York 1999, p. 231-248.

30. S. C. S. Lai, N. P Lebedeva, T. H. M Housmans and M. T. M. Koper, *Top Catal.,* **46** (2007) 320.

31. M. Salmerón, S. Ferrer, M. jazzar and G. A. Somorjai, *Phys. Ref. B* **28** (1983) 6758.

32. S. Baud, C. Ramseyer, G. Bihlmayer, S. Blügel, C. Barreteau, M. C. Desjonquéres, D. Spanjaard and N. Bernstein, *Phys. Rev. B,* **70** (2004) 235423.

33. D. R. Lide (Ed.), CRC Handbook of Chemistry and Physics, 80th ed., CRC Press, Boca Raton 1999/2000.

34. S. Trasatti, *Electrochim. Acta*, **35** (1990) 269.

35. S. Trasatti, *"Electrode potential and double layer"*, Handbook of fuel cells Vol 2, W. Vielstich (Ed.), John Wiley & Sons Ltd, Chichester 2003.

36. C. Barbero, J.J. Silver and L. Sereno, *J. Electroanal. Chem.* **291** (1990) 81.

37. T. Iwasita and X. Xia, *J. Electroanal. Chem.,* **411** (1996) 95.

38. P. A. Thiel and T. E. Madey, *Surf. Sci. Rep.,* **7** (1987) 211.

39. K. Ataka, T. Yotsyanagi and M. Osawa, *J. Phys. Chem.,* **100** (1996) 10664.

40. J. Zhang, M. Huang, H. Ma, F. Tian, W. Pan and S. Chen, *Electrochem. Commun.,* **9** (2007) 1298.

41. E. Gileadi, B. T. Rubin and J. O'M. Bockris, *J. Phys. Chem.,* **69** (1965) 3335.

42. C. Harting and E. Spohr, *Chemical Physics,* **319** (2005) 185.

43. T. Frenlink, W. Visscher and J. A. R. van Veen, *Langmuir,* **12** (1996) 3702.

44. T. H. M. Housmans, A. H. Wonders and M. T. M. Koper, *J. Phys. Chem. B,* **110** (2006) 10021.

45. J. R. C. Salgado, J. J. Quintana, L. Calvillo, M. J. Lázaro, P. L. Cabot, I. Esparbé and E. Pastor, *Phys. Chem. Chem. Phys.,* **10** (2008) 6796.

46. T. Iwasita and V. F. C. Nart, *Prog. Surf. Sci.,* **55** (1997) 271.

47. T. Iwasita and F. C. Nart, *"Advances in Electrochemical Science and Engineering"*, Vol. 4, H. Gerischer and C. W. Tobias (Eds.), Wiley, New York 1995, p. 123.

48. T. Iwasita, X. H. Xia, H. D. Liess and W. Vielstich, *J. Phys. Chem. B,* **101** (1997) 7542.

49. M. T. M. Koper, A. P. J. Jansen, R. A. van Santen, J. J. Lukkien and P. A. J. Hibers, *J. Chem. Phys.,* **109** (1998) 6051.

50. D. Cao, G. Q. Lu, A. Wieckowski, S. A. Wasileski and M. Neurock, *J. Phys. Chem. B* **109** (2005) 11 622.

51. T. Jarvi and E. M. Stuve, *"Electrocatalysis"*, J. Lipkowski and P. N. Ross (Eds), Wiley-VCN, New York, 1998.

52. S. Sriramulu, T. Jarvi and E. M. Stuve, *J. Electroanal. Chem.,* **467** (1999) 132.

53. E. Herrero, W. Chrzanowski and A. Wieckowski, *J. Phys. Chem.,* **99** (1995) 10 423.

54. R. Parsons and T. J. VanderNoot, *J. Electroanal. Chem.* **257** (1988) 9.

55. J. Willsau, O. Wolter and J. Heitbaum, *J. Electroanal. Chem. Interfacial Electrochem.,* **185** (1985) 163.

56. T. D. Jarvi, S. Sriramulu and E. M. Stuve, *J. Phys. Chem. B,* **101** (1997) 3649.

57. A. Hamnett, *Compr. Chem. Kinet.,* **37** (1999) 635.

58. N. M. Markovic and P. N. Ross, *Surf. Sci. Rep.,* **45** (2002) 117.

59. T. Iwasita, *Electrochim. Acta,* **47** (2002) 3663.

60. J. P. Guthrie, *Can. J. Chem.,* **53** (1975) 898.

61. J. G. M. Winkelman, O. K. Voorwinde, M. Ottens, A. A. C. M. Beenackers and L. P. B. Janssen, *Chem. Eng. Sci.,* **57** (2002) 4067.

62. A. Miki, S. Ye, T. Senzaki and M. Osawa, *J. Electroanal. Chem.,* **563** (2004) 23.

63. E. A. Batista, G. R. P. Malpass, A. J. Motheo and T. Iwasita, *Electrochem. Commun.,* **5** (2003) 843.

64. E. A. Batista, G. R. P. Malpass, A. J. Motheo and T. Iwasita, *J. Electroanal. Chem.,* **571** (2004) 273.

65. K. Taneda and Y. Yamazaki, *Electrochim. Acta,* **52** (2006) 1627.

66. S. Song and P. Tsiakaras, *Appl. Catal. B: Environ.,* **63** (2006) 187.

67. J. Wang, S. Wasmus and R. F. Savinell, *J. Electrochem. Soc.,* **142** (1995) 4218.

68. C. Lamy, A. Lima, V. LeRhun, F. Delime, C. Coutanceau and J-M. Leger, *J. Power Sources,* **105** (2002) 283.

69. Z. Qi and A. Kaufman, *J. Power Sources,* **112** (2002) 121.

70. D. Cao and S. H. Bergens, *J. Power Sources*, **124** (2003) 12.

71. V. Livshits and E. Peled, *J. Power Sources,* **161** (2006) 1187.

72. Y. Zhu, S. Y. Ha and R. I. Masel, *J. Power Sources,* **130** (2004) 8.

73. S. Ueda, M. Eguchi, K. Uno, Y. Tsutsumi and N. Ogawa, *Solid State Ion.* **117** (2006) 2175.

74. T. H. M. Housmans and M. T. M. Koper, *J. Phys. Chem. B,* **107** (2003) 8557.

75. X. H. Xia, T. Iwasita, F. Ge and W. Vielstich, *Electrochim. Acta,* **41** (1996) 711.

76. A. V. Tripkovic and K. Dj. Popkovic, *Electrochim. Acta,* **41** (1996) 2385.

77. S. –G. Sun and Y. Lin, *Electrochim. Acta,* **44** (1998) 1153.

Publication I

A. Santasalo, T. Kallio and K. Kontturi, Performance of Liquid Fuels in a Platinum-Ruthenium-Catalysed Polymer Electrolyte Fuel Cell, *Platinum Metals Rev.*, **53** (2) (2009) 58-66.

DOI: 10.1595/147106709X416040

Performance of Liquid Fuels in a Platinum-Ruthenium-Catalysed Polymer Electrolyte Fuel Cell

HIGHER MOLECULAR WEIGHT COMPOUNDS AS FUELS FOR A PEFC

By Annukka Santasalo, Tanja Kallio* and Kyösti Kontturi

Research Group of Physical Chemistry, Department of Chemistry, Helsinki University of Technology, PO Box 6100, FI-02015 TKK, Finland; *E-mail: tanja.kallio@tkk.fi

Crossover and performance of different 1 M low molecular weight organic fuels with a platinum-ruthenium (60:40) catalyst in a unit fuel cell were studied at different temperatures. Large, negatively charged or complicated molecules were found to have the lowest crossover rates through the Nafion® 115 membrane, and methanol had the highest permeability at all temperatures. The smallest molecule, formic acid, dissociates in water, resulting in a less severe crossover problem. In a PtRu-catalysed fuel cell, compounds with only one carbon atom exhibit superior performance compared to molecules having a carbon chain; with methanol and formaldehyde producing power densities up to five times higher than those achieved with molecules having a longer carbon chain. However, it should be noted that PtRu does not catalyse the breaking of the C–C bond; therefore, larger molecules can only be oxidised to derivative products. However, larger organic molecules show a lower rate of crossover through the Nafion® membrane, which enables more concentrated solutions to be used to decrease the volume of the fuel. With the addition of a third metal to the PtRu-based catalyst, higher molecular weight molecules are good candidates for energy sources in a fuel cell.

Introduction

Polymer electrolyte fuel cells (PEFCs) are promising electrochemical power generators, especially for transport and portable applications. Pure hydrogen or a hydrogen-rich gas is often used as the fuel in order to obtain high electrical efficiency at ambient temperature. However, storage, transport and refuelling are more problematic for a gaseous fuel than for a liquid. If fuel reforming is used, this renders the system even more complex. Therefore, research has recently been focused on the use of hydrogen carriers such as aqueous solutions of small organic solvents, which offer easier storage, improved safety and high energy densities (between 1750 and 7080 Wh l^{-1} depending on the component) compared to hydrogen gas (180 Wh l^{-1} at 1000 psi and 25°C) (1).

At present, of the liquid systems, only the direct methanol fuel cell (DMFC) has been widely studied (2–7). Disadvantages of methanol include its toxicity, high flammability and tendency to permeate through the widely-used Nafion® membrane – a phenomenon known as 'crossover'. However, several other organic fuels that possess higher boiling points and lower crossover rates than methanol have shown promising preliminary results (8–13).

At low temperatures, Pt nanoparticles are widely used as catalyst materials for organic fuels in the fuel cell anode. However, pure Pt catalysts only extract the hydrogen atoms from the carbon chain. They cannot cleave the carbon–carbon bond or oxidise the carbon–oxygen bond at the range of potentials normally encountered in a liquid-fuelled fuel cell. Therefore, Ru is added to offer a possible catalyst site for water to decompose to hydrogen and hydroxyl (OH) groups at lower potentials (6, 14), enabling the organic fuel to be oxidised completely to carbon dioxide.

The aim of the present study is to compare the behaviour of different liquid fuels for a PtRu (60:40) catalysed PEFC. The chosen fuels are all short-chained carbon compounds. The crossover rates of the fuels through the commonly used Nafion® 115 (N-115) membrane were explored, followed by their performance in a PEFC with a Nafion® 115 membrane as the electrolyte.

Measurement Conditions and MEA Preparation

The solutions used were prepared from methanol (Fluka, p.a.), formaldehyde (Merck, p.a.), formic acid (Riedel-de Haën, p.a.), ethanol (Altia, Grade A), acetaldehyde (Merck, p.a.), 1-propanol (Merck, extra pure), 2-propanol (Merck, p.a.), ethylene glycol (Aldrich, 99.89%), glycerol (Fluka, p.a.) and ultrapure water (Milli-Q® (MQ), Millipore, 18.2 MΩ cm).

To observe the crossover phenomenon with as few variables as possible, the crossover experiments were performed in a two-compartment diffusion cell. The Nafion® 115 membrane was pressed between the two compartments, then one side of the cell was filled with a 1 M solution of the fuel and the other with deionised water. 30 µl samples were taken every 10 min for 60 min and were analysed with a gas chromatograph (HP 6890 GC) using an HP Innowax column at a heating rate of 5°C min^{-1}. An internal standard of 10 µl of 1,4-dioxane was added to each sample.

The membrane electrode assembly (MEA) was made by spraying a mixture of 2 mg cm^{-2} catalyst powder (anode: Pt:Ru (60:40) on Vulcan XC-72 carbon (40%); cathode: Pt on Vulcan (40%)), Nafion® liquid ionomer (5 wt.%, Aldrich) and 2-propanol on the surface of the Nafion® 115 membrane. After spraying both sides, the MEA was hot pressed at a temperature of 130°C and a pressure of 50 kN for 2 min.

All measurements were performed in a fuel cell with an active area of 7.26 cm^2. The 1 M liquid fuels were fed to the anode compartment at room temperature at a rate of 1.5 ml min^{-1}, and the gas (Instrument Oxygen 5.0, AGA) to the cathode at 270 ml min^{-1}. The cell was allowed to stabilise overnight (liquid fuel 0.2 ml min^{-1} and oxygen 30 ml min^{-1} at 30°C) before the measurements were taken. Prior to each fuel change, the cell was rinsed with MQ-water for 2 h. All measurements were made at temperatures of 30°C, 50°C and 70°C.

Fuel Cell Efficiency and Crossover Rates

The results obtained show that fuel cell efficiency, defined as current density at a particular cell voltage, is temperature-related. Fuel cell efficiency increases with increasing temperature for all the fuels tested, as shown in Figure 1 for a DMFC. However, the crossover rate also increases with temperature, as shown in Figure 2. Figures 1 and 2 present the behaviour of methanol; the results for the other fuels are similar.

Increasing the temperature of the DMFC from 30°C to 50°C increases the fuel cell efficiency by

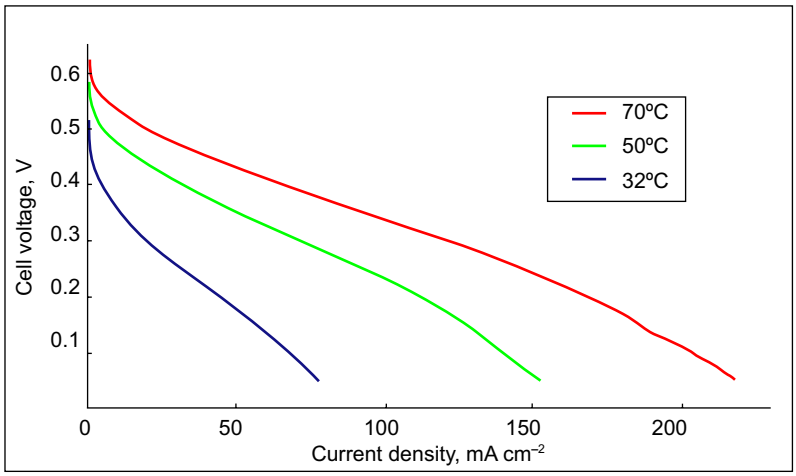

Fig. 1 Effect of temperature on the efficiency of the direct methanol fuel cell (DMFC)

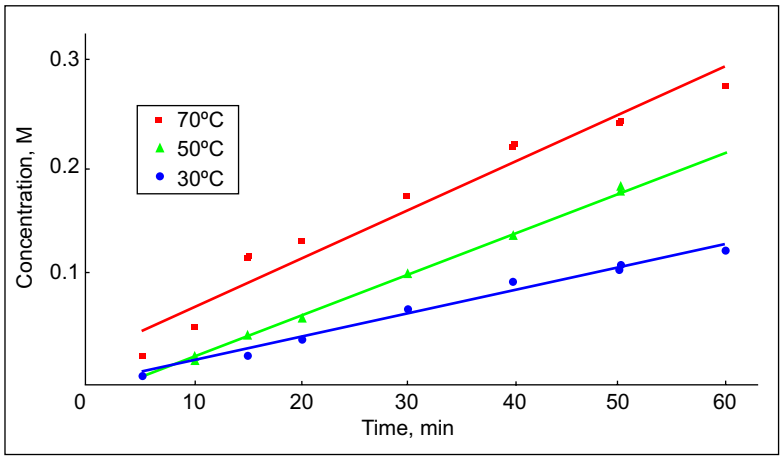

Fig. 2 Effect of temperature on the crossover of 1 M methanol through the Nafion® 115 membrane

96%, and from 50°C to 70°C by 43% (Table I). This is due to the faster electrode kinetics at the anode and the cathode when the temperature is increased. For other fuels, a temperature change from 30°C to 50°C leads to an increase in efficiency of between 36% and 109%, while an increase from 50°C to 70°C increases efficiency by 31% to 77% (Table I). The open circuit potential (OCP) of the fuel cell represents the difference in potential between the anode and the cathode when there is no external current flow. This also shows a slight increase when the temperature is raised, but this phenomenon is related to the catalyst material of the electrodes and the fuel used. Therefore, only the OCP for each fuel at 50°C is presented in Table I.

Raising the temperature also increases the fuel crossover from the anode to the cathode (Figure 2). Changing the temperature from 30°C to 70°C more than doubles the amount of methanol being transported to the cathode, causing a decrease in fuel cell performance. The crossover rate of the fuel depends not only on the temperature but also on the fuel and membrane used (15). Crossover through the Nafion® 115 membrane during the

Table I

Open Circuit Potentials (OCPs) in a Fuel Cell and Increase in Fuel Cell Efficiency when the Temperature is Raised*

Fuel	Number of carbons in chain	OCP at 50°C, V	Increase in fuel cell efficiency with temperature,%	
			From 30°C to 50°C	From 50°C to 70°C
Methanol	C_1	0.58	96	43
Formaldehyde	C_1	0.57	79	43
Formic acid	C_1	0.64	36	32
Ethanol	C_2	0.53	73	49
Acetaldehyde	C_2	0.54	54	77
Ethylene glycol	C_2	0.46	109	76
1-Propanol	C_3	0.44	63	50
2-Propanol	C_3	0.81	55	48
Glycerol	C_3	0.44	107	31

** All measurements were carried out at a potential of 0.05 V*

first 60 minutes in the diffusion cell at 25°C is presented for all the studied fuels in Figure 3. The crossover information for formic acid and glycerol was not included because of very low crossover for these fuels and the difficulty of analysing very small volumes of dilute formic acid samples.

Figure 3 demonstrates that methanol, being a small and neutral molecule which behaves similarly to water, permeates easily through the membrane. This results in losses in fuel cell efficiency. In contrast, formaldehyde, an even smaller molecule, has a lower crossover rate, due to the formation of methylene glycol with water (16) which due to its larger size permeates less easily through the Nafion® 115 membrane.

Permeability of alcohols through the membrane decreases with increasing size and complexity of the molecule, which justifies the interest in higher alcohols. Even though the crossover of ethanol and 2-propanol is not as severe as that of methanol, these fuels have shown a tendency to swell the membrane, influencing the MEA structure (17, 18). This results from the fact that the alcohols replace water molecules in the proton conducting membrane, decreasing the mobility of the protons, which increases electrolyte resistance. As shown in Figure 3, for most fuels the crossover through the Nafion® 115 membrane at 25°C over 60 minutes is linear, but for 1-propanol and ethylene glycol the crossover increases sharply after 30 minutes. This fact strongly supports the idea that these larger organic molecules might interact with the membrane, causing changes to the membrane morphology.

Open Circuit Potentials with Different Fuels

For all the fuels, the theoretical OCP can be calculated from thermodynamic values. For the fuels studied, the calculated OCP values lie between 1.00 V and 1.25 V under standard conditions. However, in real processes, the OCP is substantially lower due to mixed potentials caused by fuel crossover lowering the total potential of the cathode, and activation overpotentials caused by surface phenomena at both electrodes.

Figure 4 shows that the observed OCP of a PtRu-catalysed fuel cell lies between 0.4 V and 0.6 V at 50°C for all the fuels tested except 2-propanol, which produces a higher OCP of 0.8 V (Table I), in accordance with previous results (13, 18). The high OCP of 2-propanol is presumably the result of two different phenomena. Firstly, 2-propanol has a low crossover rate through the Nafion® 115 membrane (Figure 3), resulting in lower cathode overpotentials. Secondly, when the OH-group is situated on the central carbon atom of the molecule, the electronegative oxygen draws electrons from the carbon, which then attracts electrons from the C–C bonds. This changes the adsorption of the molecule to the catalyst surface, which leads to a different oxidation path to that seen for primary alcohols. This causes lower overpotentials at the anode, again resulting in a higher OCP.

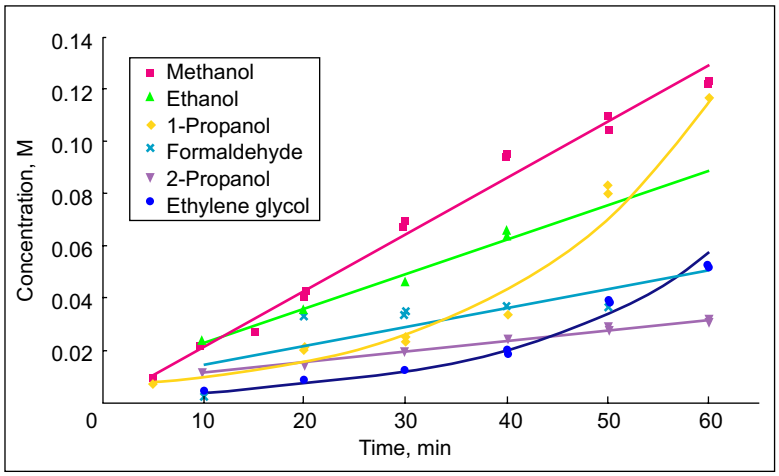

Fig. 3 Crossover of one-, two- and three-carbon fuels through the Nafion® 115 membrane at 25°C

Another fuel also reaches slightly higher overpotentials than other alcohols and aldehydes. Formic acid produces an OCP of 0.64 V (Table I). Formic acid has previously been shown to have a very small crossover through cation exchange membranes, due to the anionic nature of the dissolved molecule (19). Formic acid has also shown higher electrochemical activity compared to methanol (20). These phenomena would be expected to result in a higher OCP than that seen for light alcohols with high crossover rates.

The lowest OCP values (under 0.5 V) are attained with 1-propanol, ethylene glycol and glycerol (Table I). The low OCP of 1-propanol is probably caused by the dramatic increase in 1-propanol crossover after the fuel has been in contact with the Nafion® 115 membrane for 40 minutes (Figure 3). The OCP values of ethylene glycol and glycerol are around 0.1 V lower than those of methanol and ethanol. It is reasonable to assume that this is due to the OH-groups connected to every carbon atom in the diol and triol, changing the adsorption mechanisms on the PtRu surface.

Performance of One-Carbon Fuels

Figure 4 shows that organic molecules containing only one carbon atom are superior fuels for the PtRu-catalysed fuel cell, producing current densities at least three times higher than larger molecules. The difference between methanol and formaldehyde performance is surprisingly minor. Methanol has a higher energy density and a higher OCP, therefore it might have been expected to offer better performance. The observed result indicates that the performance loss when using methanol as a fuel is significant, likely due to severe methanol crossover. Investigation of new membrane materials to decrease methanol crossover may eventually lead to increased OCP and improved efficiency of the DMFC.

Formaldehyde exhibits a much lower crossover than methanol and performs better at lower current densities, but when higher current densities are reached, its performance declines gradually. As mentioned earlier, formaldehyde forms methylene glycol in water, and this greatly increases the size of the reactant. At the high current densities as the reaction rate increases, neither the products nor the reactant are able to diffuse from or to the surface fast enough, causing a rapid decrease in performance starting from 90 mA cm^{-2} (Figure 4). Therefore, the rate determining step for formaldehyde seems not to be the electrode kinetics as is the case for methanol.

The smallest one-carbon molecule, formic acid, produces roughly half the current density of the other C_1 fuels, even though the crossover of formic acid is nearly negligible. However, when using a more concentrated solution, formic acid performs better because the current density rises with more concentrated solutions, which is not the case for alcohols (19).

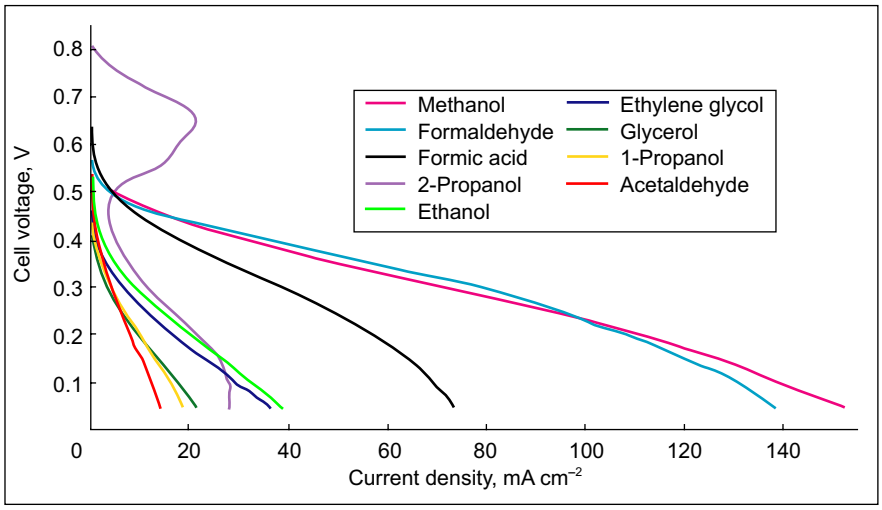

Fig. 4 The efficiency of the investigated one-, two- and three-carbon liquid fuels in a single cell at 50°C

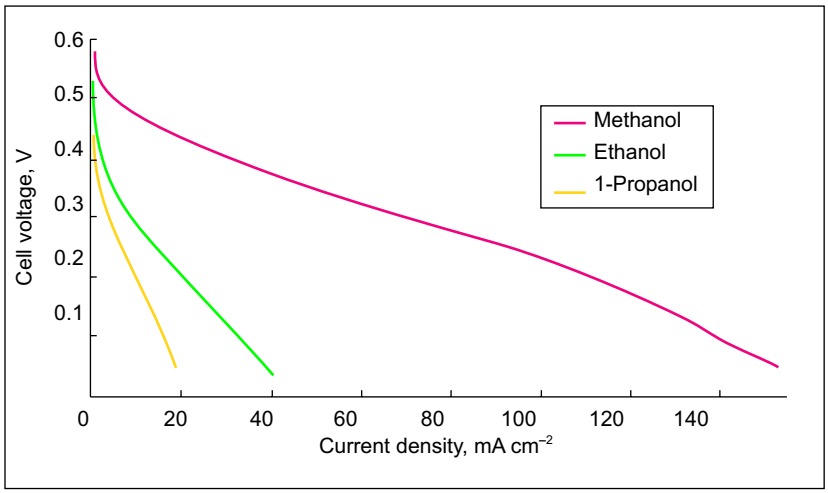

Fig. 5 Comparison of the efficiency of primary alcohols in a single cell at 50°C

To explore more carefully the effect of the length of the carbon chain in the fuel, the performances of the studied primary alcohols are presented in Figure 5. This figure illustrates that current density with methanol is more than three times higher than has been obtained with ethanol, and up to seven times higher than with 1-propanol. The longer the carbon chain, the lower the performance. This is due to partial oxidation of molecules with several carbon atoms, which is not seen in one-carbon molecules. These results are in accordance with a previous study (21), suggesting that the PtRu catalyst cannot effectively dissociate the C–C bond. However, it is clear that PtRu is an excellent catalyst for C_1 fuels at low temperatures.

Performance of Two- and Three-Carbon Fuels

In contrast to the case of C_1 molecules, ethanol shows more than double the current densities measured for its corresponding aldehyde, acetaldehyde, even though the OCP values of the two fuels remain nearly identical (Figure 6). This indicates that at low temperatures on the PtRu electrode, oxidation of ethanol and acetaldehyde stops at acetic acid, which is not oxidised further. Therefore, acetaldehyde displays inferior performance to ethanol. Experiments with acetic acid as a fuel gave such poor performance that the data have been excluded from this study. The other C_2 alcohol, ethylene glycol, performed in an almost identical way to ethanol, despite the fact that the

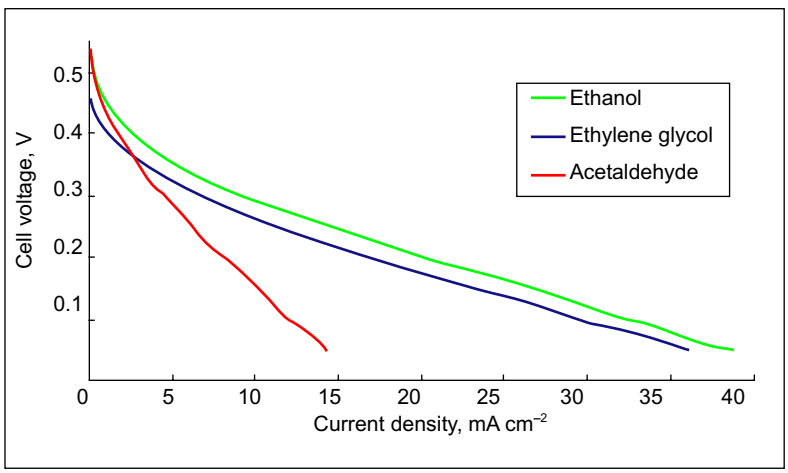

Fig. 6 Comparison of the efficiency of C_2 fuels in a single cell at 50°C

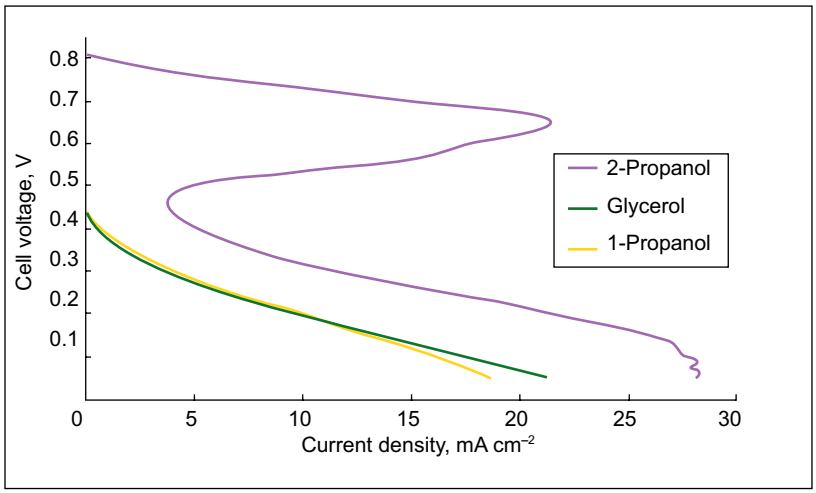

Fig. 7 Comparison of the efficiency of C_3 fuels in a single cell at 50°C

OCP of the former molecule was nearly 0.1 V lower. This indicates that the electrode processes of ethylene glycol differ from those of ethanol. Further studies need to be carried out to determine specific reaction mechanisms.

Figure 7 shows the performance of C_3 alcohols in terms of fuel cell efficiency. Similarly to the C_2 alcohols, the primary alcohol (1-propanol) and glycerol perform equally. However, in this case the primary alcohol also has a low OCP. These C_3 alcohols produce roughly half the current density of C_2 alcohols. Furthermore, the polarisation curve of the secondary alcohol 2-propanol behaves differently to that of the other compounds. Firstly, the OCP of 2-propanol is very high at 0.81 V, which is almost 0.3 V higher than that measured for methanol. Secondly, even at low current densities, 2-propanol reacts to form an intermediate, most likely acetone (22), which does not undergo further oxidation but remains at the surface, impeding the adsorption of 2-propanol. Therefore, when a current density of 20 mA cm^{-2} is reached, the surface of the catalyst is completely blocked by this intermediate, resulting in a rapid drop in current. At lower potentials, around 0.5 V, the intermediate either desorbs into the solution, allowing 2-propanol to adsorb on to the catalyst sites, or is oxidised further.

In contrast to our results, two separate research groups have reported fuel cell performances for 2-propanol involving no rapid current drop (13, 18). However, Qi *et al.* (13) also conclude that

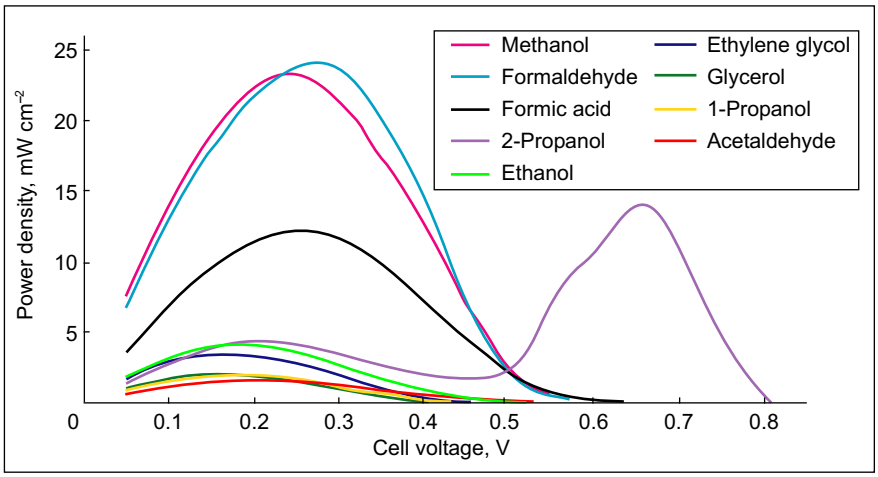

Fig. 8 The power densities of all the investigated one-, two- and three-carbon fuels in a single cell at 50°C

the electrode surface of the PtRu catalyst is being poisoned with intermediates of 2-propanol oxidation and suggest a periodic cleaning of the surface by an electrical pulse.

Power densities of the fuels can be calculated from the cell voltage and current density (Figure 8). The highest power densities were reached with C_1 fuels, providing almost five times more power than fuels with a carbon chain. Almost all the fuels studied have their power density maximum between 0.15 V and 0.3 V. However, 2-propanol produces an additional power density peak at a potential of 0.66 V. Even though 2-propanol cannot produce higher power density than C_1 fuels (due to the catalyst used), it can still provide the highest power density of the fuels containing a carbon chain at 0.22 V.

Fuel Choice for a PtRu-Catalysed Fuel Cell

The results found during this study are in agreement with previous work by several groups (6, 23, 24) showing that a PtRu catalyst performs best for methanol and other C_1 fuels. The crossover of methanol is the most severe of all the organic components studied. Methanol also produces the highest current density when used with a PtRu catalyst, therefore much research on DMFCs has concentrated on the development of impermeable electrolyte materials. However, the highest power density is produced by formaldehyde, which also seems to oxidise completely on the PtRu surface. Formaldehyde exhibits a lower crossover than methanol through the Nafion® 115 membrane, therefore it may be another possible candidate fuel for use in a PEFC.

Formic acid produces only half the current density of other C_1 fuels, even though it has the lowest crossover rate through the Nafion® 115 membrane and therefore, the highest OCP of the C_1 fuels. Formic acid has shown promising results when used in a fuel cell at high concentrations, even as high as 12 M (19). On the other hand, the PtRu catalyst appears not to be the optimum catalyst material for formic acid oxidation. Palladium-based and platinum-bismuth catalysts have both shown higher performances than the PtRu catalyst (25, 26).

Unfortunately, the PtRu catalyst shows no activity towards breaking the C–C bond, resulting in only partial oxidation of fuels with carbon chains. To improve the performance of the oxidation reaction for organic molecules with higher molecular weight, a second or third metal must be introduced with the Pt catalyst. For instance, tin alloyed with Pt has shown promising results towards ethanol oxidation (27, 28). Electrooxidation kinetics for organic molecules with higher molecular weight are extremely complicated and difficult to control. However, their crossover through the Nafion® 115 membrane is low and therefore they are interesting candidates and worthy of further study.

Of all the investigated organic molecules with a carbon chain, 2-propanol exhibits the most interesting results, producing the highest OCP and power density. However, there remains a problem with the formation of an intermediate which blocks the catalyst surface at higher current densities, causing a rapid drop in current. Further work is needed to characterise this intermediate and prevent its formation. Nevertheless, of the fuels tested in this study, 2-propanol appears to be the only light organic compound containing more than one carbon atom that has an appropriately high OCP. Therefore it would be an interesting focus for further research.

Conclusions

This paper presents the main features of temperature dependence, crossover and fuel cell efficiency for different fuels oxidised using a PtRu catalyst in a fuel cell. When the temperature of a fuel cell is increased, the performance increases. However, at the same time more fuel is transferred from the anode to the cathode compartment through the membrane. This crossover depends on the size and the charge of the fuel molecule, as well as the concentration of the fuel solution. Therefore, organic compounds with high molecular weight might offer a solution to the crossover problem.

Acknowledgements

The financial support of the Academy of Finland is gratefully acknowledged.

References

1 W. Qian, D. P. Wilkinson, J. Shen, H. Wang and J. Zhang, *J. Power Sources*, 2006, **154**, (1), 202

2 J. H. Yang and Y. C. Bae, *J. Electrochem. Soc.*, 2008, **155**, (2), B194

3 P. Hernández-Fernández, S. Rojas, P. Ocón, A. de Frutos, J. M. Figueroa, P. Terreros, M. A. Peña and J. L. G. Fierro, *J. Power Sources*, 2008, **177**, (1), 9

4 U. A. Icardi, S. Specchia, G. J. R. Fontana, G. Saracco and V. Specchia, *J. Power Sources*, 2008, **176**, (2), 460

5 V. Baglio, A. Stassi, A. Di Blasi, C. D'Urso, V. Antonucci and A. S. Aricò, *Electrochim. Acta*, 2007, **53**, (3), 1360

6 P. S. Kauranen, E. Skou and J. Munk, *J. Electroanal. Chem.*, 1996, **404**, (1), 1

7 V. Saarinen, T. Kallio, M. Paronen, P. Tikkanen, E. Rauhala and K. Kontturi, *Electrochim. Acta*, 2005, **50**, (16–17), 3453

8 J. Wang, S. Wasmus and R. F. Savinell, *J. Electrochem. Soc.*, 1995, **142**, (12), 4218

9 W. J. Zhou, B. Zhou, W. Z. Li, Z. H. Zhou, S. Q. Song, G. Q. Sun, Q. Xin, S. Douvartzides, M. Goula and P. Tsiakaras, *J. Power Sources*, 2004, **126**, (1–2), 16

10 S. Song, W. Zhou, Z. Liang, R. Cai, G. Sun, Q. Xin, V. Stergiopoulos and P. Tsiakaras, *Appl. Catal. B: Environ.*, 2005, **55**, (1), 65

11 C. Rice, S. Ha, R. I. Masel, P. Waszczuk, A. Wieckowski and T. Barnard, *J. Power Sources*, 2002, **111**, (1), 83

12 M. Umeda, H. Sugii, M. Mohamedi and I. Uchida, *Electrochemistry (Tokyo, Jpn.)*, 2002, **70**, (12), 961

13 Z. Qi and A. Kaufman, *J. Power Sources*, 2002, **112**, (1), 121

14 J.-M. Léger, *J. Appl. Electrochem.*, 2001, **31**, (7), 767

15 T. Kallio, K. Kisko, K. Kontturi, R. Serimaa, F. Sundholm and G. Sundholm, *Fuel Cells*, 2004, **4**, (4), 328

16 E. A. Batista and T. Iwasita, *Langmuir*, 2006, **22**, (18), 7912

17 S. Song, W. Zhou, J. Tian, R. Cai, G. Sun, Q. Xin, S. Kontou and P. Tsiakaras, *J. Power Sources*, 2005, **145**, (2), 266

18 D. Cao and S. H. Bergens, *J. Power Sources*, 2003, **124**, (1), 12

19 Y.-W. Rhee, S. Y. Ha and R. I. Masel, *J. Power Sources*, 2003, **117**, (1–2), 35

20 M. Weber, J.-T. Wang, S. Wasmus and R. F. Savinell, *J. Electrochem. Soc.*, 1996, **143**, (7), L158

21 I. de A. Rodrigues, J. P. I. De Souza, E. Pastor and F. C. Nart, *Langmuir*, 1997, **13**, (25), 6829

22 S.-G. Sun and Y. Lin, *Electrochim. Acta*, 1998, **44**, (6–7), 1153

23 A. Aramata and M. Masuda, *J. Electrochem. Soc.*, 1991, **138**, (7), 1949

24 S. Lj. Gojkovic, T. R. Vidakovic and D. R. Durovic, *Electrochim. Acta*, 2003, **48**, (24), 3607

25 Y. Zhu, Z. Khan and R. I. Masel, *J. Power Sources*, 2005, **139**, (1–2), 15

26 F. J. Vidal-Inglesias, J. Solla-Gullón, E. Herrero, A. Aldaz and J. M. Feliu, *J. Appl. Electrochem.*, 2006, **36**, (11), 1207

27 C. Lamy, A. Lima, V. LeRhun, F. Delime, C. Coutanceau and J.-M. Léger, *J. Power Sources*, 2002, **105**, (2), 283

28 W. J. Zhou, B. Zhou, W. Z. Li, Z. H. Zhou, S. Q. Song, G. Q. Sun, Q. Xin, S. Douvartzides, M. Goula and P. Tsiakaras, *J. Power Sources*, 2004, **126**, (1–2), 16

The Authors

Annukka Santasalo started her doctoral studies at Helsinki University of Technology, Finland, in 2007. After a visit to Professor Juan Feliu's laboratory in Alicante, Spain, in spring 2008, she has focused her research on electrocatalysis in polymer electrolyte fuel cells. Her current research activities are centred on finding new catalyst materials, including different platinum group metals, to form alloys for electrooxidation of alcohols both in acid and alkaline media.

Dr Tanja Kallio is an academic research fellow at Helsinki University of Technology and has a D.Sc. (Tech.) degree from the same university. Her fields of research are electrochemical catalysis and polymer membrane electrolytes for polymer electrolyte fuel cells and enzymatic fuel cells.

Professor Kyösti Kontturi has a D.Sc. (Tech.) degree from Helsinki University of Technology and is now Professor of Physical Chemistry and Electrochemistry at that university. He has been interested in transport processes in electrolyte solutions, irreversible thermodynamics, electrochemistry at liquid–liquid interfaces, drug delivery, membrane electrochemistry and nanotechnology. Currently his field of research is mainly in electrochemistry of ionic liquids and nanotechnology. Professor Kontturi has published 220 articles in peer reviewed journals.

Publication II

A. Santasalo, F. J. Vidal-Iglesias, J. Solla-Gullón, A. Berná, T. Kallio and J. M. Feliu, Electrooxidation of Methanol and 2-propanol Mixtures at Platinum Single Crystal Electrodes, Electrochim. Acta, **54** (2009) 6576-6583.

Electrochimica Acta 54 (2009) 6576–6583

Contents lists available at ScienceDirect

Electrochimica Acta

journal homepage: www.elsevier.com/locate/electacta

Electrooxidation of methanol and 2-propanol mixtures at platinum single crystal electrodes

A. Santasalo[a], F.J. Vidal-Iglesias[b,*], J. Solla-Gullón[b], A. Berná[b], T. Kallio[a], J.M. Feliu[b]

[a] Research Group of Physical Chemistry, Department of Chemistry, Helsinki University of Technology, P.O. Box 6100, 02015 TKK, Finland
[b] Instituto de Electoquímica, Universidad de Alicante, Apartado 99, 03080 Alicante, Spain

ARTICLE INFO

Article history:
Received 22 April 2009
Received in revised form 9 June 2009
Accepted 13 June 2009
Available online 23 June 2009

Keywords:
Alcohol mixture
Platinum single crystals
Methanol
2-Propanol
Electrooxidation

ABSTRACT

In the present work the electrooxidation of methanol, 2-propanol and different mixtures of both alcohols has been studied on the three platinum basal planes in three different electrolytes (H_2SO_4, $HClO_4$ and NaOH). The results indicate that, like in the case of both individual alcohols, the electrooxidation of the mixture is a structure sensitive reaction and that Pt(1 1 1) leads to higher current densities for some mixture compositions as compared to what could be expected from the contribution of the individual compounds. The effect of the methanol concentration in the mixture points out that 2-propanol is the main reacting fuel at the Pt(1 1 1) surface. Interestingly, the addition of methanol clearly has a positive effect on 2-propanol oxidation. For a specific mixture composition, while results from cyclic voltammetry indicate a modest twofold increase in current density, chronoamperometric results after 10 min experiment show a nearly 200 times higher current density. IR experiments have been performed to gain information about the enhancement mechanism. Nevertheless, we have found that both methanol and 2-propanol seem to follow the same mechanism as they follow in the absence of the other alcohol, and therefore the enhancement could be probably related to a competitive adsorption for the active surface sites.

1. Introduction

Direct alcohol fuel cells (DAFC) are promising electrochemical power generators especially for portable applications. However, electrooxidation kinetics of alcohols is slow and consequently DAFC power densities are low for practical applications. At present, methanol is one of the most widely studied organic fuels [1–15] and it is known to produce high current densities in DAFC with platinum based catalysts [16]. Nevertheless, during the reaction, the platinum surface becomes poisoned by strongly adsorbed intermediates such as carbon monoxide, due to the dissociative chemisorption of methanol [14,15]. This adsorbed CO, both in linear and bridge-bonded form, has been observed at platinum surfaces [1,14,15]. The reported methanol electrooxidation products are CO_2, HCHO, HCOOH and $HCOOCH_3$ [17,18]. The mechanism of methanol electrooxidation on Pt follows a "dual-pathway" with the additional complication that CO may be also considered as reactive intermediate [18,19]. In addition, methanol electrooxidation on the three basal planes of platinum has been shown to be a structure sensitive reaction [10,18,20]. Among them, Pt(1 1 1) was found to be the least reactive towards methanol decomposition, while Pt(1 1 0) was considered to be the most active. Nevertheless, in a very recent paper, Housmans et al. have investigated the selectivity and structure sensitivity of the methanol oxidation pathways on basal planes and stepped platinum single crystal electrodes by monitoring the mass fractions of CO_2 (m/z 44) and methylformate (m/z 60) using on-line electrochemical mass spectrometry (OLEMS) [21]. They found that methanol oxidation on Pt basal planes showed an increase in maximum activity in the order Pt(1 1 1) < Pt(1 1 0) < Pt(1 0 0). The order obtained is different to that previously reported by Herrero et al. (Pt(1 1 1) < Pt(1 0 0) < Pt(1 1 0)) [10] and it was attributed to differences in the electrode pre-treatment which greatly influences the surface structure of the Pt(1 0 0) and Pt(1 1 0) electrodes. In addition, on the basis of the onset potential of the reaction (<0.6 V), the Pt(1 1 0) was reported to be the most active, followed by the Pt(1 1 1) and Pt(1 0 0) surfaces [21].

Besides the studies with the three basal planes, methanol electrooxidation was also performed on stepped Pt surfaces in order to clarify how exactly the step density influences these reactions. Shin and Korzeniewski suggested that an increase of the step density catalyzes methanol decomposition [22], whereas Tripkovic and Popovic showed that the increase in the step density leads to a decrease in the surface activity towards methanol electrooxidation [23], both using Pt[n(1 1 1) × (1 0 0)] stepped surfaces. In addition, Housmans and Koper studied methanol oxidation on Pt[n(1 1 1) × (1 1 0)] stepped surfaces, and reported an increase in

* Corresponding author.
E-mail address: fj.vidal@ua.es (F.J. Vidal-Iglesias).

0013-4686/$ – see front matter © 2009 Elsevier Ltd. All rights reserved.
doi:10.1016/j.electacta.2009.06.033

the activity with the step density, suggesting that the presence of steps with a (1 1 0) orientation catalyzes methanol decomposition, CO oxidation and also the direct methanol oxidation [24]. These kind of studies are relevant, not only from a fundamental point of view, but also from a practical one, because in practical applications the stepped surfaces may be considered as models of surface defects, always present on dispersed electrodes.

The 2-propanol oxidation has not received as much attention as methanol's. Nevertheless, 2-propanol is an interesting fuel and in comparison with methanol it is less toxic, it has a higher boiling point and it is less prone to crossover through the electrolyte membrane to the cathode side [25,26]. In fuel cell studies, the electrooxidation of 2-propanol over platinum or platinum-containing catalysts supplies, at low current densities, higher voltages than methanol [25]. The products from this oxidation are acetone and carbon dioxide [27,28]. In this way, the number of papers concerning this reaction has greatly grown in the recent years [29–32]. One of the most relevant papers concerning the electrooxidation of 2-propanol on platinum single crystals was published in 1996 by Sun and Lin [28]. Nevertheless, they employed Pt single crystals cooled down in an oxidative atmosphere (air) which is known to introduce surface defects on the electrodes. In a very recent paper, platinum–ruthenium electrodes have been also used for 2-propanol oxidation and rate enhancement has been observed, by not only increasing the current density of the main peak (CV experiments) but also decreasing the onset potential [32]. Finally, and from a more applied point of view, the open circuit potential of 2-propanol is much higher for a 60:40 PtRu catalyst fuel cell than that of methanol providing a broader possible potential area [26]. In summary, it is well established that the nature and the structure of the electrode material play a key role in the adsorption and electrooxidation of both organic fuels.

An interesting alternative to the use of these pure organic fuels may be their combination to form a binary mixture. In a previous paper, Gojkovic et al. [33] studied the electrooxidation of methanol + 2-propanol mixtures, concluding that these mixtures can deliver a significant anodic current over the entire potential range from 0.2 to 0.8 V, which is not observed with pure methanol or pure 2-propanol. Unfortunately, this study was exclusively carried out with polyoriented platinum nanoparticles and consequently the effect of the surface structure could not be evaluated.

The aim of this work is to study the structure sensitivity of this methanol + 2-propanol binary fuel oxidation on platinum. To our knowledge no work has been focused on the effect of the surface structure in this type of alcohol mixtures. In this way, this paper describes the first results concerning the electrooxidation of alcohol mixtures in platinum single crystals. The interest is focused on finding synergetic conditions in which the reactivity of the mixture could be higher than that expected from the individual contributions. This would lead to electrocatalytic effects on heterogeneous surfaces from changes in the solution composition.

2. Experimental

Platinum single crystals were oriented, cut, and polished from small single crystal beads (2.5 mm diameter) by the procedure described previously [34]. The electrodes were flame-annealed, cooled down in a H_2 + Ar atmosphere and protected with water in equilibrium with this gaseous mixture in the usual way [35]. It has been shown that this treatment leads to well-defined surfaces [36]. A single crystal platinum bead, obtained by melting and slowly cooling a Pt wire, was used as a well-defined polycrystalline surface having a uniform distribution of all surface sites.

Electrochemical experiments were carried out in two conventional three-electrode cells using large Pt counter electrodes. The potentials were measured against a reversible hydrogen electrode (RHE) connected to the cell through a Luggin capillary. One cell was filled with the electrolyte in the absence of alcohol or alcohol mixture under study. The second cell contained the alcohol, or alcohol mixture, at controlled concentration. Solutions were prepared by the addition of 2-propanol and/or methanol to 0.1 M $HClO_4$, 0.5 M H_2SO_4 or 0.5 M NaOH. All reagents were of p.a. quality (Merck). Solutions were prepared using Millipore Milli-Q water. Oxygen was eliminated by bubbling Ar (Air Liquide N50) for 20 min. The Ar atmosphere was maintained inside the cell during the experiments. To keep a constant concentration of the alcohols in solution, the Ar was previously bubbled through a solution of the same composition as the one in the electrochemical cell. Before any experiment was started, the potential was always kept at 0.05 V. The electrode potential was controlled using a PGSTAT30 AUTOLAB system.

Initial cyclic voltammograms recorded at 50 mV s^{-1} were always performed in the cell without the alcohol or alcohol mixture in order to check the surface structure of the electrode after flame annealing. Subsequently, the electrode was transferred to the second cell with the solution under study where the sweep rate used was 20 mV s^{-1}. Before the chronoamperometric measurements, the electrode was removed from the second cell, washed carefully with ultrapure water to remove possible CO residues and placed back in the second cell at 0.05 V. The chronoamperometric measurements were performed at 0.5 V vs. RHE for 600 s.

Spectroelectrochemical experiments were carried out with a Nicolet Magna 850 spectrometer equipped with a narrow-band DC-coupled MCT-A detector. The spectroelectrochemical cell was provided with a prismatic CaF_2 window bevelled at 60°. A reversible hydrogen electrode (RHE) and a platinum foil were used as reference and counter electrodes, respectively. Unless otherwise stated,

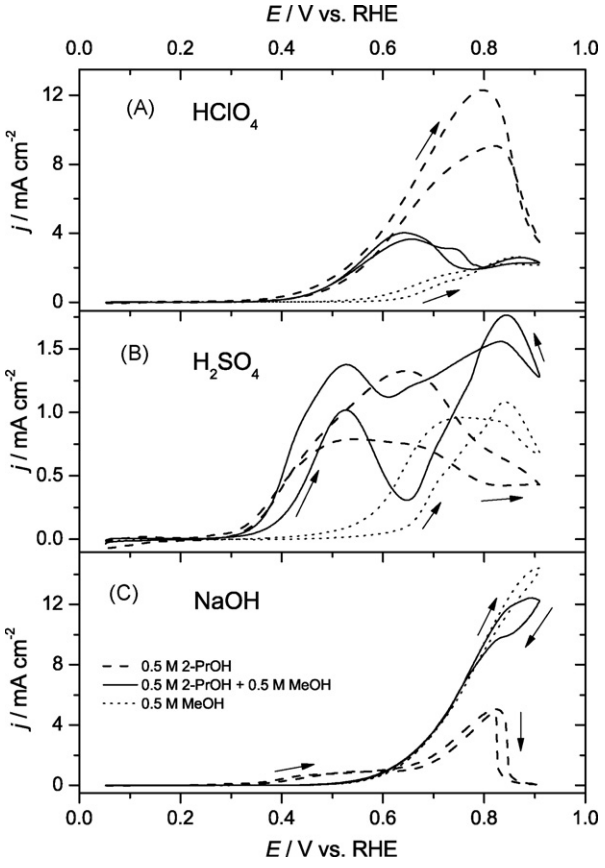

Fig. 1. Electrooxidation of 0.5 M 2-propanol, 0.5 M methanol + 0.5 M 2-propanol mixture and 0.5 M methanol on polyoriented platinum in 0.1 M $HClO_4$ (A), 0.5 M H_2SO_4 (B) and 0.5 M NaOH (C). Scan rate 20 mV s^{-1}. Third scans are shown.

the spectra were collected with p-polarized light with a resolution of 8 cm^{-1}. The spectra are presented as the ratio $-\log(R_2/R_1)$, where R_2 and R_1 are the reflectance values corresponding to the single beam spectra recorded at the sample and reference potentials (0.10 V RHE), respectively. Each one of these single beam spectra is calculated from 100 interferograms during the single potential spectra and from 13 interferograms for the time-dependent spectra.

3. Results and discussion

Fig. 1 shows the oxidation on a polyoriented Pt single crystal of 2-propanol, methanol and a 1:1 mixture of both alcohols in three different supporting electrolytes (0.1 M $HClO_4$, 0.5 M H_2SO_4 and 0.5 M NaOH). The voltammetric profiles obtained in H_2SO_4 (Fig. 1B) are quite similar to those reported previously by Gojkovic et al. [33] for the alcohol mixture electrooxidation despite the different H_2SO_4 concentration (0.1 M H_2SO_4). In addition, and although the alcohol mixture concentration was also more diluted (0.1 M methanol + 0.1 M 2-propanol) the profile of the curves (only positive sweeps were given by Gojkovic et al. [33]) are also similar. However, minor current densities were recorded by Gojkovic, due to the lower alcohol concentrations. In the case of $HClO_4$ and NaOH, no previous information has been published. In any case, the results obtained do not show any enhancement. Only in H_2SO_4 higher current densities are observed, although in this media much lower current densities where obtained for the electrooxidation of the equimolar mixtures of both alcohols on the polyoriented platinum surface. It is important to notice that the current densities obtained in H_2SO_4 are clearly lower than those obtained with other electrolytes indicating that the anion adsorption plays a key role on the adsorption of the pure alcohols and their mixtures. Moreover, alkaline medium seems to be the most active for the alcohol mixture oxidation on polycrystalline platinum, as it is indicated by the highest current density and the lower poisoning rate. In this case the mixture behaves similarly to methanol although it gets poisoned earlier.

3.1. Effect of the Pt surface structure

To evaluate the possible influence of the surface structure on the electrooxidation of the alcohol mixture, similar experiments to those performed with the polyoriented surface were carried out for the three Pt basal planes. Fig. 2 shows the oxidation of methanol, 2-propanol and the equimolar mixture of both alcohols on the three Pt single crystal electrodes in the three supporting electrolytes. In case of the pure alcohol oxidations, and in spite of the fact that this is not the scope of the present study, some relevant features must be commented to further understand the results obtained for the oxidation of the alcohol mixtures. For the $HClO_4$ experiments, the voltammetric profiles for methanol oxidation (Fig. 2A) correlate quite well with the results of Housmans et al. [21] and where the maximum activity towards the electrooxidation of methanol decreased in the order: Pt(1 0 0) > Pt(1 1 0) > Pt(1 1 1) in 0.1 M $HClO_4$. This order is different to that reported earlier [10] and illustrates how the differences in the flame annealing step (specifically the cooling step in air or in hydrogen-containing atmosphere) affect the surface structure of the electrode and its reactivity. Incidentally, the comparison of the voltammetric profiles of the electrodes in the clean supporting electrolytes clearly reflects that the surface order is different after both pre-treatment steps.

In the case of 2-propanol, only Sun's group [28] has studied its oxidation in 0.1 M H_2SO_4 on platinum single crystal electrodes which were cooled down in air. The results reported are not in agreement with those presented in Fig. 2, due to the presence of the surface defects that arise from the cooling procedure. The results obtained in perchloric acid and with the electrodes

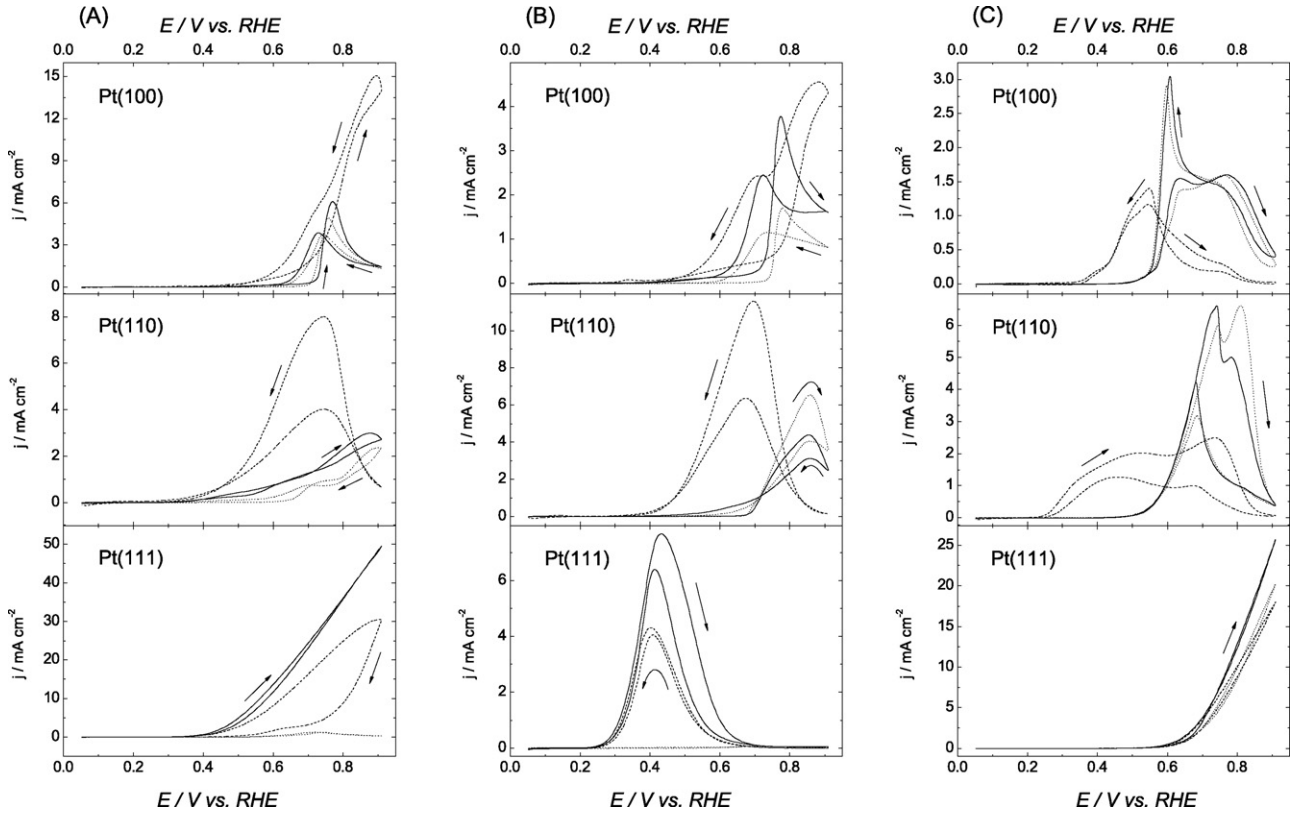

Fig. 2. Electrooxidation of 0.5 M 2-propanol (dashed line), 0.5 M methanol + 0.5 M 2-propanol mixture (solid line) and 0.5 M methanol (dotted line) on Pt(1 0 0), Pt(1 1 0) and Pt(1 1 1) in 0.1 M $HClO_4$ (A), 0.5 M H_2SO_4 (B) and 0.5 M NaOH (C). Scan rate 20 mV s^{-1}. Third scans are shown.

cooled in a H_2/Ar atmosphere (Fig. 2A), indicate that the maximum activity towards 2-propanol oxidation decreases in the order Pt(1 1 1) > Pt(1 0 0) > Pt(1 1 0).

The electrooxidation of small alcohols is reported to be facile in alkaline media [37,38]. However, this is not always the case neither on all the crystal surfaces nor for all small alcohols. In fact, Fig. 2 demonstrates that the current densities obtained for the three platinum basal planes for 2-propanol oxidation in alkaline media are clearly lower than those obtained in perchloric acid. On the other hand, in the case of methanol, the current density increases in comparison with the acidic electrolyte, for Pt(1 1 0) and Pt(1 1 1) surfaces, but not on Pt(1 0 0).

Analyzing the effect of the supporting electrolyte exclusively in acidic media, higher current densities have been reached for the electrooxidation of all the studied solutions in perchloric acid than in sulphuric acid on Pt(1 0 0) and Pt(1 1 1) surfaces. This is a strong evidence to support sulphate anions competition for the adsorption sites on these two surfaces, as it has been previously reported for the case of methanol oxidation on Pt(1 1 1) [12]. Kita et al. [39] reported that for Pt(1 1 1) current densities up to 10 times higher were observed in $HClO_4$ than in H_2SO_4, while for Pt(1 0 0) the enhancement factor was around two. This behaviour could indicate a stronger anion adsorption on Pt(1 1 1) than on Pt(1 0 0) [40,41]. Nevertheless, in H_2SO_4, the onset potential for both the oxidation of 2-propanol and the alcohol mixture is lower (≈100 mV) than in $HClO_4$. Finally, on Pt(1 1 0) current densities are slightly higher in the H_2SO_4 electrolyte solution, indicating that sulphate anion adsorption is not as strong as for the other two basal planes [39].

In the case of the alcohol mixture, the obtained results (Fig. 2) clearly indicate that the oxidation on platinum single crystal surfaces is similar to that observed with one of the pure alcohols. Thus, whereas for Pt(1 0 0) and Pt(1 1 0), regardless of the supporting electrolyte, the profiles resemble to those corresponding to methanol oxidation, for Pt(1 1 1) the profiles are similar to those obtained with 2-propanol, although in NaOH, both pure alcohols show very similar voltammetric profiles. However, the most relevant point is that for Pt(1 1 1), and only for this surface, a clear enhancement in the electrocatalytic activity in comparison with the pure alcohols is observed. Moreover, this enhancement is found in the three supporting electrolytes under study, suggesting that the specific surface structure of this electrode may be the key point of the enhanced electrocatalytic activity.

The enhancement obtained in case of the Pt(1 1 1) electrode for the oxidation of the equimolar alcohol mixture was confirmed by performing chronoamperometric measurements at 0.5 V for 600 s in $HClO_4$ (Fig. 3). $HClO_4$ was selected as supporting electrolyte in these experiments because much higher current densities can be obtained in comparison to the other two electrolytes, as previously shown in Fig. 2. The observed trend is the same to that previously reported by analyzing cyclic voltammetry data in $HClO_4$ (Fig. 2A) and confirm that Pt(1 1 1) is the only electrode surface that provides an electrocatalytic enhancement for the oxidation of the alcohol mixture. Thus, whereas for Pt(1 0 0) and Pt(1 1 0) electrodes, the current densities obtained after 600 s and at 0.5 V follow the order 0.5 M 2-propanol > 0.5 M 2-propanol + 0.5 M methanol > 0.5 M methanol, for Pt(1 1 1), the trend is 0.5 M 2-propanol + 0.5 M methanol > 0.5 M 2-propanol > 0.5 M methanol indicating again the enhanced activity of this surface for the alcohol mixture electrooxidation. In fact, on Pt(1 1 1) the current density obtained after 600 s for the mixture is over 60-fold higher (580 $\mu A\,cm^{-2}$) than that obtained with 2-propanol (9 $\mu A\,cm^{-2}$) and about 190-fold higher than for methanol electrooxidation (3 $\mu A\,cm^{-2}$).

From the results obtained for the three platinum basal planes (Figs. 2 and 3) and also for the polyoriented platinum electrode (Fig. 1), we can state that only Pt(1 1 1) produces a much higher current density with the alcohol mixture than with the two pure alcohols. This result is not only confirmed by using a potentiodynamic technique such as cyclic voltammetry but also by using potentiostatic conditions such as those of chronoamperometric experiments.

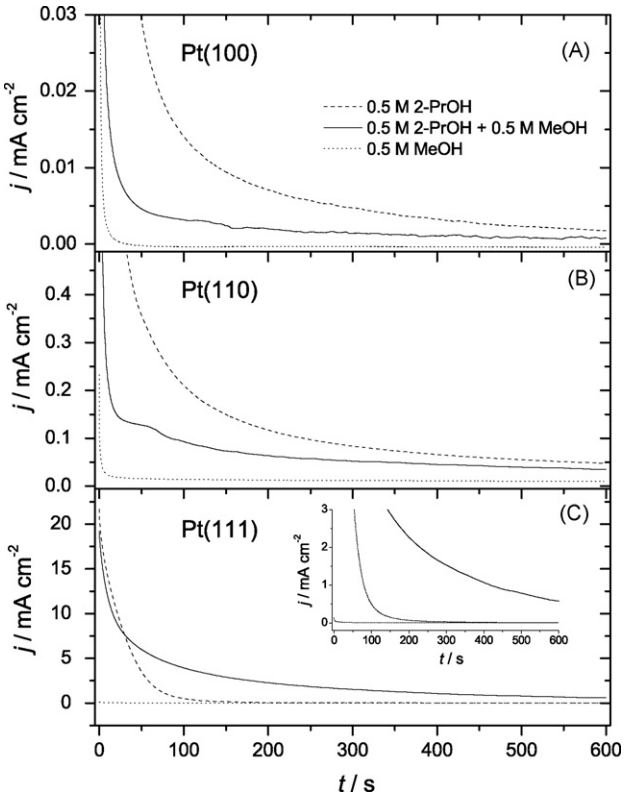

Fig. 3. Chronoamperometric measurements for 0.5 M 2-propanol, 0.5 M 2-propanol + 0.5 M methanol mixture and 0.5 M methanol at Pt(1 0 0) (A), Pt(1 1 0) (B) and Pt(1 1 1) (C) in 0.1 M $HClO_4$. Step potential: 0.5 V vs. RHE.

In order to better understand this enhanced activity on the Pt(1 1 1), we have examined how Pt(1 1 1) became poisoned with time for consecutive cycles by cyclic voltammetry. Fig. 4 shows the differences between the first and the third cycles in 2-propanol and also in the (1:1) alcohol mixture.

As it can be observed, a much slower poisoning rate results for the alcohol mixture than for 2-propanol, although cycle 1 is very similar for both oxidations. In addition, in both cases the onset oxidation potential is shifted to more positive potentials with increasing the number of cycles. In terms of current density the current density of the peak of 2-propanol oxidation is about 40% lower in the third cycle when compared with the first cycle, while the effect in the mixture is lower than 10%. Finally, it is also important to point out that for the alcohol mixture the voltammetric profile is quite similar to that corresponding to the first cycle (Fig. 4B) whereas for 2-propanol, the modification is more noticeable and there is practically no oxidation in the negative potential sweep.

3.2. *Effect of the binary fuel composition for Pt(1 1 1)*

From the results presented up to now, it has been demonstrated that the oxidation of the 2-propanol + methanol mixture on a Pt(1 1 1) electrode shows a similar voltammetric profile to that characteristic of 2-propanol, suggesting that practically only 2-propanol is oxidized. Nevertheless an evident slower poisoning rate was observed in comparison to pure 2-propanol, which must be related to the presence of methanol in the same solution. To study the effect of methanol in the electrooxidation process, the

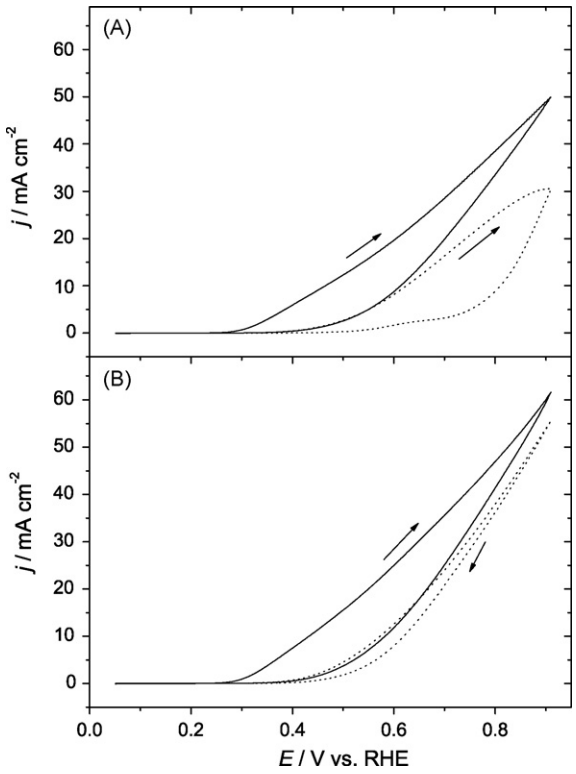

Fig. 4. Electrooxidation of 0.5 M 2-propanol (A) and a 0.5 M methanol + 0.5 M 2-propanol mixture (B) on Pt(1 1 1) in 0.1 M $HClO_4$. First (solid line) and third (dotted line) cycles are presented. Scan rate 20 mV s^{-1}.

2-propanol concentration was kept constant (0.5 M) whereas the methanol concentration was systematically modified and the reactivity of the mixtures was evaluated. Fig. 5 shows the voltammetric profiles of the third cycle of the oxidation of three different alcohol mixtures and, for sake of comparison, those obtained for the two pure alcohols. In a similar way to that reported in Fig. 4, the results obtained for the first cycle for 2-propanol and the different mixtures, were quite similar. Nonetheless, by comparing the third cycle, the mixture with the highest activity (attending to the maximum current observed in the voltammogram) corresponds to the 0.5 M

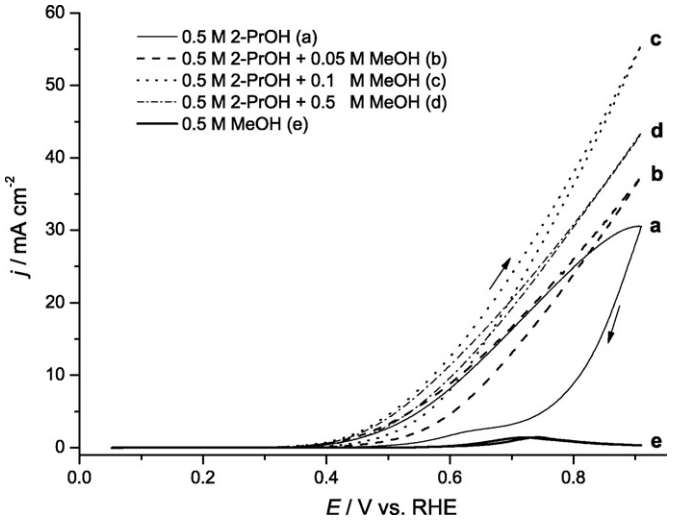

Fig. 5. Electrooxidation of 0.5 M 2-propanol, 0.5 M methanol and 0.5 M 2-propanol + *x* M methanol mixtures (concentrations are shown in the figure legend) on Pt(1 1 1) in 0.1 M $HClO_4$. Scan rate 20 mV s^{-1}. Third scans are shown.

2-propanol + 0.1 M methanol mixture. As it can be observed, and in comparison with the pure 2-propanol oxidation (curve "a" in Fig. 5), the overall oxidation current density increases by adding methanol until a maximum value is reached at this particular mixture composition. From that point, the current density clearly decreases. Although it has not been included in Fig. 5, a 0.5 M 2-propanol + 1 M methanol experiment was also carried out, but the voltammetric profile is similar to that from the 0.5 M 2-propanol + 0.5 M methanol mixture.

In the electrochemical oxidation process, it is clear that both 2-propanol and methanol must compete for the adsorption sites on the Pt(1 1 1) surface and consequently, taking into account that the adsorption sites are constant, the higher the methanol concentration the lower the 2-propanol adsorption will be. Besides, the 2-propanol oxidation gets strongly poisoned with the consecutive cycles while the mixtures seem to be more stable with time (Fig. 4) although the initial current densities are similar in both cases. In this way, taking into account these two different features, it seems that the main role of the presence of methanol is to compete for the

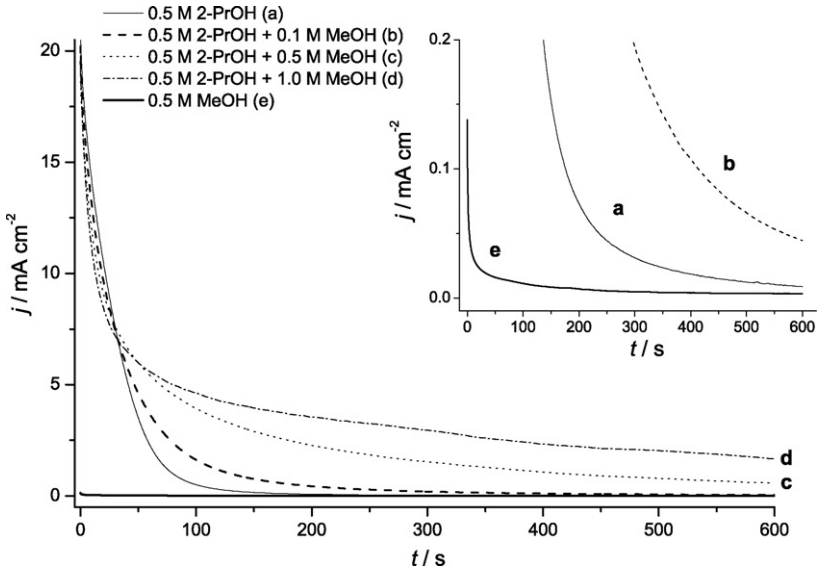

Fig. 6. Chronoamperometric measurements for 0.5 M 2-propanol, 0.5 M methanol and 0.5 M methanol + *x* M 2-propanol mixtures (concentrations are shown in the figure legend) on Pt(1 1 1) in 0.1 M $HClO_4$. Step potential: 0.5 V vs. RHE.

adsorption sites where the 2-propanol is adsorbed and then become inactive, as observed for the oxidation of pure 2-propanol solution. Therefore, the presence of methanol decreases the rate of the self-inactivation step observed in the 2-propanol electrooxidation process.

In a similar way to that shown in Fig. 3, chronoamperometric experiments were performed with the different 2-propanol–methanol mixtures to study the effect of methanol concentration in long time experiments. Fig. 6 shows the results for the two pure alcohols and three different 2-propanol + methanol mixtures. As it can be observed, after 10 min at 0.5 V, the higher current density is observed for the mixture containing the highest methanol concentration (0.5 M 2-propanol + 1 M methanol). It must be noted that the current density recorded after this period of time is practically 200 times higher (1.7 mA cm^{-2}) than that recorded for pure 2-propanol (9 μA cm^{-2}) with the same concentration and about threefold higher than for the mixture containing a 0.5 M methanol concentration (0.58 mA cm^{-2}). The results obtained in the potentiostatic experiments indicate that it is more advisable to increase the optimal methanol concentration found in the voltammetric analyses, for long term experiments, with the main objective of decreasing as much as possible the poisoning rate of the surface without reaching a methanol-like behaviour (curve "e" in Fig. 5). That is the reason why, for the long time experiments, it is convenient the use of a higher methanol concentration (being the best of the employed 0.5 M 2-propanol + 1 M methanol), whereas in cyclic voltammetry experiments, the highest currents were obtained with a lower methanol concentration (0.5 M 2-propanol + 0.1 M methanol). In this latter case there is less competition for the adsorption sites and the surface becomes less contaminated than in the case of pure 2-propanol.

3.3. Spectroelectrochemical analysis of products and intermediates

In order to gain information about the enhanced oxidation mechanism and detect possible reaction intermediates or products, IR experiments were carried out with Pt(1 1 1). These results are shown in Figs. 7 and 8 for 2-propanol and for 2-propanol + methanol oxidation, respectively. Oxidation of 2-propanol spectra (Fig. 7) show bands from species that are only present in solution, as observed in experiments carried out with s- and p-polarized light experiments. Negative bands at 2900 cm^{-1} were observed due to the depletion of 2-propanol, consumed at the sampling voltage. Positive bands appear at 1700, 1428, 1369 and 1240 cm^{-1}. All these bands correspond to acetone, produced in solution after 2-propanol dehydration. The 1700 cm^{-1} band corresponds to ν[CO] vibration of the carbonyl group, the 1428 cm^{-1} band corresponds to the $\nu_{asy}[CH_3]$ asymmetric tension, that at 1368 cm^{-1} to the $\nu_{sy}[CH_3]$ symmetric band and that at 1240 cm^{-1} to the ν[COH] tension, all of them from acetone molecule in solution. This latter point was confirmed by the observation of the same bands for deuterated water experiments. In addition, in the spectra obtained with deuterated water no band was observed due to C=C double bond at 1600 cm^{-1}, so propene formation by 2-propanol dehydration or 2-propenol formation as a result of the tautomeric equilibrium with acetone can be ruled out. Nevertheless, this 1600 cm^{-1} was previously observed by Sun and Lin [28]. Finally, a very weak CO_2 band at 2345 cm^{-1} is only observed at 0.9 V, indicating that the oxidation to CO_2 does take place in negligible amount and that essentially only acetone is produced. The CO_2 can come from acetone or from direct 2-propanol oxidation. In this way, the results obtained indicate that no adsorbed molecules have been detected by IR. Nevertheless, it is important to note that, as it has been previously shown in Fig. 4 with the consecutive cycles experiment, the surface becomes poisoned and the current density decreases. Consequently, the surface

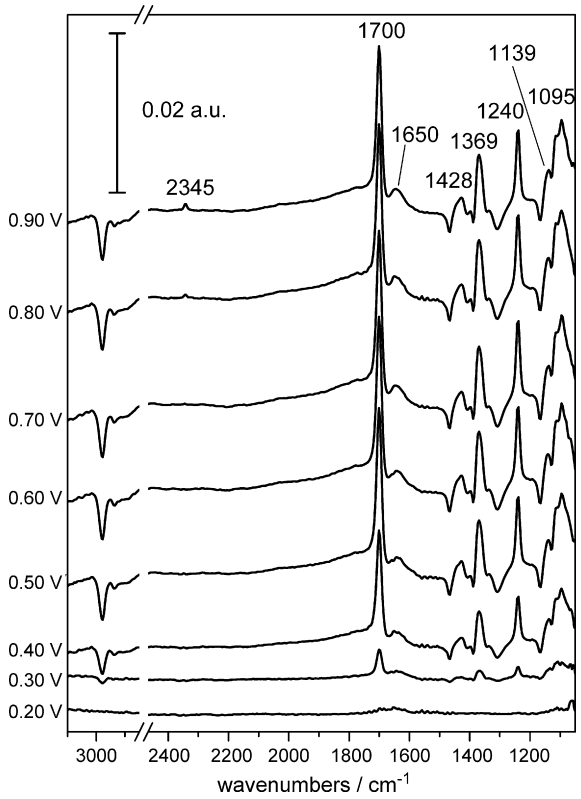

Fig. 7. FTIRS spectra collected in 0.1 M $HClO_4$ + 0.5 M 2-propanol solution for Pt(1 1 1).

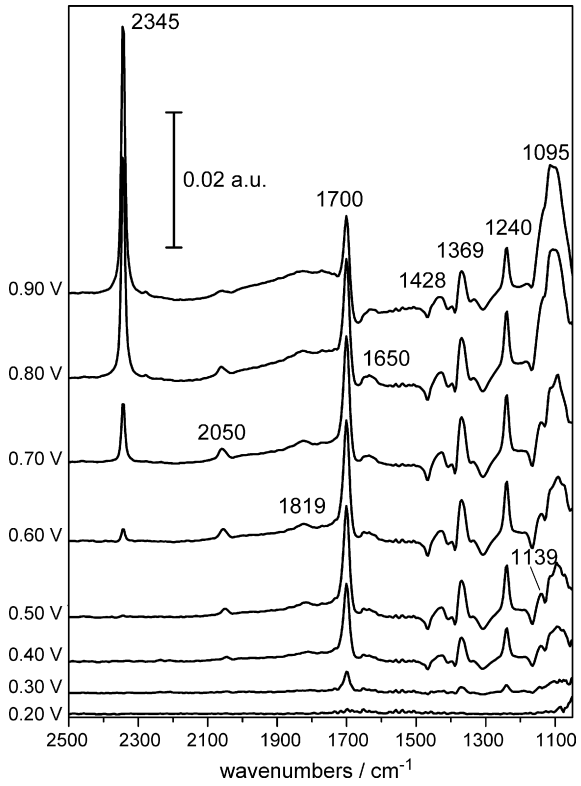

Fig. 8. FTIRS spectra collected in 0.1 M $HClO_4$ + 0.5 M 2-propanol + 0.5 M methanol solution for Pt(1 1 1).

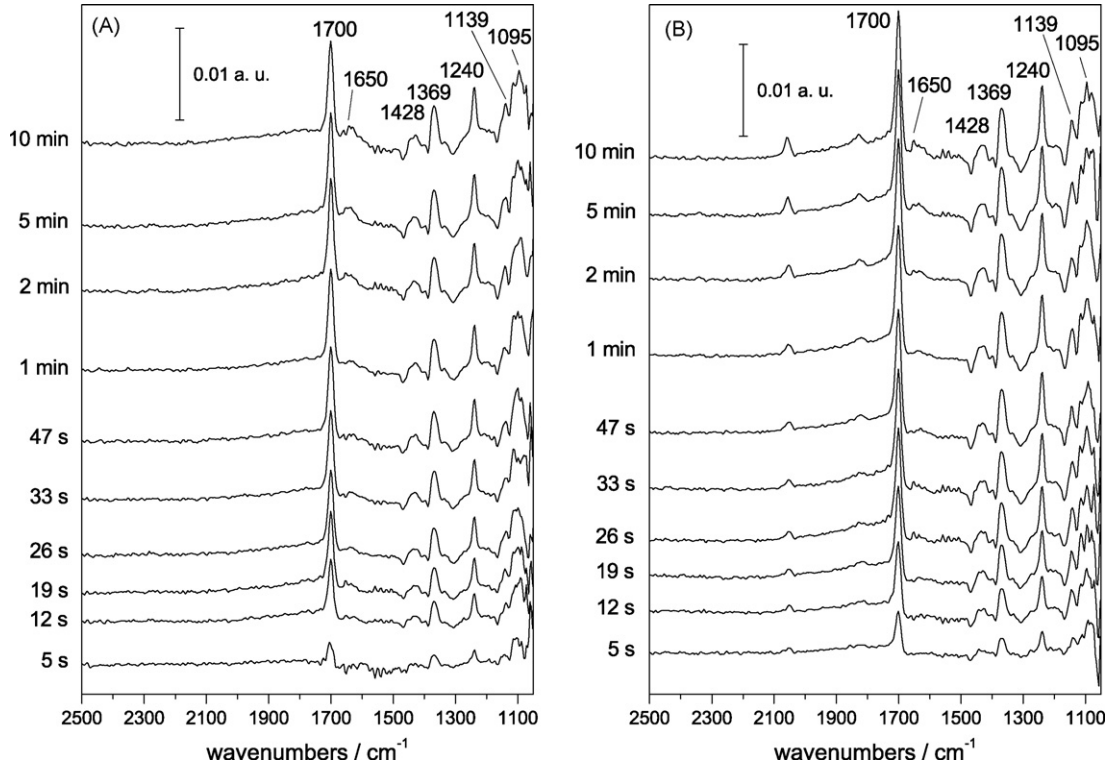

Fig. 9. Time dependent infrared spectra collected at several times (5 s to 10 min) for Pt(1 1 1) electrode in 0.1 M $HClO_4$ + 0.5 M 2-propanol solution (A) and 0.1 M $HClO_4$ + 0.5 M 2-propanol + 0.5 M methanol solution (B) at 0.5 V vs. RHE.

poisoning/inactivation cannot be explained in terms of the presence of IR sensitive adsorbed molecules which, acting as a surface poison, block the active surface sites.

In case of the 0.5 M methanol + 0.5 M 2-propanol mixture, the spectra (Fig. 8) show bands at 2050 and 1819 cm^{-1} due to linear and bridge adsorbed CO, as a result of methanol dissociative adsorption, in addition to the bands related to acetone that are still observed due to 2-propanol oxidation. Moreover, a clear CO_2 band at 2345 cm^{-1} is observed at lower potentials than in case of 2-propanol. Similar bands at similar electrode potentials were previously observed with pure methanol [18] indicating that 2-propanol seems not to affect the methanol electrooxidation mechanism. In this way, from the IR experiments, no clear conclusion can be reached about the enhancement observed in the oxidation of the alcohol mixture because both methanol and 2-propanol, seem to follow the same mechanism as that in the absence of the other alcohol.

Following the same experimental conditions than those employed in Figs. 3 and 6, time dependent transient spectra were collected for the electrooxidation of 2-propanol (Fig. 9A) and 2-propanol + methanol mixture (Fig. 9B) on Pt(1 1 1). For the 2-propanol oxidation, a clear increase in the acetone signals is observed within the first 2 min after that, the signal remains practically constant. Nevertheless, no new bands were observed as a function of time, suggesting that, although inactivation/poisoning takes place in this process, as reported in Fig. 3, no adsorbed species acting as poison have been detected by IR. On the other hand, for the 2-propanol + methanol oxidation, the acetone signals increase in a similar way than in case of pure 2-propanol, but together with the signals corresponding to linear and bridge CO. Again, no new bands were observed when increasing the time. Consequently, the obtained IR results do not provide any evidence to gain an insight into the catalytic improvement reported for the oxidation of the 2-propanol + methanol mixture. However, it is clear that both 2-propanol and methanol must compete for the adsorption sites to be further oxidized. In this way, and taking into account that the oxidation current of methanol is too low (Figs. 2A and 3C) to justify the enhancement, the presence of methanol must modify/alter the adsorption process of 2-propanol producing a lower degree of surface inactivation than in absence of methanol. Unfortunately, this surface inactivation process in case of 2-propanol is not fully understood and according to the IR results could not be justified in terms of adsorbed poisoning species. More work is in progress to gain information about the electrooxidation mechanism for the 2-propanol + methanol binary fuel oxidation.

In the oxidation of 2-propanol it is observed a decrease in electrocatalytic activity after successive potential scans. This deactivation response is characteristic of the formation of irreversible adsorbed species that block the electrode surface. When a mixture of 2-propanol and methanol is used, this decrease is not observed because the formation of this particular adsorbate is inhibited. However, in the infrared spectra collected during the spectroelectrochemical experiments, the only detected product of the 2-propanol oxidation was acetone in solution, because the same bands were observed in spectra with p-polarized and s-polarized light. The only difference between the spectra corresponding to the 2-propanol and the 2-propanol/methanol mixture was the observation of adsorbed CO as a result of the dissociative adsorption of methanol.

As it has been reported, acetone in solution is the main product, but there could be other minor products from side reactions. These products could be for 2-propanol:

$$CH_3CHOHCH_3 \xrightarrow[\text{dehydration}]{H^+} CH_3CH{=}CH_2 + H_2O$$

or for acetone:

$$CH_3COCH_3 \xrightarrow[\text{tautorium}]{H^+} CH_3COH{=}CH_2$$

Both products have a double carbon bond with π-electrons that are well-known to interact with metal transition electrodes and

especially platinum [42]. These reactions probably are not very important in solution, but the Lewis acidic character of the electrode at positive charge densities can favour its formation on the electrode surface. These products are expected to adsorb with the C=C double bond parallel to the surface and because of the surface selection rule [43] this vibration would be infrared inactive and therefore cannot be detected. Only the terminal methyl group could be observed by infrared, but this contribution is obscured by the methyl groups of acetone whose concentration is much higher.

In this way, when methanol is present in solution, the formation of CO adsorbed on the electrode surface breaks the long range domains probably needed for the formation and adsorption of the species involved in the 2-propanol oxidation. Thus, adsorbed CO formation is a key step to reduce the formation of blocking species coming for the side reactions during 2-propanol oxidation and resulting in an enhanced electrocatalytic activity. This hypothesis can initially be considered to be tentative although more light could be shed if previous experiments, where quartz crystal microbalance is used, are taken into account [44]. Lin et al. studied the oxidation of 2-propanol in basic medium for a polyoriented platinum electrode by FTIR spectroscopy and Electrochemical Quartz Crystal Microbalance (EQCM). As in the present case, the authors did not identify any poisoning species by FTIR spectroscopy. However, EQCM studies provided quantitative results of surface mass variation, suggesting the adsorption of 2-propanol or its dissociative products on the polyoriented Pt surface in basic medium.

4. Conclusions

In the present paper, the electrooxidation of methanol, 2-propanol and different mixtures of both alcohols have been studied by cyclic voltammetry and chronoamperometry on the three platinum single crystals and in three different supporting electrolytes (H_2SO_4, $HClO_4$ and NaOH). Moreover IR experiments were performed with Pt(1 1 1) in $HClO_4$.

The results obtained indicate that the electrooxidation of the mixture is a structure sensitive reaction and that, exclusively with the Pt(1 1 1), a clear enhancement in the electrooxidation process is obtained in comparison with the oxidation of the pure alcohols. In addition, this enhancement is observed in the three different supporting electrolytes indicating that the specific surface structure of this electrode is the responsible of the enhanced electrocatalytic activity. In addition, for the Pt(1 1 1) in $HClO_4$, the 2-propanol/methanol concentration ratio was studied.

The results obtained in this paper confirm that the use of 2-propanol + methanol mixtures can be very interesting not only from a fundamental point of view but also for its possible application in fuel cells, although more work is still necessary to fully comprehend the oxidation mechanism when both alcohols are present in the solution. Thus, in terms of current density, an enhancement of 200 times is reached for the electrooxidation of 0.5 M 2-propanol + 1 M methanol mixture after 10 min at 0.5 V in comparison to that obtained for the 0.5 M 2-propanol. IR experiments have confirmed that acetone is the main product for 2-propanol or 2-propanol + methanol oxidation although CO_2 was also observed in the case of the mixture due to the methanol oxidation. Nevertheless, the IR analyses using Pt(1 1 1) have not provided evidences to explain the enhanced process. In this way, it seem that the main role of the methanol is to compete for the adsorption sites where the 2-propanol can be adsorbed modifying its adsorption process and diminishing the surface inactivation observed in case of pure 2-propanol oxidation. More work is in progress to gain information about the electrooxidation mechanism for the 2-propanol + methanol binary fuel oxidation. Thus, a more detailed study with stepped surfaces containing (1 1 1) sites, concerning the effect of (1 1 1) terraces and (1 1 1) steps will be carried out in order to understand the catalytic enhancement.

Acknowledgments

This work has been financially supported by the MICINN-FEDER (Spain) through project CTQ2006-04071/BQU. FJVI also thanks the European Social Funding. Santasalo and Kallio want to give their sincere gratitude to the Academy of Finland. In addition, Santasalo would like to address her gratitude to the Finnish cultural foundation and Helsinki University of Technology for providing a financial possibility to work for 6 months in the University of Alicante.

References

[1] A. Lam, D.P. Wilkinson, J. Zhang, Electrochim. Acta 53 (2008) 6890.
[2] U.A. Icardi, S. Specchia, G.J.R. Fontana, G. Saracco, V. Specchia, J. Power Sources 176 (2008) 460.
[3] T. Shudo, K. Suzuki, Int. J. Hydrogen Energy 33 (2008) 2850.
[4] V. Saarinen, T. Kallio, M. Paronen, P. Tikkanen, E. Rauhala, K. Kontturi, Electrochim. Acta 50 (2005) 3453.
[5] T. Iwasita, Electrochim. Acta 47 (2002) 3663.
[6] S. Wasmus, A. Küver, J. Electroanal. Chem. 461 (1999) 14.
[7] C.L. Campos, C. Roldán, M. Aponte, Y. Ishikawa, C.R. Cabrera, J. Electroanal. Chem. 581 (2005) 206.
[8] J.S. Spendelow, P.K. Babu, A. Wieckowski, Curr. Opin. Solid State Mater. 9 (2005) 37.
[9] L. Dubau, F. Hahn, C. Coutanceau, J.-M. Léger, C. Lamy, J. Electroanal. Chem. 554 (2003) 407.
[10] E. Herrero, K. Franaszczuk, A. Wieckowski, J. Phys. Chem. 98 (1994) 5074.
[11] X.H. Xia, T. Iwasita, F. Ge, W. Vielstich, Electrochim. Acta 41 (1996) 711.
[12] S.C.S. Lai, N.P. Lebedeva, T.H.M. Housmans, M.T.M. Koper, Top. Catal. 46 (2007) 320.
[13] T.D. Jarvi, S. Sriramulu, E.M. Stuve, Colloid Surf. A: Physicochem. Eng. Aspects 134 (1998) 145.
[14] B. Beden, F. Hahn, S. Juanto, C. Lamy, J.-M. Léger, J. Electroanal. Chem. 225 (1987) 215.
[15] J.-M. Léger, S. Rousseau, C. Coutanceau, F. Hahn, C. Lamy, Electrochim. Acta 50 (2005) 5118.
[16] C. Lamy, A. Lima, V. LeRhun, F. Delime, C. Coutanceau, J.M. Léger, J. Power Sources 105 (2002) 283.
[17] K.I. Ota, Y. Nakagawa, M. Takahashi, J. Electroanal. Chem. 179 (1984) 179.
[18] T. Iwasita, in: W. Vielstich, A. Lamm, H.A. Gasteiger (Eds.), Handbook of Fuel Cells, vol. 2, J. Wiley & Sons, England, 2003, p. p. 603.
[19] M.W. Breiter, Electrochemical Processes in Fuel Cells, Springer-Verlag, Berlin, 1969.
[20] C. Lamy, J.M. Leger, J. Clavilier, R. Parsons, J. Electroanal. Chem. 150 (1983) 321.
[21] T.H. Housmans, A.H. Wonders, M.T.M. Koper, J. Phys. Chem. B 110 (2006) 10021.
[22] J. Shin, C. Korzeniewski, J. Phys. Chem. B 99 (1995) 3419.
[23] A.V. Tripkovic, K.D. Popovic, Electrochim. Acta 41 (1996) 2385.
[24] T.H. Housmans, M.T.M. Koper, J. Phys. Chem. B 107 (2003) 8557.
[25] D. Cao, S.H. Bergens, J. Power Sources 124 (2003) 12.
[26] A. Santasalo, T. Kallio, K. Kontturi, Platinum Met. Rev. 53 (2009) 59.
[27] E. Pastor, S. González, A.J. Arvia, J. Electroanal. Chem. 395 (1995) 233.
[28] S.G. Sun, Y. Lin, Electrochim. Acta 41 (1996) 693.
[29] M.E.P. Markiewicz, D.M. Hebert, S.H. Bergens, J. Power Sources 161 (2006) 761.
[30] I.A. Rodrigues, F.C. Nart, J. Electroanal. Chem. 590 (2006) 145.
[31] J. Liu, J. Ye, C. Xu, S.P. Jiang, Y. Tong, J. Power Sources 177 (2008) 67.
[32] C.G. Lee, H. Ojima, M. Umeda, Electrochim. Acta 53 (2008) 3029.
[33] S.Lj. Gojkovic, A.V. Tripkovic, R.M. Stevanovic, J. Serb. Chem. Soc. 72 (2007) 1419.
[34] J. Clavilier, S.G. Sun, D. Armand, M. Petit, J. Electroanal. Chem. 205 (1986) 276.
[35] A. Rodes, M.A. Zamakhchari, K. El Achi, J. Clavilier, J. Electroanal. Chem. 305 (1991) 115.
[36] A. Al-Akl, G. Attard, R. Price, B. Timothy, Phys. Chem. Chem. Phys. 3 (2001) 3261.
[37] C. Lamy, J.M. Léger, S. Srinivasan, in: J.O'M. Bockris, B.E. Conway, R.E. White (Eds.), Direct Methanol Fuel Cells: From a Twentieth Century Electrochemist's Dream to a Twenty-first Century Emerging Technology, Modern Aspects of Electrochemistry No. 34, Kluwer Academic/Plenum Publishers, New York, 2001, p. p. 65.
[38] J.S. Spendelow, A. Wieckowski, PhysChemChemPhys 9 (2007) 2654.
[39] H. Kita, Y. Gao, H. Hattori, J. Electroanal. Chem. 373 (1994) 177.
[40] F.C. Nart, T. Iwasita, M. Weber, Electrochim. Acta 39 (1994) 961.
[41] T. Iwasita, F.C. Nart, M. Weber, Electrochim. Acta 39 (1994) 2093.
[42] F. Zaera, Chem. Rev. 95 (1995) 2651.
[43] R.G. Greenler, J. Chem. Phys. 44 (1966) 310.
[44] H. Lin, G.L. Chen, Z.S. Zheng, J.Z. Zhou, S.P. Chen, Z.H. Lin, Acta Phys. Chem. Sin. 21 (2005) 1280.